CXCR5 EXPRESSING T HELPER CELLS MEDIATE PROTECTIVE IMMUNITY AGAINST TUBERCULOSIS

by

Samantha R. Slight

B.S. Microbiology, Brigham Young University, 2008

Submitted to the Graduate Faculty of

School of Medicine in partial fulfillment

of the requirements for the degree of

Doctor of Philosophy

University of Pittsburgh

2013

UNIVERSITY OF PITTSBURGH

SCHOOL OF MEDICINE

This dissertation was presented

by

Samantha R. Slight

It was defended on

April 2, 2013

and approved by

Tim D. Oury, M.D. Ph.D., Professor of Pathology

Jon D. Piganelli, Ph.D., Associate Professor of Pediatrics

Doug Reed, Ph.D., Assistant Professor of Immunology

Todd A. Reinhart, ScD, Professor of Infectious Diseases and Microbiology

Anuradha Ray, Ph.D., Professor of Medicine and Immunology

Dissertation Advisor: Shabaana A. Khader, Ph.D., Assistant Professor of Pediatrics

CXCR5 EXPRESSING T HELPER CELLS MEDIATE PROTECTIVE IMMUNITY AGAINST TUBERCULOSIS

Samantha R. Slight, Ph.D.

University of Pittsburgh, 2013

COPYRIGHT

Copyright permission was granted for the use of parts from:

1. **Slight SR,** Rangel-Moreno J, Gopal R, Lin Y, Fallert Junecko BA, Mehra S, Selman M, Becerril-Villanueva E, Baquera-Heredia J, Pavon L, Kaushal D, Reinhart TA, Randall TD, and Khader SA. (2013). CXCR5+ T helper cells mediate protective immunity against tuberculosis. *J Clin Invest*. 123 (2): 712-726.
2. **Slight SR** and Khader SA. (2012). Chemokines shape the immune response to tuberculosis. *Cytokine Crowth Factor Rev.* 24 (2): 105-113.

Letters are on file with Samantha R. Slight

CXCR5 EXPRESSING T HELPER CELLS MEDIATE PROTECTIVE IMMUNITY AGAINST TUBERCULOSIS

Samantha R. Slight, Ph.D.

University of Pittsburgh, 2013

One third of the world's population is infected with *Mycobacterium tuberculosis* (Mtb). Although most infected people remain asymptomatic, they have a 10% lifetime risk of developing active tuberculosis (TB). Thus, the current challenge is to identify immune parameters that distinguish individuals with latent TB from those with active TB. Using human and experimental models of Mtb infection, we show that organized ectopic lymphoid structures containing $CXCR5^+$ T cells are found in Mtb-infected lungs. In addition, we show that in experimental Mtb infection models, the presence of $CXCR5^+$ T cells inside ectopic lymphoid structures are associated with immune control. Furthermore, in a mouse model of Mtb infection, we show that activated $CD4^+$ $CXCR5^+$ T cells accumulate in Mtb-infected lungs, and produce proinflammatory cytokines. Absence of CXCR5 in mice results in increased susceptibility to TB due to defective T cell localization within the lung parenchyma. We show that CXCR5 expression on T cells mediates correct T cell localization within TB granulomas, efficient macrophage activation, promoting protection against Mtb infection and facilitating lymphoid follicle formation. These data show a novel role for $CD4^+$ $CXCR5^+$ T cells in protective immunity against TB and highlight their potential use for future TB vaccine design and therapy.

TABLE OF CONTENTS

LIST OF TABLES

LIST OF FIGURES

ACKNOWLEDGEMENTS

My graduate school experience has been challenging and demanding, but also has been the most character building period of my life. I realize that many people have helped and supported me through my graduate career, and I owe sincere and wholehearted thanks to all of them.

Foremost, I have been extremely blessed to have Shabaana Khader as a mentor. I am so grateful she took me on as a rotation student the Spring of 2009. Since then, she has inspired and motivated me by her fantastic positive attitude and enthusiasm for science. She is one of the most intelligent and driven people I have ever met and has been invaluable as a mentor, teacher, and friend. She has provided me with valuable guidance and advice and taught me how to troubleshoot and always bring my research to the highest level of excellence. I am grateful for her patience with all my steps in learning and always encouraging me to be the best that I can be. She always looks out for me. I would not have reached this point without her.

The Khader Lab has had a group of talented lab personnel that have passed through the lab over the years that I have been extremely grateful to have the opportunity to work with them. They have all contributed in their own way and without of which this thesis work would not have been accomplished. I first want to thank Yinyao Lin who was the first postdoctoral student I met in the lab and who taught me much of the techniques that I have used to accomplish this work. I am very grateful for his patience in teaching me. Radha Gopal has provided much assistance and support in completing this project and has been a great friend more than just a colleague.

Additional thanks for technical assistance, critical scientific discussions and advice, and friendship from Lokesh Gulani, Leticia Monin, Daniel Mallon, and Nikhil Nuthalapati. In addition, we have had a good number of collaborators who have made this work possible who will be noted throughout this dissertation, but I specifically want to recognize Javier Rangel-Moreno. He had been there through all the revisions of our CXCR5 paper working extensive hours and weekends to create the beautiful images we have needed for the manuscript. None of this would have been possible without his scientific contribution and talent and I am very grateful for him. Also, Alison Logar who runs our flow cytometry core and has taught me the tricks of the trade. She has also been a wonderful friend.

I also would like to thank my committee members, Drs Tim Oury, Jon Piganelli, Anuradha Ray, Doug Reed, Todd Reinhart, and Shabaana Khader for their time in meeting every six months to discuss, troubleshoot, and advise on my research project to bring it to a finished product. I also would like to thank Dr. Reinhart and Beth Fallert Junecko for their technical assistance on the paper and for his grant advisement as part of the T32 PART training program. Also, Dr. Piganelli for always checking up on me in Rangos and for all his advisement.

Finally, I would like to thank my family and friends. I am so grateful to have made such wonderful and lifelong friends here in Pittsburgh who have been a great support. It will definitely be bittersweet in leaving here. Most importantly, I would like to thank my family for their love and encouragement. There is no doubt in my mind that whatever challenges I may face, my family is and will always be there for me. I am so grateful for my parents always encouraging me to fulfill my dreams, for providing support, advice, love, and never limiting me. For my brother, sister and brother-in-law, I'm so thankful for your understanding, support and being a strength to

me. You are all an example. I love my family and relatives so much and without their support I would not be here today.

ABBREVIATIONS

AIDS	Acquired Immunodeficiency Syndrome
APC	Antigen Presenting Cell
A-TB	Active Tuberculosis
B6	C57BL/6
BALT	Bronchus Associated Lymphoid Tissue
BSL	BioSafety Level
CALT	Conjunctiva Associated Lymphoid Tissue
CFU	Colony Forming Units
CR	Complement Receptor
ELO	Ectopic Lymphoid Organ
ESAT-6	6 kDa Early Secretory Antigenic Target
DC	Dendritic Cell
DCSIGN	DC-specific intercellular adhesion molecule-3-grabbing nonintegrin
DLN	Draining Lymph Node
DOTS	Directly Observed Therapy, Short Course
FDC	Follicular Dendritic Cell
FFPE	Formalin Fixed Paraffin Embedded
GALT	Gut Associated Lymphoid Tissue

GC	Germinal Center
HEV	High Endothelial Venuole
HIV	Human Immunodeficiency Virus
iBALT	inducible Bronchus Associated Lymphoid Tissues
BMDC	Bone Marrow Dendritic Cell
ICOS	Inducible T- cell Costimulator
IFN	Interferon
Ig	Immunoglobulin
IL	Interleukin
iNOS	inducible Nitric Oxide Synthase
i.v.	Intravenous
LT	Lymphotoxin
L-TB	Latent Tuberculosis
LTi	Lymphoid Tissue inducer
MAdCAM-1	Mucosal Cell Addressin Cell Adhesion Molecule 1
MALT	Mucosa Associated Lymphoid Tissue
ManLAM	Manosylated Lipoarabinamannam
MDR	Multi-Drug Resistant
Mtb	*Mycobacterium tuberculosis*
MTEC	Mouse Tracheal Epithelial Cells
NALT	Nasal Associated Lymphoid Tissue
NHP	Non-Human Primate
NK	Natural Killer

NO	Nitric Oxide
PCNA	Proliferating Cell Nuclear Antigen
PNA	Peanut Agglutinun
PNAd	Peripheral Lymph Node Addressin
PRRs	Pattern Recognition Receptors
ROI	Reactive Oxygen Intermediates
SLO	Secondary Lymphoid Organ
SP-A	Surfactant Protein-A
TB	Tuberculosis
STAT	Signal Transducer and Activator of Transcription
Tfh	T Follicular Helper
Th	T Helper
TLR	Toll Like Receptor
Tg	Transgenic
TGF	Tumor Growth Factor
TNF	Tumor Necrosis Factor
Treg	T regulatory
VCAM-1	Vascular Cell Adhesion Molecule 1
XDR	Extensively Drug Resistant

1.0 INTRODUCTION

1.1 *MYCOBACTERIUM TUBERCULOSIS*

Twenty years ago, the World Health Organization declared TB a global health emergency. The disease, caused by the bacterium Mtb, most commonly affects the lungs. Transmission occurs from person to person through aerosol droplets generated through the cough of someone with an active respiratory Mtb infection. Even though a TB vaccine exists and an effective drug regimen is available, TB still ranks as the second leading cause of death from an infectious disease in the world, only behind Human Immunodeficiency Virus (HIV). The ever increasing global health burden of TB can be contributed by a number of factors including: 1) the emergence and growth of multi-drug resistant (MDR) and extensively drug resistant (XDR) strains of Mtb; 2) social inequality and widespread poverty; and 3) the increasing acquired immunodeficiency syndrome (AIDS) epidemic. Despite this dismal outlook, hope lies in the growing body of immunological knowledge and new scientific tools at our fingertips in providing novel breakthroughs in the treatment and prevention of TB.

1.1.1 Disease Outcomes

The clinical manifestation of TB is diverse and depends on a number of host factors and host-microbe interactions [2]. Following initial exposure to Mtb, several disease outcomes are possible:

active disease, latent disease, and reactivated disease (Figure 1) [2]. Although active TB and reactivated TB place the largest strain on health care systems, only a small proportion of those infected actually develop symptoms. Approximately 5-10% of the population will develop a primary infection with clinical symptoms of active disease. Symptoms typically develop within 2 years of the initial infection and most commonly include coughing, fatigue, fever, and chest pain [3]. The disease primarily affects the lungs, the initial site of infection, but the infection can spread to other organs such as the spleen, lymph nodes, liver, joints, peritoneum, kidneys, and central nervous system causing widespread symptoms and damage. Patients with active disease are typically placed on a combination drug therapy including isoniazid, rifampin, pyrazinamide, and ethambutal for 6 months or longer [4]. Incomplete drug treatment for active disease contributes to the growing MDR and XDR TB cases worldwide and has prompted the implementation of the

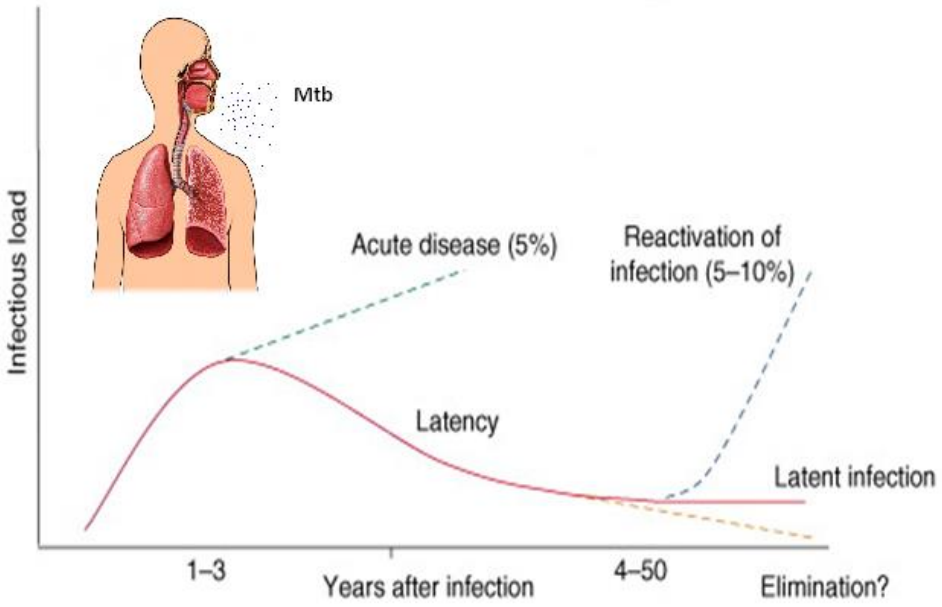

Figure 1: The progression of Mtb infection in humans.

Following aerosol exposure to Mtb, approximately 5% of individuals develop active disease within the first two years. Others develop latent infection, which 90% maintain for life. However, 5-10% of individuals reactivate TB. The immune conditions and cellular architecture required for maintaining immune control during latent infection require further investigation. Figure modified from previous work [1].

Directly Observed Therapy, Short Course (DOTS) regimen [4].

Active TB may be the primary cause of TB hospitalizations, but latent TB is the largest reservoir of the tubercule bacilli. The majority of cases, approximately 90%, of individuals infected with Mtb are able to mount a protective cell-mediated immune response that inhibits the growth of the mycobacteria without complete eradication [5]. This is referred to as a latent TB infection. These patients are characterized as having a positive skin reaction to tuberculin, but having no observable symptoms of pulmonary or extrapulmonary TB [5]. In contrast to active disease, latent Mtb-infected individuals are not considered infectious.

If latent TB were controlled throughout the life of the person, it would pose no eminent threat to the host or close contacts. However, 10% of latently infected individuals reactivate and develop post-primary active TB [4]. Factors such as age, immune status, malnutrition, smoking and coexisting diseases are known to increase risk of reactivation, but detection methods to determine those that will and those who will not reactivate are ill defined [4]. It is becoming clear that latency encompasses a wide range of conditions and by determining the molecular and cellular differences between active and latent TB, it may be possible to identify patients who are at risk for reactivation.

1.1.2 The TB Granuloma

The hallmark characteristic of TB is the granuloma where it is easily identified on chest x-rays in activated, latent, and reactivated infection. At the most rudimentary level, the granuloma is an organized immune cell aggregate composed of infected macrophages at the center surrounded by a dense leukocytic wall [6]. The granuloma is thought to be a protective defense to concentrate the immune response for effective bacterial killing and to prevent mycobacterial spreading [7].

However, the observation that granulomas develop in both latent and active infection suggests that formation is inadequate for protection. Further, in active infection, the caseous core can foster an environment where extracellular bacteria can exist and where increased cell death in the granuloma can act as a nutritional source for replicating bacteria [8]. The granuloma can also act as an infectious source to seed new granulomas within the lung [9]. Thus, a very delicate and dynamic balance between Mtb replication and the immune response must be maintained. By identifying the cellular differences and biomarkers characteristic of latent and active granulomas, we may further understand what specific granulomatic structure sustains long-term bacterial control.

In humans, a spectrum of granulomas are observed in TB, but the classic granuloma is caseous, meaning it has a necrotic core. Mtb-infected macrophages are clustered at the center where they can undergo a number of changes including the fusion into multinucleated giant cells and/or differentiation into foam cells [6, 10]. Macrophages constitute the majority of the cells within the granuloma. As immune cells infiltrate the lung, a leukocyte cuff forms containing $CD4^+$ T helper (Th) cells, $CD8^+$ T cells, natural killer (NK) cells, dendritic cells (DCs), neutrophils, and fibroblasts. B cells form distinct lymphocytic aggregates and epithelial cells are also known to contribute to the formation of this complex and dynamic structure. The increased number of immune cells and Mtb-infected macrophage cell death form the caseum within the granuloma, which increases in size as the infection progresses [7]. Cytokine production is primarily localized in the periphery of the granuloma where it is thought that the majority of cross-talk occurs rather than in the core [11-12]. The receptors required for localization of these critical immune cells within the granuloma is a significant area of investigation.

1.1.3 Animal Models

TB is a disease that only occurs naturally in humans. However, studying human TB can be challenging with considerable variation in age of the subject, duration of infection, bacterial strains, and genetic differences. Not to mention, patients with latent and active infection and those receiving antibiotic treatment further contribute to disease diversity. Fortunately, TB research has several animal models for studying infection, although many aspects should be considered when selecting an appropriate animal model. The primary animal models used for Mtb infection research include the non-human primate (NHP), the mouse, the guinea pig, and the rabbit, with the mouse considered the most commonly used animal model. An important issue with other regards to TB research is the need for a biosafety level (BSL)- 3 facility. As such, several other mycobacteria animal models have developed, such as the zebrafish model infected with *M. marinum*, that are suitable for BSL-2 work.

Historically, the guinea pig was the first model used by Robert Koch, the original pioneer of TB research, when he infected a guinea pig with infectious brain or lung tissue from humans who died of TB [13]. The lung pathology of a guinea pig is very similar to humans with large mononuclear cells that undergo necrosis forming caseous granulomas. However, guinea pigs are highly susceptible to infection and limited reagents are available for study [14]. Further, rabbits develop similar lung pathology as humans with more innate resistance to TB, however, similar limitations as the guinea pig also exist with this model [15-16]. Recently, zebrafish have become an excellent model for real-time visualization of granuloma development using *M. marinum* as these fish embryos are transparent [17]. Although caseous granulomas develop in the zebrafish, lesions contain few lymphocytes suggesting innate immunity may play a larger role in

granuloma formation in zebrafish [18]. Despite limitations to this model, new insights into host immunity are obtainable with the ease of new technology and genetics available.

The most exploited model in TB is the mouse model [19]. It is both economical and easily manipulated, with a vast amount of immunological resources available. Various routes of infection including intravenous (i.v.) and the low dose aerosol model have been utilized for Mtb infection. Intravenous delivery of Mtb is advantageous in that it produces a considerable host immune response with a systemic infection. However, the immune response to systemic infection differs substantially from an infection through a natural aerosol route where fewer bacteria are deposited directly in the lung. Chiefly, a considerable amount of bacteria is required for i.v. infection to infect the lung as bacteria circulate and reside in the spleen and liver [20]. Further, bacteria are also deposited within the parenchyma of the lung rather than the alveoli as seen in an aerosol infection. The development of specialized equipment to deliver ~100 colony forming units (cfu) of Mtb bacteria, which is considered a low dose of Mtb, has made the use of the aerosol model more convenient. Microscopic aerosol droplets are deposited in the lower lung closely mimicking a natural TB infection making it the most acceptable route of infection [21-22].

Some limitations exist in the mouse model of tuberculosis namely differences in granuloma development and the inability to naturally develop latent TB. Mtb-infected mice develop a chronic infection that persists throughout the life of the mouse [23]. Further, the granulomatic response, which begins to develop around day 21 post infection, does not progress to a necrotic phase, except in certain strains of mice [24-25]. The murine granuloma starts with the accumulation of macrophages followed by infiltration of lymphocytes and the organization of distinct $CD4^+$ T cells aggregates and interspersed $CD8^+$ T cells throughout the lung. Tight clusters of B cells can also be observed in the granuloma [24]. Human granulomas are more

structured in comparison to the mouse granuloma, however, great insights into granuloma development have resulted from murine TB research. The versatility of the mouse model with its capacity for genetic manipulation and vast immunological resources make it an ideal model for determining protective immune mechanisms against Mtb.

Although the mouse model has contributed immensely to our understanding of TB, it does not reproduce classical latency. This deficiency can be overcome with the use of NHPs, which develop various types of pathological lesions and outcomes similar to human infection [26]. Mtb granulomas contain a classical structure of multinucleated giant cells and caseation with liquefacation and cavity formation occurring in the NHP lung with active TB. Cost, containment requirements, and ethical concerns for NHP research has limited the use of this model in TB, but it still remains our greatest resource in studying latent TB and for examining TB/AIDS co-infection and reactivation [26].

1.2 MTB HOST DEFENSE

1.2.1 Initiation of Infection

The first line of defense against aerosolized Mtb is the alveolar macrophage within the lung. Although crucial for eliciting an immune response, the macrophage is also used by the bacterium to evade immune recognition and destruction ensuring survival within the host. Several pattern recognition receptors (PRRs) are implicated in the internalization of Mtb, namely complement receptors (CR) 1, 3, and 4, CD14, the mannose receptor, scavenger receptors and the pulmonary surfactant protein (Sp-A) [27-31]. Once inside the host cell, the maturation of the phagosome is a

relatively short process. However Mtb arrests phagosome development and prevents lysosome fusion [32]. The inability of the macrophage to proceed through this pathway is thought to be dependent upon the bacterial expression of surface manosylated lipoarabinamannam (ManLAM) and other Mtb lipids such as PIMs that prevents the acquisition of lysosomal hydrolases [33-36]. The arrest of the phagosome provides an ideal environment for Mtb replication and evasion from the host that requires adaptive immunity to overcome.

The development of adaptive immunity is dependent on the uptake of Mtb antigen by antigen presenting cells (APCs) mainly dendritic cells (DCs), but also macrophages and B cells. DCs, in addition to complement receptors and the mannose receptor, also express DC-SIGN (DC-specific intercellular adhesion molecule-3-grabbing nonintegrin), which interacts with Mtb surface carbohydrates for cellular uptake [37-38]. In contrast to human macrophages, DCs prevent intracellular growth of Mtb and are able to upregulate activation markers following internalization through DC-SIGN and signaling through toll-like receptors (TLRs) 2, 4, and 9 [38-41]. Mtb-stimulated DCs traffic to the lymph node following maturation and upregulation of the CC-chemokine receptor CCR7 where they present antigen to naïve T cells and produce proinflammatory cytokines initiating the T cell adaptive immune response. T cell priming occurs in the mouse model 8-10 days following challenge [42-44]. Additionally, IL-12p40 is required to induce chemokine responsiveness of Mtb-exposed dendritic cells as IL-12p40 deficient DCs were unable to migrate from the periphery to secondary lymphoid organs (SLOs), but could be rescued with the addition of IL-12p40 homodimer [45-46].

A major consequence of Mtb induced macrophage and DC activation is the production of proinflammatory cytokines and chemokines (Mtb cytokine and chemokine secretion will be discussed in depth in section 1.3 and 1.4, respectively) responsible for initiating immune cell

recruitment for granuloma formation and for shaping the adaptive immune response. In the mouse model, this cytokine and chemokine production can be detected in the lung starting at day 15 post infection and coincides with cellular accumulation and control of the bacterium [24]. Cytokines can induce activation of macrophages and killing of Mtb by driving production of reactive oxygen intermediates (ROIs) and inducible nitric oxide synthase (iNOS). It is clear, that Th1 skewing cytokines, namely interferon (IFN)-γ and tumor necrosis factor (TNF)-α, produced by other innate or adaptive immune cells in close proximity to Mtb-infected macrophages drive this process.

1.2.2 $CD4^+$ T Helper Cells

It is well established that $CD4^+$ T helper cells are critical in protection against Mtb in both mice and humans [47]. Patients infected with HIV-1 are estimated to have a 30 times greater risk of developing tuberculosis. Mice deficient of $CD4^+$ T cells succumb ~120 days post infection with increased neutophilic influx and reduced lymphocyte accumulation in the lung [48]. Following Mtb infection, distinct activation profiles of DCs drive naïve T helper cells to become polarized into Th1, Th17, or T regulatory (Treg) phenotypes in the draining lymph node. These cells then migrate to the lung in response to Mtb-induced chemokines to elicit effector functions by day 15 post challenge in the mouse model [49]. Th1 cells, which are driven by IL-12p70 production and the expression of T-bet, are thought to be the primary cells responsible for bacterial control by IFNγ and TNFα–induced macrophage activation [50]. The arrival of antigen-specific Th1 cells correlates with cessation of bacterial growth in the lungs of Mtb-infected mice [51]. Th1 cells localized near Mtb-infected macrophages are essential for cross-talk and subsequent

activation and microbial killing in the lung [52]. It remains undisputed that the $CD4^+$ Th1 pathway is critical for Mtb protective immunity.

Th17 differentiation is initiated by IL-6, IL-1β, and TGF-β production and requires IL-23 for maintenance [53-56]. In recent work, Th17 cells were found in the lung following infection with Mtb, however, the absence of IL-23/IL-17 did not result in increased susceptibility early in infection [57]. IL-23KO mice had reduced inflammation within the lung, but similar bacterial numbers as control mice prior to day 100 post infection, suggesting Th17 cells do not play a key role in early adaptive immunity [57-58]. However, IL23KO mice had higher bacteria after 100 days indicating a role in chronic Mtb host defense. In contrast, Th17 cells are essential in generating protective memory responses in several vaccine models[59]. Thus, our expanding knowledge of Th17 cells in Mtb infection is rapidly evolving and will be beneficial in the design of an effective vaccine.

Treg cells induced by IL-6 and TGF-β cytokines and the expression of FoxP3 are critical in homeostatic regulation, but overproduction can lead to lack of infection control [60]. $Foxp3^+$ Treg cells are found in the lung during Mtb infection and are specifically localized within the granuloma and peribronchial regions [61]. Selective depletion of $Foxp3^+$ cells in mixed bone marrow chimeric mice resulted in 10-fold less bacteria in the lungs of Mtb-infected mice [61]. Further, adoptive transfer of antigen-specific $Foxp3^+$ Treg cells prevented effector cell expansion and increased the bacterial burden in the lung suggesting that Tregs are primarily detrimental to the generation of a protective immune response in Mtb infection [62].

The involvement of newly emerging cell subsets such as T follicular helper cells, Th22 cells, and Th9 cells in Mtb infection remain to be defined. In addition, it is now understood that T helper cells may possess some degree of plasticity [63]. The phenotypic flexibility of these

subsets in host defense against Mtb may be advantageous allowing the T helper cell to adapt to various immune environments as the infection progresses. It is becoming clear that multifunctional IFNγ^+TNFα^+IL-2^+ Th1 rather than single positive IFNγ^+ Th1 cells correlate with better protective immune responses against Mtb [64]. The plasticity of all $CD4^+$ Th cell subsets is an important focus for future study in Mtb infection.

1.2.3 $CD8^+$ T cells

It is generally accepted that $CD4^+$ T cells are critical during Mtb infection, but evidence for $CD8^+$ T cell involvement has been lacking. CD8-deficient mice are not more susceptible and have no defects in granuloma development, despite the presence of $CD8^+$ T cells in peripheral lesions of the lung [65-66]. Although, this early evidence shifted the primary focus to $CD4^+$ T cells, further analysis suggests that $CD8^+$ T cells may also be required for optimal defense against Mtb infection. During the chronic phase of infection, CD8-deficient mice were reported to have increased lymphocytic and neutophilic influx [65]. In addition, antibody depletion studies suggest both CD8 and CD4 cells are needed during Mtb infection, although the role for $CD4^+$ cells is more prominent in the murine model [67]. In addition, adoptive transfer of immune $CD8^+$ T cells reduced the bacteria burden within the lung of Mtb-infected mice [20, 68]. In humans, Mtb specific $CD8^+$ T cells were found to directly kill Mtb-infected macrophages through granulysin production [69-70]. Additional evidence has shown that $CD8^+$ T cells produce the proinflammatory cytokines IFNγ and TNFα to further contribute to bacterial control [71]. Thus, it is clear that $CD8^+$ T cells are involved in Mtb infection and interact with $CD4^+$ T cells to contribute to the outcome of TB [72].

1.2.4 B cells

The function of B cells and antibodies in TB remains an enigma. Although important for numerous microbial pathogens in protection and immunological memory, B cells, by themselves, are thought to confer little protection against TB [73]. Historically, passive immune therapy was used to transfer humoral immunity with variable protective results, and was replaced by the advent of antibiotics as a superior treatment [74]. Variability in passive immunity is likely contributed to differences in the preparation of antisera and treatment durations. Further, B cell deficiencies in both humans and mice fail to increase susceptibility to Mtb infection, questioning whether B cells markedly participate in Mtb immunity [75-77]. However, B cell aggregates are a dominant structure in both human, NHP, and mouse Mtb-infected lungs and become more organized as the infection progresses [11, 24, 78-79]. The absence of B cells in mice disrupts granuloma formation and increases pulmonary inflammation indicating B cells are required for maintenance of pulmonary host architecture and for retaining the host immune balance in the Mtb-infected lung [77]. Many questions remain to be answered on the role of these structures in Mtb immunity and whether B cells play a greater role towards protection.

1.3 CYTOKINES IN MTB INFECTION

Resistance to Mtb is dependent upon cellular signals initiated by Mtb-specific lymphocytes to activate macrophage killing mechanisms. Experimental models have firmly established that these soluble factors, or cytokines, are responsible for the cell-to-cell communication instigated in inflammation. Cytokines are vital for a vast number of innate and adaptive immune responses in

TB for regulating not only macrophage activation, but inducing the differentiation of leukocytes, driving granuloma formation, and maintaining a balanced host microenvironment. In the mouse model of Mtb, induction of cytokine and effector molecules specific to the Th1 pathway, namely IL-12, IFN-γ, TNF-α, and iNOS occurs between days 15-21 and coincides with T helper cell accumulation within the lung [80]. The functions of these proteins in host resistance to Mtb are well documented in both the mouse model and Mtb-infected humans.

1.3.1 Interleukin-12

Mtb is a potent inducer of the multifunctional cytokine IL-12, which can be expressed as either a homodimer (IL-12p40$_2$) or a heterodimer composed of IL-12p40 and the IL-12p35 subunit (IL-12p70) [81]. In the mouse model, both IL-12p35 and IL-12p40 deficient mice are more susceptible to Mtb infection compared to wild type controls. However, a deficiency in IL-12p40 is more detrimental to the host compared with IL-12p35 deficiency, suggesting a role for IL-12p40 outside of IL12p70 expression [50, 82]. IL-12p40 is induced early in infection in response to TLR stimulation predominantly by macrophages and DCs and signals through the IL-12 receptor formed by the IL12Rβ1 and β2 chains. Signaling through this receptor on DCs by the IL-12p40 homodimer, activates the homing ability of Mtb-primed DCs for migration to secondary lymphoid organs [45]. In the absence of IL-12p40, mice failed to generate activated $CD4^+$ Th1 cells due to the inability of DCs to become responsive to homeostatic chemokines that drive migration from the lung to the draining lymph node (DLN) [45]. Activation of DCs could be restored with treatment of IL-12p40$_2$, and IL-12p40 deficient mice can be partially rescued with administration of exogenous IL-12p40$_2$ [45, 82]. Upon arrival of DCs to the DLN, IL-12p70 is instrumental in driving the differentiation of naïve T cells to a Th1 phenotype [81]. Th1 cells migrate to the Mtb-

infected lung where they are responsible for producing IFNγ and TNFα proinflammatory cytokines. IL-12 is further required to maintain pulmonary Th1 effector function during chronic Mtb infection [83]. The important role for IL-12 pathway is emphasized in human patients with Mendelian defects in IL12Rβ1 and IL-12p40 who demonstrate increased susceptibility to mycobacterial infections [84]. Recently, human dendritic cells producing IL-12 are demonstrated to also drive naïve T helper cell induction of a T follicular helper cell phenotype and CXCR5 expression suggesting newer cell subsets may evolve under Mtb Th1 cytokine conditions [85].

1.3.2 Interferon-γ

The importance of IFNγ in mycobacterial protection is clearly demonstrated by the severity and increased susceptibility to mycobacterial infections in individuals with defects in IFNγ signaling pathways [86]. The major defined effect of IFNγ is the activation of macrophages by signaling through the IFNγ receptor comprised of two subunits, R1 and R2. Activation stimulates antimicrobial expression of LRG47 and nitrogen and oxygen radical intermediates that can kill the intracellular pathogen [87-88]. Recently, IFNγ has been linked to induction of autophagy known to reduce Mtb intracellular bacterial burden within phagocytes [89]. However, macrophages are not the only cell acted upon by IFNγ. New evidence suggests that IFNγ is a powerful immunomodulator of non-hematopoietic cells, as bone marrow chimeric mice deficient of IFNγR within lung epithelial and endothelial cells were unable to control chronic Mtb infection [90].

During Mtb infection, numerous cell subtypes have been identified in both mice and humans that are capable of producing IFNγ, namely $CD4^+$ Th cells, $CD8^+$ T cells and NK cells [72, 91]. As a result, it is often difficult to assess the major cell contributor of IFNγ as mice deficient in

one cell subset compensate production with another. However, IFNγ protection is a key function of $CD4^+$ Th cells. In the Mtb-infected mouse, ~5% of pulmonary leukocytes are producing IFNγ without restimulation [72]. Further analysis determined that ~90% of IFNγ producing cells were $CD3^+$ T cells, of which ~65% were $CD4^+$ T cells and ~35% were $CD8^+$ T cells confirming that Th1 cells are significant producers of IFNγ during Mtb infection [72]. However, adoptive transfer of antigen-specific IFNγ deficient $CD4^+$ T cells into IFNγ-/- mice controlled Mtb infection compared with transferred wild type $CD4^+$ T cells indicating other CD4-dependent Mtb protective mechanisms exist [44]. In addition, a mouse lacking any component of the IFNγ signaling pathway, IFNγ, IFNγR, and STAT1 remains one of the most susceptible genetically modified animals to date in Mtb infection with high bacterial burdens, large infiltration of polymorphonuclear neutrophils and extensive necrosis [92-93]. Increased neutophils in mice deficient in IFNγ signaling pathways is due to regulation of IL-17 by IFNγ, as IL-17 is known to control neutrophil recruitment [94]. It is clear that IFNγ is essential to restrict bacterial replication and prevent fatal infection in Mtb-infected humans and mice.

1.3.3 Tumor Necrosis Factor-α

TNFα is another potent proinflammatory cytokine in Mtb infection as definitely proven by multiple studies with genetically modified mice, soluble TNF receptors, and blocking antibodies [95]. Likewise, patients with severe autoimmune disease are treated with immunosuppression therapy using TNFα blockers that increase the risk of developing reactivated TB demonstrating a critical role for TNFα in control of Mtb infection [96-97]. TNF-α can exist in both soluble form and membrane bound and is known to act through the trimeric receptors, TNFR1 and TNFR2 [95].

Mice deficient in TNF have an initial delay of cellular influx into the lung, where recruited T cells fail to colocalize with macrophages, and necrosis ensues [98]. TNFα-/- mice begin to succumb to infection ~28 days post infection following low dose, aerosol Mtb infection [98]. Chronic Mtb-infected mice and NHPs that were TNF neutralized had increased tissue bacterial burden with fluid accumulation in the alveolar space [99-100]. The heightened bacterial burden in TNFα gene deficient mice is attributed to the bactericidal activity of TNFα in activating macrophages that is synergistic with IFNγ [101–102]. In addition, TNFα is important for chemokine production in macrophages and the subsequent recruitment and organization of immune cells into the granuloma [98, 101]. In vitro assays have demonstrated that Mtb-infected murine macrophages neutralized with TNFα have decreased levels of the chemokines CCR5, CXCL9, and CXCL10 [103]. Further, mice deficient in TNFα exhibit disrupted granuloma formation in the lung, likely attributable to decreased chemokine production [101]. Cells primarily responsible for TNFα production in humans and experimental models include macrophages and antigen specific $CD4^+$ T cells and $CD8^+$ T cells [71, 104-105]. It has further been described that a population of $CD4^+$ T cells are multifunctional and capable of producing both IFNγ and TNFα and may play a role in Mtb host defense[106] . The contribution of TNFα to Mtb infection is undisputable with functions in bacterial killing, cell survival, lymphocyte recruitment and granuloma formation.

1.3.4 Nitric Oxide

The production of reactive oxygen intermediates, reactive nitrogen intermediates, and LRG-47 are effective host defenses against infectious pathogens. NO is a signaling molecule synthesized when the guanidine nitrogen of L-arginine is oxidized by nitric oxide synthases (NOS), which

are either constitutively expressed (neuronal NOS and endothelial NOS) or induced (inducible NOS). Expression is driven by the production of proinflammatory cytokines TNFα, IFNγ, and IL-1β, individually or synergistically [107]. iNOS plays an essential role in generating NO during Mtb infection and killing Mtb within infected macrophages in the mouse [108-109]. Mtb-infected iNOS-/- mice had higher rates of dissemination and increased neutrophilic necrosis that led to exacerbated TB, compared with B6 control mice [110]. In chronic infection, mice treated with aminoguianidine, an iNOS inhibitor, showed worsened pathology and increased bacillary load, while mice latently infected with Mtb, also known as the Cornell mouse model, developed reactivated infection [111].

In contrast to the mouse model of TB, the role of iNOS in human TB remains controversial. Few reports have identified antimycobacterial effects of NO, however, iNOS expression is upregulated in human Mtb-infected granulomatic lesions [107, 112]. Early growth inhibition of Mtb in human alveolar macrophages is shown to be independent of IFN-γ mediated NO activation as exogenous IFN-γ added to Mtb infected macrophages produced no antimicrobial activity [113]. However, macrophages and epithelial cells are capable of making NO during Mtb infection [107, 112-115]. One study suggests that alveolar macrophages can make NO when infected with Mtb and this correlated with inhibition of Mtb growth [116]. Importantly, polymorphisms in *iNOS* in -1026G allele, rs2274894 (intron), and rs8078340 (promoter) found in Brazilian, African-American, and South African populations, repectively, were associated with increased susceptibility to TB, supporting the potential protective role for NO in human infection [117].

1.4 CHEMOKINES IN MTB INFECTION

In addition to cytokines, chemokines are critical for protective immunity against Mtb. Chemokines are a large family of structurally related proteins that are known to interact with a number of G-protein linked receptors to drive angiogenesis, development, the trafficking of APCs to SLOs and the recruitment of immune cells to sites of inflammation [118-121]. Each chemokine is categorized into four subfamilies based on structural similarities in their first two of four cysteine residues: C, CC, CXC, and CX_3C [118-120]. Based on their expression in inflammation or in SLOs, chemokines can be further divided into inflammatory or homeostatic chemokines [122]. However, it is becoming clear that homeostatic chemokines can also be induced in response to inflammation [24, 123-126].

The availability of several animal models of TB has greatly benefited our overall understanding of chemokines in Mtb infection. In the mouse model of low dose aerosol Mtb infection, mRNA for a number of chemokines and their corresponding receptors have been reported to be upregulated in the lung between days 12-21 post infection (Table 1) and this coincides with the recruitment of specific immune cells into the lung (Figure 2). Specifically, the early accumulation of a variety of different innate cells such as neutrophils, NK1.1 cells, γδ T cells and macrophages (Figure 2a), as well as later accumulation of adaptive effector cells such as $CD4^+$ T cells, $CD8^+$ T cells and B cells appear to coincide with induction of specific chemokine mRNAs in Mtb-infected murine lung (Figure 2b). The coordinated expression of chemokines likely plays an important role in granuloma formation. Although granulomas seen in the mouse model of TB are not organized similar to granulomas seen in Mtb-infected humans and NHPs, the use of novel chemokine deficient mice in the mouse model of TB has been pivotal

Table 1: Chemokine Induction in Mtb-infected mice.

Fold induction of chemokine and chemokine receptor genes in the murine lung were quantified using microarray at day 12 (D12), day (D15) and day 21 (D21) following *M. tuberculosis* infection [80]. Table was adapted from [127].

Symbol	Gene Name	D12		D15		D21	
		Fc	FDR	FC	FDR	FC	FDR
CXCL1	chemokine (C-X-C motif) ligand 1	**1.70**	0.04	**4.58**	0.00	**118.27**	0.00
CXCL2	chemokine (C-X-C motif) ligand 2	1.10	0.70	**2.06**	0.02	**29.73**	0.00
CXCL3	chemokine (C-X-C motif) ligand 3	**2.73**	0.00	**3.86**	0.00	**36.53**	0.00
CXCL5	chemokine (C-X-C motif) ligand 5	**19.07**	0.00	**9.47**	0.00	**192.71**	0.00
CXCL9	chemokine (C-X-C motif) ligand 9	**2.78**	0.00	**93.97**	0.00	**2134.40**	0.00
CXCL10	chemokine (C-X-C motif) ligand 10	1.39	0.13	**20.54**	0.00	**357.38**	0.00
CXCL11	chemokine (C-X-C motif) ligand 11	1.00	1.38	**1.99**	0.02	**86.67**	0.00
CXCL12	chemokine (C-X-C motif) ligand 12	1.05	1.11	1.16	0.64	**2.09**	0.05
CXCL13	chemokine (C-X-C motif) ligand 13	1.40	0.16	1.43	0.19	**42.89**	0.00
CXCL16	chemokine (C-X-C motif) ligand 16	-1.25	0.90	-1.07	1.15	**3.82**	0.01
CXCL17	chemokine (C-X-C motif) ligand 17	-1.02	1.34	-1.01	1.17	**1.99**	0.05
CCL1	chemokine (C-C motif) ligand 1	1.00	1.09	1.05	1.33	**4.21**	0.02
CCL2	chemokine (C-C motif) ligand 2	1.51	0.07	**4.45**	0.00	**232.36**	0.00
CCL3	chemokine (C-C motif) ligand 3	-1.28	0.74	1.33	0.29	**61.40**	0.00
CCL4	chemokine (C-C motif) ligand 4	1.29	0.21	2.04	0.01	**147.32**	0.00
CCL5	chemokine (C-C motif) ligand 5	-1.30	0.63	1.24	0.45	**8.95**	0.00
CCL7	chemokine (C-C motif) ligand 7	1.12	0.59	**2.58**	0.01	**108.37**	0.00
CCL8	chemokine (C-C motif) ligand 8	**1.82**	0.02	3.97	0.00	**61.61**	0.00
CCL9	chemokine (C-C motif) ligand 9	1.20	0.51	1.41	0.14	**3.76**	0.01
CCL11	chemokine (C-C motif) ligand 11	-1.24	0.68	1.60	0.09	**2.06**	0.07
CCL12	chemokine (C-C motif) ligand 12	**2.81**	0.00	**3.13**	0.00	**69.50**	0.00
CCL17	chemokine (C-C motif) ligand 17	**1.72**	0.04	1.52	0.12	1.77	0.11
CCL19	chemokine (C-C motif) ligand 19	-1.44	0.45	1.41	0.25	**11.09**	0.00
CCL20	chemokine (C-C motif) ligand 20	1.00	1.09	1.00	1.09	**75.02**	0.00
CCL21A	chemokine (C-C motif) ligand 21a	-1.07	1.15	1.04	1.03	-1.11	1.20
CCL22	chemokine (C-C motif) ligand 22	1.44	0.10	1.31	0.35	**3.48**	0.01

in documenting the individual, as well as the overlapping, and redundant roles of chemokines and their ligands in Mtb infection. The specific roles of inducible and homeostatic chemokines in Mtb infection will be further discussed.

1.4.1 Inflammatory Chemokines in Mtb Infection

Cellular recruitment in response to pulmonary inflammation requires the upregulation of cytokines, the expression of adhesion molecules on the cell surface and endothelium, and the production of inducible chemokines. The majority of identified chemokines are inducible, and

are expressed in response to inflammation. During Mtb infection, a number of inflammatory chemokines are produced, namely CXCR1/2 (neutrophil recruiter), CXCR3 (lymphocyte recruiter), and CCR2/5 (lymphocyte and myeloid recruiter) ligands (Table 1) [80]. In in vitro cultures, these chemokines are produced from Mtb infected macrophages in as little as 2 hours with peak expression within ~24 hours post infection [128-130]. However, in vivo detection of pulmonary chemokines in the mouse is delayed until days 12-21 post infection (Table 1) [80]. The most highly discussed chemokines in Mtb, IFNγ inducible chemokines CXCL9/10/11, are thought to be important for the recruitment of Th1 cells to the Mtb infected lung and will be further discussed.

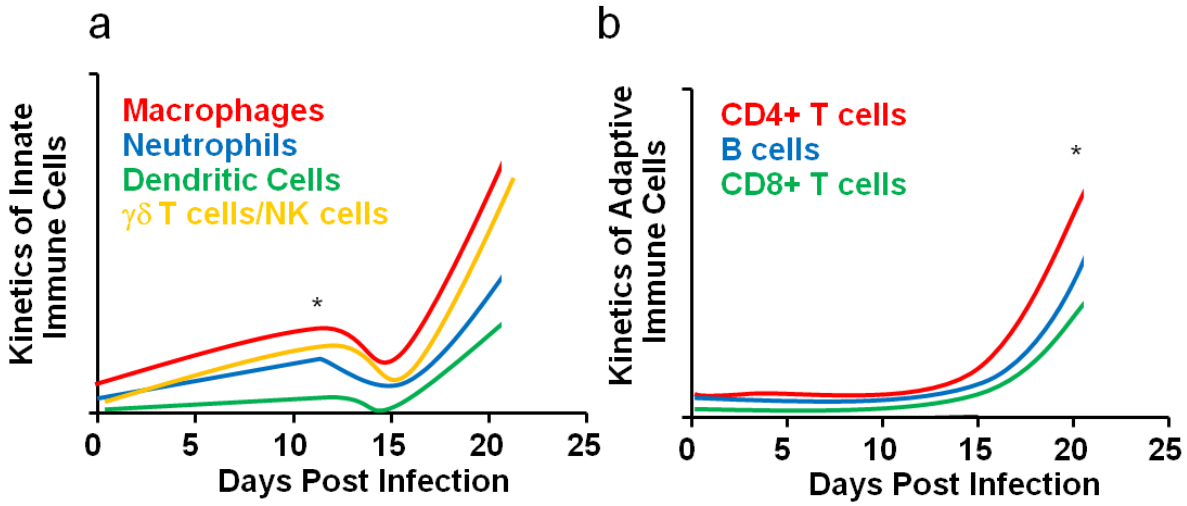

Figure 2: Timing of accumulation of immune cells in the murine lung following Mtb infection.

Innate cells such as neutrophils, γδ T cells, DCs, and macrophages likely respond to early induction of chemokines and accumulate in the Mtb-infected lung (a). Following initiation of adaptive immune responses, cytokine-producing $CD4^+$, $CD8^+$ T cells as well as B cells then respond to appropriate chemokines induced in the lung and accumulate to mount protective immune responses against Mtb infection (b). *Indicates the timing of arrival of different immune cells to the lung following Mtb infection determined by flow cytometry,.

is an inflammatory chemokine receptor that is upregulated on naïve T cells rapidly following DC-induced T cell activation [131]. T-bet, the Th1 master transcription factor directly transactivates the CXCR3 promoter in Th1 cells and CTL cells to mediate migration into sites of inflammation [132]. CXCR3 is highly expressed by $CD4^+$ T helper type 1 cells and $CD8^+$ T cells, it is also detected on B cells, NK and NKT cells and results in migration towards three chemokines namely, CXCL9/MIG, CXCL10/IP-10, and CXCL11/ITAC [132]. CXCL9-11 expression is induced during Mtb infection (Table 1) and expression is localized within TB granulomas [133-134]. Further, CXCR3 expressing T cells are found in Mtb-infected NHP lungs and BAL [134] as well as Mtb-infected mouse lungs [135]. To investigate the mechanistic role of CXCR3 in response to Mtb infection, *Cxcr3-/-* mice on the C57BL/6 background were infected with low doses of aerosolized Mtb, but did not show any defects in bacterial control [136]. However, tubercle granuloma formation was impaired with associated decrease in the number, size, and density of granulomas in the lung [136]. Furthermore, higher expression of CXCL9 was found to differentiate disease severity in human TB patients [137-138] and a new potential protective SNP in the promoter of CXCL10 has been reported [139], suggesting that despite bacterial control in the absence of *Cxcr3* in murine models, CXCR3 receptor and its ligands may play important roles in human TB.

1.4.2 Homeostatic Chemokines in Mtb

Constitutive expression of "homeostatic" chemokines accounts for the accumulation of naïve T cells, B cells and resident macrophages in SLOs, as well as for the recruitment of dendritic cells following antigen exposure. Four chemokines are responsible for SLO organization, specifically CCL19, CCL21, CXCL12, and CXCL13. Interestingly, CCL19, CXCL12 and CXCL13 mRNAs

are upregulated in the lung at D21 during an Mtb infection (Table 1) and play a critical role in protective immunity.

Migration of T cells and DCs to the paracortical T-cell zones of secondary lymphoid organs is dependent upon the expression of the homeostatic chemokines CCL19 and CCL21. Naïve and central memory T cells, as well as DCs express CCR7 and respond to this chemokine gradient [140-141] and the expression of these chemokines are required for effective T-cell priming [142-144]. Accordingly, following Mtb pulmonary infection, DCs upregulate CCR7 [45, 145-146] and migrate to the draining lymph node [45, 49].Consistent with this role for CCR7 in DC migration, *Ccr7* deficient mice exhibit impaired DC migration to the mediastinal lymph node, resulting in delayed dissemination of Mtb to peripheral organs [147-148], and delayed activation of T cells [148]. Similarly, mice that have a genetic mutation leading to the loss of CCL19 and CCL21ser expression (*plt/plt* mutant mice) have defects in DC migration to the DLN [49] and decreased induction of T cells producing IFNγ in the lymphoid organs [24]. The delayed generation of IFNγ-producing activated T cells in the lymphoid organs correlated with delayed accumulation of IFNγ producing T cells in Mtb-infected lungs, and resulted in increased susceptibility to Mtb infection [24]. These data together support a role for CCL19 and CCL21 expression in the lymphoid organs to mediate optimal DC migration and T cell priming during Mtb pulmonary infection.

CXCL13, the only ligand for CXCR5, is a homeostatic chemokine expressed constitutively in secondary lymphoid organs [149] and produced by follicular dendritic cells and stromal cells for the specific localization of B cells and Tfh cells within the lymphoid follicle [150-154]. Recently, CXCL13 expression has been detected in non lymphoid tissues and associated with inflammation seen in conditions such as chronic obstructive pulmonary disease, rheumatoid arthritis and TB [11, 155-156]. CXCL13 is upregulated during an Mtb infection (Table 1) [80] and

expression is localized specifically within lymphoid follicles containing B cells adjacent to the granuloma [24, 147, 157]. In the absence of *Cxcl13*, integrity of the B cell follicle and formation of the granuloma is severally compromised [24]. Furthermore, B cells isolated from Mtb infected murine lungs expressed CXCR5 and migrated to CXCL13 in vitro [77], suggesting that both T cells and B cells expressing CXCR5 may be important during TB. Accordingly, mice deficient in CXCL13 are more susceptible to Mtb low dose aerosol infection, due to defects in correct T cell localization within the TB granulomas and leading to decreased macrophage activation and mycobacterial control [24]. Future research will focus on delineating the specific role of CXCR5 on T cells and B cells in formation of lymphoid structure formation within TB granulomas and their specific role in mycobacterial control.

1.5 ECTOPIC LYMPHOID FOLLICLES

Ectopic lymphoid follicles, also known as ectopic lymphoid organs (ELOs), were first identified as permanent structures seen in rabbits, rats, and guinea pigs [158]. Unlike conventional secondary lymphoid organs (SLOs), ELOs are not preprogrammed and develop after birth. ELOs can be found in nearly every organ in the body and are characterized based on location as gut associated lymphoid tissue (GALT), bronchus associated lymphoid tissue (BALT), nasal associated lymphoid tissue (NALT), mucosa associated lymphoid tissue (MALT) and conjunctiva associated lymphoid tissue (CALT). In humans and mice, little evidence of BALT formation can be found in the lung, but in response to antigenic stimulation, mice and humans can develop lymphoid follicles throughout the lung, known as inducible bronchus associated lymphoid tissues (iBALT) [158-159]. They differ from BALT in that they do not always form near airways and can be

found in the parenchyma. Further, BALT contains an overlying epithelial layer and do not form in response to antigen. iBALT are reported to be induced during several inflammatory disease conditions of either autoimmune or infectious nature.

BALT was initially described more than 30 years ago as a dominantly lymphocytic aggregate found mainly in the upper bronchi [160-161]. Today, we compare these structures to SLOs with organized B cell follicles, separated T cell areas, macrophages, stromal cells, and follicular dendritic cells (FDCs) [159]. Follicular dendritic cells have a similar function in BALT as they do in SLOs presenting antigen and providing co-stimulatory signals to B cells for activation and successive class-switching in the germinal center [162-164]. B cells in BALT can develop into plasma cells as IgG cells are detected under some inflammatory conditions; however, the majority of cells are $IgM^{lo}IgD^{hi}$ [165-166]. Further, T cells are also known to interact with antigen-loaded DCs and undergo multiple rounds of proliferation in BALT [167]. Lymphocytes enter through high endothelial venules (HEV) that develop and express peripheral lymph node addressin (PNAd) and vascular cell adhesion molecule 1 (VCAM-1) rather than mucosal cell addressin cell adhesion molecule 1 (MAdCAM-1) used in Peyer's patches [168-169]. The inflammatory conditions required for formation of iBALT will be further discussed.

1.5.1 Chemokine and Cytokine Induced Formation

iBALT only appear in the lung after prolonged periods of antigen stimulation in response to infection or autoimmune disease disorders [170]. It is clear iBALT is not a constitutive structure in the lungs of humans and mice and forms in a process called lymphoid neogenesis, which is thought to utilize similar mechanisms to SLO development [168]. Homeostatic chemokines are an important component of lymphoid organ formation during embryogenesis and are also detected

within iBALT [170]. The increased expression of CXCL13, CCL19, and CCL21 are essential for SLO development and immunity as mice deficient in *Cxcl13* or *Cxcl19* are lacking numerous lymph nodes and have disorganized splenic architecture [171-172]. CXCL13 is primarily produced by FDCs and other reticular stromal cells in SLOs, which allow the recruitment of CXCR5+ cells to the B cell follicular zone [173-174]. CXCL13 is a unique chemokine in that it is not redundant and will only recruit cells expressing CXCR5, namely B cells and Tfh cells [174]. In addition to CCL21 and lymphotoxin (LT)-α expression, ectopic expression of CXCL13 is known to lead directly to lymphoid neogenesis [171]. In contrast, CCL19 and CCL21 are produced or expressed on HEVs, DCs, and stromal cells in the T cell zone recruiting naïve T cells and activated DCs expressing CCR7 [172]. These chemokines are thought to act similarly in iBALT to recruit and compartmentalize cells although development and structure appear to differ depending upon the source of inflammation.

Although the induced expression of homeostatic chemokines can be independent of cytokine production in the formation of iBALT, the majority of chemokines expressed in ELOs is attributable to TNF family members, specifically LT-α/β, TNF-α, and LIGHT [175]. In addition to the TNF family members, IL-17 has also been linked to iBALT development by inducing CXCL13 and CCL19 expression [176]. The ELO developmental process is thought be initiated similar to SLOs by Lymphoid Tissue inducer (LTi) cells that drive the differentiation of mesenchymal cells into stromal cells through engagement of the surface receptor, LTβR [177]. These stromal cells then produce the homeostatic chemokines necessary to recruit and organize lymphocytes [172]. However, recent evidence suggests initiation of ectopic lymphoid follicles does not parallel conventional lymph nodes. In response to LPS induced inflammation, iBALT develops independent of LTi cells and instead requires the transcription factors RORγt and Id2

driven by IL-17 producing CD4+ T cells [176]. IL-17 promoted CXCL13 expression, independent of LT-α, which was critical for lymphoid follicle formation [114]. Despite the similarities between SLOs and ELOs, the early events in lymphoid follicle development and maintenance remain relatively unknown and require further investigation.

1.5.2 ELOs in Autoimmune Inflammation

Ectopic lymphoid organs often develop in autoimmune disorders [170]. Autoreactive T and B cells are associated with the development of iBALT [178] that typically is seen in the immune targeted organ in such diseases as Sjogren's syndrome [123, 179-180], rheumatoid arthritis [123, 181], multiple sclerosis [182-183], and diabetes [184-185]. Immune targeted organs include the exocrine glands [186-188], joints and lungs [189-190], central nervous system [182-183], and the pancreas, respectively [191]. Typical ELO formation contained FDCs, CD4+ and CD8+ T cells, CD20+ B cells, CD38+ plasma cells, and CD68+ macrophages with reticular networks [186-188]. Further, lymphoid aggregates were found to contain proliferating Ki-67-expressing cells and HEVs that express PNAd similar to SLOs [123, 183, 188-189, 191]. In RA, CXCL13 has been shown to be produced by FDCs and hematopoietic cells such as monocyte-derived macrophages (CD68+) that recruit CXCR5+ T and B cells [192]. Further, induction of homeostatic chemokines is attributed to the cytokines LT-α and LT-β [193–194], and also to LIGHT in diabetes[184, 191] .

It is interesting to note that disease severity was associated with ectopic lymphoid follicle formation as patients containing highly developed germinal centers had more severe complications [186]. In Sjogren's syndrome, patients containing ectopic lymphoid follicles in exocrine glands showed lower saliva production, indicating ELOs contribute to impairment of salivary gland function [188, 195-196]. Rheumatoid arthritis patients with ELOs were found to have

higher plasma cells in the synovium, suggesting lymphoid follicles may contribute to autoreactive B cell generation [197]. Further, in multiple sclerosis patients, ELOs were associated with severe pathology in the cerebral cortex and aggressive clinical progression [182]. Formation of these lymphoid aggregates was attributed to the expression of the homeostatic chemokines CXCL13, CCL21, and CCL19 and studies in gene deficient mice indicate that absence of these homeostatic chemokines disrupt ELO development [184, 191, 193-194, 198-200]. However, disruption of ELOs did not always ameliorate disease [200].

These studies demonstrate that ELO formation in autoimmune disease correlates with homeostatic chemokine expression, autoantibody production, and clinical symptoms. Despite the presence of ELOs in autoimmunity, it remains uncertain the role these structures play in disease. It appears ectopic lymphoid aggregates promote autoimmunity in some diseases, but may be a result of the autoimmunity itself in others. Studies with transgenic mice expressing CXCL13, CCL19, and CCL21 generate ectopic lymphoid follicles, but do not develop autoimmunity indicating that additional mechanisms are required for a destructive immune response [171, 201-203]. It is evident that a greater understanding of the cellular and molecular mechanisms in autoimmunity is required to determine the function of ELOs.

1.5.3 ELOs in Infectious Disease

Numerous infections are known to trigger the development of ectopic lymphoid tissues including *Helicobacter pylori* in the stomach [204-207], *Borrelia burgdorferi* in the skin [208-210], and *M. tuberculosis*, *Klebsiella pneumonia*, *Pseudomonas aeruginosa*, *Haemophilus influenzae* in the lung [211] among other infections [212-215]. BALT formation can also be seen in other non-infectious lung diseases such as chronic obstructive pulmonary disease (COPD) [156, 216], pulmonary fibrosis

[217], and hypersensitivity pneumonitis [211, 218]. Despite the prevalence of lymphoid follicles in infectious disease, little remains known about the function of ELOs. The current understanding of ELO formation and function in infectious disease will be further discussed.

H. pylori is a prevalent infection in humans that colonizes the gastric epithelium causing severe inflammation of the stomach lining that can be acute or chronic, but the majority of cases persist for years or life. Chemokines promoting neutrophil recruitment are highly elevated as the disease that is characterized by dense infiltration of neutrophils. However, several homeostatic chemokines, such as CCL21 and CXCL13, are also upregulated in the mucosa and lead to accumulation of lymphoid cells [204-207, 219]. In cases of gastritis in both humans and mice, it is common for ectopic lymphoid follicles expressing homeostatic chemokines, CD3+ T cells, and B cells, and prominent germinal center structures containing HEV expressing PNAd and MAdCAM to form [220]. Specifically, in humans 85% of *H. pylori* positive patients contained lymphoid follicles, which were strongly associated with a higher grade of severity [207]. Futhermore, elevated levels of CXCL13 in gastric biopsies correlated with a higher degree of gastric inflammation and higher bacterial burden suggesting ELOs may contribute to pathology [221]. Using a mouse model of chronic *H. pylori*, *Cxcr5* deficient mice, which did not form organized ectopic lymphoid follicles, exhibited decreased Th17 immune responses and decreased IgA and IgG responses by B cells, but unaltered Th1 cellular responses [126]. In addition, bacterial colonization was similar between wild type mice and *Cxcr5* deficient mice suggesting ectopic lymphoid formation does not contribute to protective immunity against *H. pylori* [126].

ELOs appear to contribute to immunity in response to influenza in mice. Using Influenza A/PR8/34 infection, mice deficient in SLOs were found to develop ELOs locally in the lung [168]. Follicles consistently contained FDCs, organized GC B cells and $CD8^+$ T cells, $CD4^+$ T cells, and

dendritic cells in interfollicular areas [168]. As expected, CXCL13, CCL19 and CCL21 expression co-localized with ectopic cells, however, induction was independent of LT-α and TNF-α [124, 168]. Interestingly, the loss of CXCL13 did not impact ELO formation in influenza infected mice, but was instead dependent upon CCL19 and CCL21 expression [124]. Importantly, SLO deficient mice infected with influenza had delayed viral clearance, but enhanced survival [168]. In addition, SLO deficient mice were capable of surviving higher doses of the virus suggesting ELOs are protective in influenza and perhaps less pathogenic than immune responses originating in the lymph node [168]. Consistent with these data, Wiley et al. induced ELO formation asymptomatically in mice using nanoparticles and found pre-existing ELOs enhanced resolution of influenza suggesting ELOs could be a future preventative target [222].

Lymphoid aggregates have been detected in the lungs of Mtb infected humans [11, 79], NHPs [78], and mice [24, 147]. Further, organized lymphoid aggregates in humans were associated with latent TB [223]. Typical follicles contained $CD4^+$ T cells, $CD8^+$ T cells, and B cells suggesting these may be ELOs [11]. However, detection of $CXCR5^+$ T cells and GC B cells has not been assessed. The homeostatic chemokines CXCL13 and CCL19, but not CCL21, were found to be upregulated in the lungs of Mtb-infected mice [24]. Further, *cxcl13-/-* mice and *plt/plt* mice were unable to control Mtb infection with higher pulmonary bacterial burden compared to wild type mice [24]. Higher susceptibility in *plt/plt* mice and *Ccr7-/-* mice was contributed to defects in T cell priming as DCs were unable to migrate to draining lymph nodes to present antigen [24, 148]. However, *Cxcl13* deficient mice were unable to organize B cell aggregates and had decreased activated macrophages [24]. These data suggest that lymphoid aggregates found in pulmonary TB are likely ELOs that may contribute to protective immunity.

The study of ELO function in infectious disease is a newly emerging field. Both CXCL13 and CCL19/CCL21 appear to contribute to initiation of ELO formation and this can be dependent or independent of LT-α and TNF-α. The contribution of ELOs to protection or pathology differ between disease making further investigation critical in elucidating the mechanism of action.

2.0 ECTOPIC LYMPHOID FOLLICLES IN *M. TUBERCULOSIS* INFECTION

2.1 ABSTRACT

One third of the world's population is infected with *M. tuberculosis.* Although most infected people remain asymptomatic, they have a 10% lifetime risk of developing active TB. Thus, the current challenge is to identify immune parameters that distinguish individuals with latent TB from those with active TB. A hallmark of pulmonary TB in both humans and experimentally infected animals is the formation of the granuloma that contains Mtb-infected macrophages. The structural differences between active TB and latent TB granulomas can differentiate important immune components required for protective immune control. Using human and experimental models, we demonstrated that organized ectopic lymphoid structures containing CXCR5+ T cells, follicular dendritic cells, and germinal center B cells form in the Mtb-infected lung. Importantly, in the non-human primate model we show that ectopic lymphoid structures are correlated with immune control. Further, the Mtb mouse model forms follicles similar to Mtb-infected humans suggesting the mouse model is a valuable tool for addressing the mechanism of ectopic lymphoid organ development and protection. Therefore, our data demonstrate a critical function for ectopic lymphoid follicles in control of Mtb infection.

2.2 INTRODUCTION

M. tuberculosis, is an intracellular pathogen that causes the disease tuberculosis, and infects about 2 billion people worldwide. Proper control of Mtb requires the colocalization of adaptive immune cells with Mtb-infected macrophages in the lung forming a granuloma, which acts as a physical barrier and promotes macrophage activation for bacterial killing [224]. Despite the presence of the granuloma in active TB, these individuals are unable to control bacterial growth suggesting differences exist between latent and active TB granulomas. The presence of B cell aggregates has long been documented in human, NHP, and mouse granulomas [11, 24, 78, 223]. In humans, B cell clusters are found in the peripheral rim of the granuloma and contain activated $CD4^+$ T cells, $CD8^+$ T cells, $CD20^+$ B cells and antigen primed $CD68^+$ monocytes/macrophages [11]. Distinct vascularization and elevated proliferation activity in lymphoid aggregates was also associated with latent TB in humans [223]. Mtb infection in cynomologus macaques identified B cell aggregates within the granuloma during primary infection with $CD3^+$ T cells, but no $CD138^+$ plasma cells were detected [78]. Further, B cells expressed higher levels of HLA-DR in the draining lymph node of macaques compared with peripheral lymph nodes suggesting B cells in the lung are activated although this was not specifically shown in lymphoid aggregates [78]. Chronic Mtb infection in the mouse model triggers formation of pulmonary lymphoid aggregates within the granuloma associated with the expression of CXCL13, which is typically expressed in SLOs [24, 147]. Mice deficient of *Cxcl13* are more susceptible to Mtb infection with higher bacterial burden in the lung and are unable to form B cell lymphoid aggregates [24]. These data suggest that B cell follicles within the lung likely form ectopic lymphoid organs that are required for immune control. In the current study, we show that B cell aggregates express the markers of bona fide ectopic lymphoid follicles containing follicular dendritic cells, $CXCR5^+$ T cells, and germinal

center B cells that co-localize with the homeostatic chemokine CXCL13 in the granuloma of human, NHP, and mouse Mtb-infected lungs. Importantly, in NHPs that develop latent infection, we identified the significant association of ELOs with immune control.

2.3 MATERIALS AND METHODS

2.3.1 Human Tissue Samples and Patient Diagnosis

Archival paraffin samples of human lung biopsies with diagnosis of TB were collected on a protocol approved by the Ethics Committee of the Instituto Nacional de Enfermedades Respiratorias and the Ethics Committee of the American British Cowdray Medical Center, Mexico City (Table 2). All subjects were of similar socioeconomic status and unrelated to the third generation as determined by a questionnaire. TB cases had symptoms (weight loss >10 kg, cough, fever, night sweats for >1 mo, or cervical or axillary lymphadenopathy) and chest radiographic findings consistent with recent pulmonary TB, a positive sputum acid-fast smear and culture confirmed for Mtb. Once the diagnostic protocol was completed, patients were discharged and proper treatment was indicated.

Table 2: Active TB patient description.

A-TB patients lung samples were analyzed for markers of ectopic lymphoid tissues including B cell lymphoid follicles, $CXCR5^+$ T cells and FDC networks.

Age	Sex	Comorbilities	Duration of symptoms prior to diagnosis	Chest x-ray /HRCT	Ectopic lymphoid structures	Final Diagnosis
64	F	Systemic Arterial Hypertension	2 months	Ground-glass opacification, Cavitation in the right upper lobe	Negative	Autopsy: Tuberculosis, Massive pulmonary hemorrhage
77	F	Diabetes Mellitus, Obesity	6 months	Bilateral, multiple centrilobular nodules	Positive	Autopsy: Acute Miliary TB, rapidly progressive; Septic Shock Hyperosmolar Coma
31	M	None	3 months	Bilateral, multiple centrilobular nodules	Positive	Active Tuberculosis
33	F	HIV	----------	----------	Negative	Tuberculosis, Massive Inflammatory Infiltrates
69	M	Bleeding in Digestive Tract	----------	----------	Negative	Tuberculosis, Tumor in Upper Right Lobe
44	F	Gastric Adenocarcinoma	----------	----------	Negative	Biopsy lower right lobe: Tuberculosis
79	F	None	----------	Pulmonary Nodules	Negative	Biopsy of the middle portion of the right lung: Tuberculosis
63	F	None	----------	Nodule detected in left lung	Negative	Tuberculosis

2.3.2 Mtb Infection in NHPs

Groups of non human primates (NHP) (Indian rhesus macaques) were used in this study at the Tulane National Primate Research Center as previously described following the recommendations of the Institutional Animal Care and Use Committee [225]. For L-TB, NHPs were infected with low dose of Mtb CDC1551 (200-500cfu) by the aerosol route [225]. Mtb exposure was confirmed by positive tuberculin skin test and PRIMAGAM, a quantiferon-type

IFNγ release assay specifically designed to confirm Mtb infection in NHPs. The NHPs did not exhibit any clinical signs of TB, as evident from normal body temperatures and weights, chest x-rays and serum levels of acute phase proteins [225]. For A-TB, NHPs were infected with high dose of Mtb CDC1551 via aerosol infection (~5000 cfu) [226]. Mtb exposure was confirmed by positive tuberculin skin test and PRIMAGAM and the NHPs exhibited clinical signs of TB, as evident from body temperatures, weights and chest x-rays [226].

2.3.3 Mtb Infection in Mice

C57BL/6 (B6) were purchased from The Jackson Laboratory, Bar Harbor, ME. Experimental mice were age-and sex-matched and used between the ages of 6-8 wks in accordance with University of Pittsburgh International Animal Care and Use Committee guidelines. Mtb strain H37Rv was cultured in Proskauer Beck medium containing 0.05% Tween 80 to mid-log phase and frozen in 1 ml aliquots at -70^{o}C. Animals were aerosol infected with ~100 CFU (low dose) of bacteria using a Glas-Col airborne infection system [227].

2.3.4 Morphometric Analysis and Immunofluoresence

Lungs from mice and NHPs were inflated with 10% neutral buffered formalin and embedded in paraffin. Lung sections were stained with H&E stain (Colorado Histo-Prep) and processed routinely for light microscopy. Formalin-fixed samples from TB patients were also used. For immunofluorescence, paraffin was removed from the formalin-fixed lung sections, washed with xylene, alcohol, and PBS. Antigens were unmasked using a DakoCytomation Target Retrieval Solution and were blocked with 5% (v/v) normal donkey serum and Fc block (5 μg/ml, 2.4G27).

Endogenous biotin was neutralized with avidin followed by biotin (Sigma-Aldrich). Murine sections were probed with goat anti-mouse CD3ε (M-20; Santa Cruz Biotechnology), rat anti-mouse B220 (RA3-6B2; BD Pharmingen), inducible NO Synthase (goat anti-mouse, M-19; Santa Cruz Biotechnology), CXCR5 (Biotin, rat anti-mouse CXCR5; BD Biosciences), and IgG (FITC-donkey anti-mouse IgG; Jackson Immunoresearch). Primary Abs were detected with secondary Ab conjugated to Alexa fluor 568 for CD3 (Alexa fluor 568, donkey anti-goat, Invitrogen). Donkey anti-rat Ab conjugated to Alexa Fluor 488 was used to visualize B220 (Molecular Probes). Some slides were incubated with PNA-FITC (SIGMA) and goat-anti PCNA (C-20, Santa Cruz Biotechnology). Rabbit anti-FITC, conjugated to alexa fluor 488 was used to amplify PNA signal (Molecular probes). To detect FDCs, slides were incubated with biotinylated, rat anti-mouse CD21-CD35 (CR2/CR1- Biolegend) and anti-follicular dendritic cell (FDCM-1, BD Pharmingen), followed by detection with SA-Alexa fluor 488 and donkey anti-rat conjugated to alexa fluor 488 (Molecular probes). CXCL13 production in infected lungs was detected with goat anti-mouse CXCL13 (R&D systems), followed by detection with donkey anti-goat-alexa fluor 568. Human and NHP tissues were probed with rabbit anti-human ICOS (ABCAM), FITC, mouse anti-human CXCR5 (clone 51505, R&D Systems), and goat anti-human CXCL13 (R&D Systems). Anti-CD3ε was further used to detect CD3 lymphocytes (clone M-20; Santa Cruz Biotechnology). For B cells, CD20 (Mouse anti-human CD20 (L26); ABCAM) and IgD (Ab-1; Lab Vision Corporation) were used with PCNA (Goat anti-PCNA (C-20); Santa Cruz Biotechnology) to detect germinal center B cells. Follicular dendritic cells in human germinal centers were further detected with anti-human CD21 (Clone 2G9; Lab Vision Corporation). Slow fade gold antifade with DAPI (Molecular Probes) was used to counterstain tissues and to detect nuclei. Images were obtained with a Zeiss Axioplan 2 microscope and were

recorded with a Zeiss AxioCam digital camera. Caudal lobes from four mice per group underwent morphometric analysis in a blinded manner using the Zeiss Axioplan microscope, which determines the area defined by the squared pixel value for each granuloma, B cell follicle and perivascular cuff as previously described [24].

2.3.5 CXCL13 In Situ Hybridization

Mouse CXCL13 cDNA was RT-PCR amplified with primers BFJ.mCXCL13_F1 (5'-GAACTCCACCTCCAGGCAGA-3') and BFJ.mCXCL13_R1 (5'-CTTTTGAGATGATAGTGGCT-3'). Human and macaque CXCL13 cDNA was RT-PCR amplified with primers (5'-AGACAGAATGAAGTTCATCT-3' and 5'-GTGGAAATATCAGCATCAGGG-3'). PCR products were ligated to the pGEM-T vector (Promega) and DNA sequenced. The pGEMT-CXCL13 plasmid was linearized by restriction digest. Gene-specific riboprobes were synthesized by in vitro transcription using a Maxiscript SP6/T7 kit (Ambion) and unincorporated nucleotides were removed using RNA Mini Quick Spin Columns (Roche). Paraffin embedded tissue specimens were pretreated as described [58], following deparaffinization in xylenes and rinsing in ethanol. In situ hybridization (ISH) with ^{35}S-labeled riboprobes was performed at 50^{o}C overnight as described [228], with 0.1M dithiothreitol included in the hybridization mix. Tissue sections were coated with NTB-2 emulsion (Kodak) and exposed at 10^{o}C for 10 days. The sections were counterstained with hematoxylin (Vector) and mounted with Permount (Fisher). Images were visualized using an Olympus BX41 microscope and captured using a SPOT RT3 digital camera (Diagnostics Instruments, Inc).

2.3.6 Statistics

Differences between the means of experimental groups were analyzed using the two tailed Student's t-test. Differences were considered significant when $p \leq 0.05$.

2.4 RESULTS

2.4.1 $CXCR5^+$ T cells accumulate within ectopic lymphoid structures of human TB granulomas

Normal human lungs do not exhibit appreciable accumulation of lymphocytes or inflammatory aggregates [155]. However, individuals with L-TB exhibit organized pulmonary lymphoid aggregates, while cellular aggregates were absent or less organized in lungs of individuals undergoing A-TB [223]. We found that lung sections from 25% of A-TB patients (Table 2) showed accumulation of lymphocytes with features of classic ectopic lymphoid structures (Figure 3), containing proliferating $PCNA^+$ GC B cells (Figure 3b), $CXCR5^+$ Tfh-like cells (Figure 3c) and $CD3^+$ T cells expressed ICOS (Figure 3d). CXCL13 protein (Figure 6e) and mRNA (Figure 3f, g) were also detected within lymphoid aggregates. $CD21^+$ follicular dendritic cells (FDCs) were also found within ELOs (Figure 3h). Localization of $CD3^+$ T cells expressing CXCR5 (Figure 3c) and numerous proliferating cell nuclear antigen (PCNA) expressing $CD20^+$ B cells inside compact B cell follicles (Figure 3b) colocalized with macrophages expressing CD68 (Figure 3i, j), suggesting these are bona fide ectopic lymphoid structures.

2.4.2 Ectopic lymphoid structures are associated with immune control during TB in the NHP model of Mtb infection

Since ectopic lymphoid structures were only seen in a minority of human A-TB granulomas analyzed, we hypothesized that generation of lymphoid structures may correlate with immune control, rather than active disease. Therefore, we characterized the presence of ectopic lymphoid structures in NHPs that were experimentally infected with aerosolized Mtb, in which similar to human infection, immune control results in L-TB and the absence of immune control results in

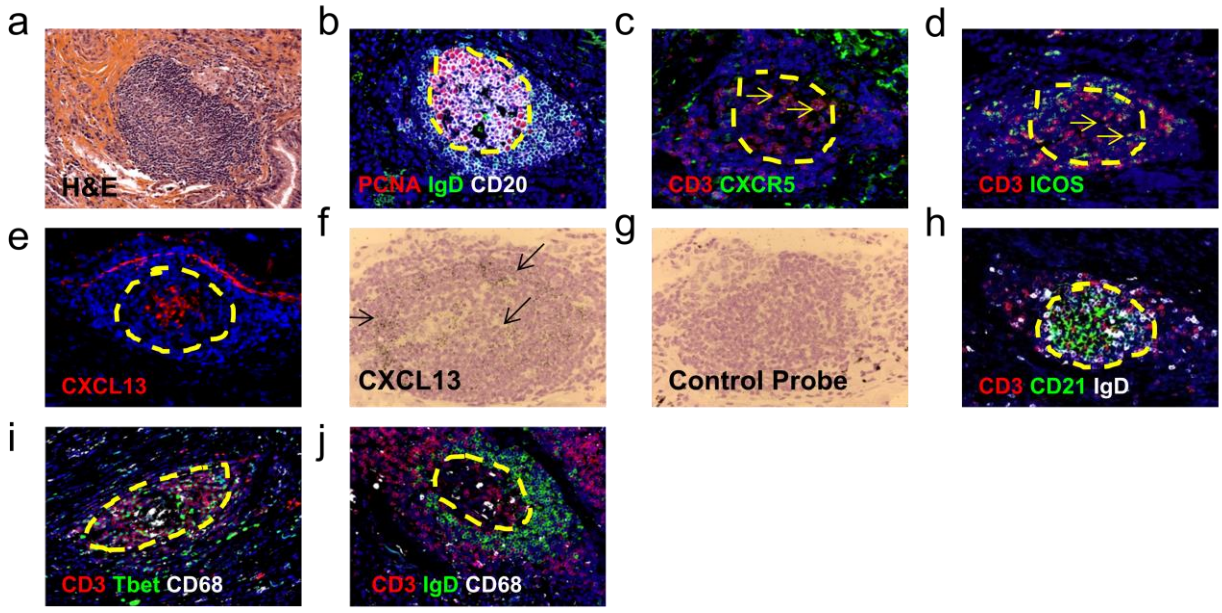

Figure 3: CXCR5$^+$ T cells accumulate within ectopic lymphoid structures of human TB granulomas.

Serial sections of FFPE lung biopsies from A-TB patients underwent H&E staining (a). Sections were analysed by immunofluorescence using antibodies specific to PCNA, IgD, and CD20 (b); CD3, CXCR5 (c); CD3, ICOS (d); CXCL13 (e); CD3, CD21, IgD (h); CD3, T-bet, CD68 (i); and CD3, IgD, and CD68 (j). All sections were counterstained with DAPI (blue). Germinal centers are outlined in yellow dashed lines and yellow arrows point to colocalization. CXCL13 mRNA was detected by ISH with a CXCL13 cRNA probe (f,g). Arrows point to strong areas of CXCL13 hybridization. Original magnification, x200; x600 (ISH).

A-TB [225]. In support of our hypothesis, 100% of lung sections from NHPs with L-TB had well-organized ectopic lymphoid structures (Figure 4a-top panel, Table 3) with distinct B cell follicles containing proliferating $CD20^+$ B cells, $CXCR5^+$ T cells and $CD21^+$ FDC networks (Figure 4b-top panel). In contrast, in NHPs with A-TB, only 46% of lung samples contained ectopic lymphoid structures (Figure 4a-lower panel, Table 3) which were smaller, less organized and diffuse. Furthermore, only 33% of samples from NHPs with A-TB contained proliferating $CD20^+$ B cells, $CD21^+$ FDC networks and $CXCR5^+$ T cells (Figure 4b-lower panel, Table 3).

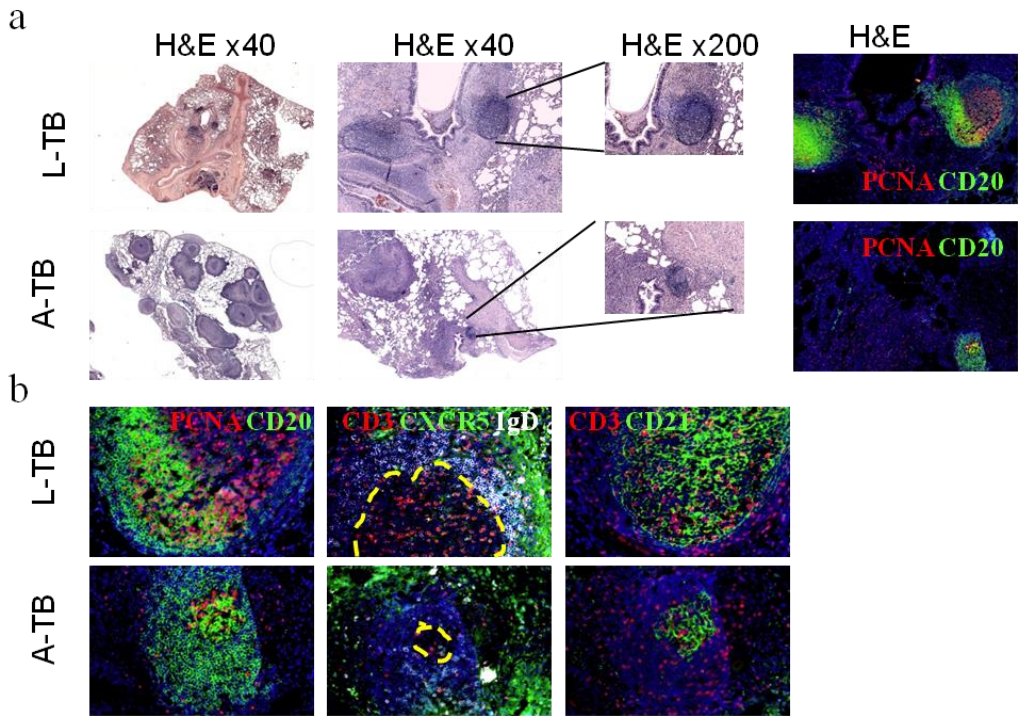

Figure 4: NHPs infected with Mtb contain ectopic lymphoid follicles.

NHPs aerosol infected with Mtb CDC1551 exhibited either L-TB or A-TB as described in Materials and Methods. Thirteen weeks after infection or at necropsy, lung FFPE serial sections were stained with H&E (a) or with antibodies specific for PCNA, CD20 (a,b); CD3, IgD CXCR5 (b); and CD3, CD21 (b). All sections were counterstained with DAPI (blue). GC, containing large, proliferating B blasts (PCNA+CD20+) is outlines in dashed yellow lines. The images shown are from a typical representative section. Original magnification, x200, unless otherwise indicated. The data represent the mean (±SD) of values from 6-15 NHPs.

Table 3: Ectopic lymphoid structures are associated with latent rather than active disease during TB in NHP Mtb infection model.

Description of frequency of NHPs with L-TB and A-TB that exhibited ectopic lymphoid structures and contained B cell follicles, proliferating B cells, $CXCR5^+$ T cells and FDC networks.

	Lymphoid follicle structures	B cell follicles	PCNA+CD20+ cells/ $CXCR5^+$ T cells	CD21+ FDC network
L-TB (n=15)	100%	100%	75%	75%
A-TB (n=13)	46%	46%	33%	33%

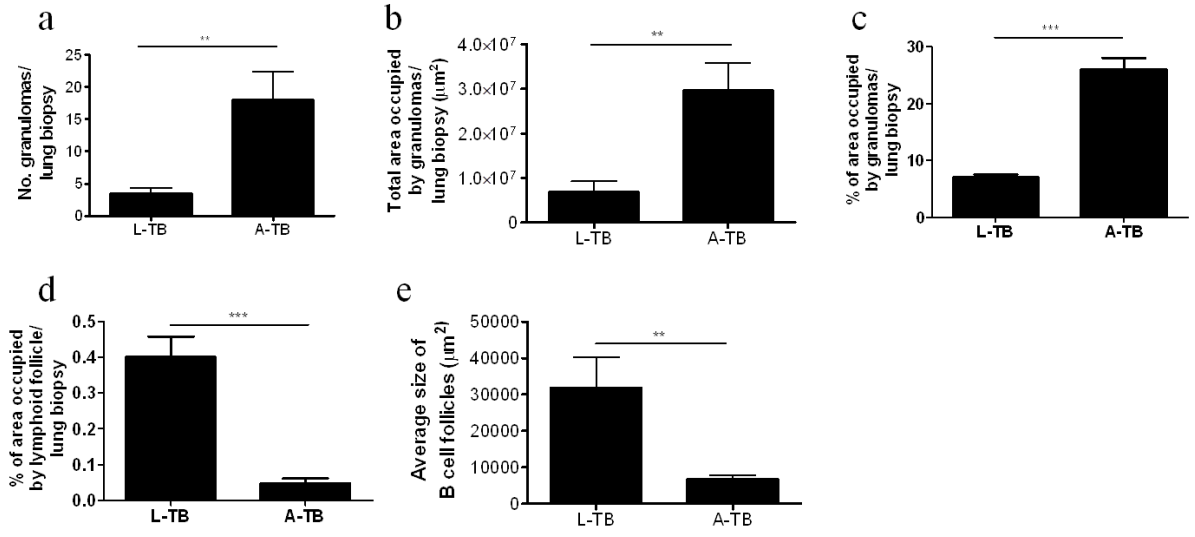

Figure 5: Ectopic lymphoid structures are associated with immune control during TB in NHP model of Mtb infection.

NHPs were aerosol infected and sacrificed as mentioned in Figure 4. Lung FFPE serial sections were stained with H&E or with antibodies specific for PCNA or CD20. The number of granulomas (a), total area occupied by granulomas (b), percentage of granuloma area occupied per biopsy (c), and average size (d) and percentage of area occupied by B cell lymphoid follicles (e) were determined with the Zeiss Axioplan microscope. The data represents the mean (±SD) of values from 6-15 NHPs. **p=0.005, ***p=0.0005

Uncontrolled disease was also evident in NHPs with A-TB as large number of necrotic granulomas occupied much of the total lung area (Figure 5a,b,c); despite this, lungs from NHPs with L-TB had significantly larger B cell follicles, which occupied a significantly larger area of the lung biopsy (Figure 5d,e), contrasting with smaller B cell follicles detected in NHPs with A-TB (Figure 5d,e). These data demonstrate that in NHPs, generation of well organized lymphoid structures containing $CXCR5^+$ T cells and B cell follicles is associated with immune control in L-TB, while loss of immune control during A-TB is associated with absent or loosely organized lymphoid aggregates.

2.4.3 $CXCR5^+$ T cells localize within ectopic lymphoid follicles in murine TB granulomas

Since $CXCR5^+$ T cells were associated with immune control, we next addressed the role of $CD4^+$ $CXCR5^+$ T cells in a well-established mouse model of TB, in which effective host immunity results in chronic infection. Although murine TB granulomas do not demonstrate all the characteristics of human TB granulomas [8], murine granulomas also form organized lymphoid structures (Figure 6a) containing CXCR5 expressing T cells ($CD3^+$ $CXCR5^+$) (Figure 6b) and $B220^+$ B cells (Figure 6c) that bound peanut agglutinin (Figure 6d) and contained complex FDC networks (Figure 6e,f). In addition, CXCL13 protein (Figure 6e,f) and CXCL13 mRNA expression was detected inside lymphoid structures (Figure 7a) and expression increased over the course of infection (Figure 7b).

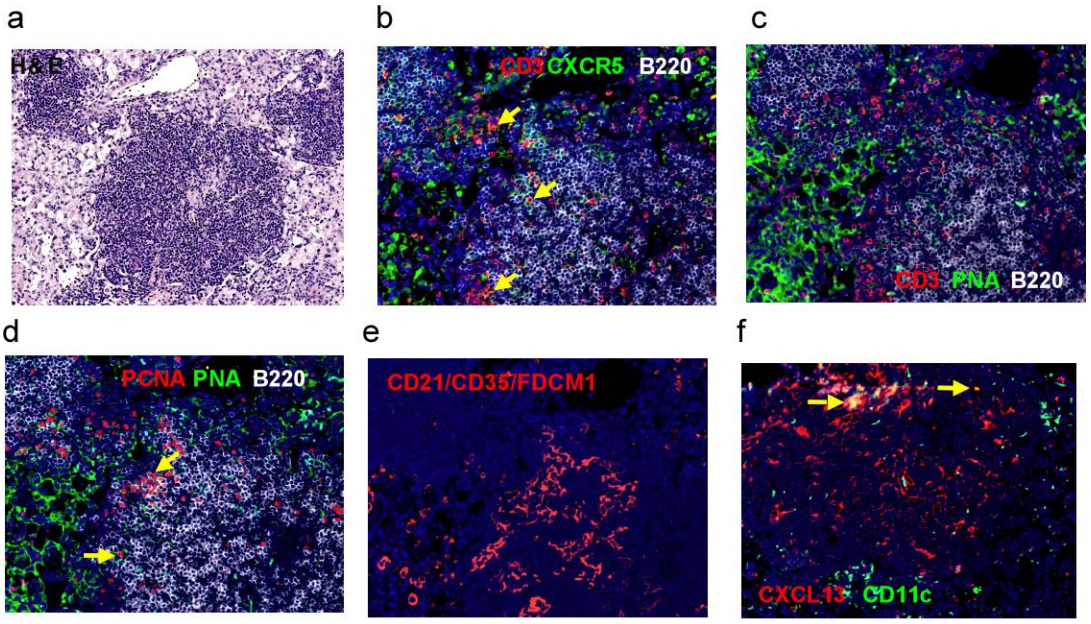

Figure 6: CXCR5$^+$ T cells localize within ectopic lymphoid follicles in murine TB granulomas

B6 mice were aerosol infected with ~100 cfu Mtb H37Rv and on day 50 post infection, FFPE serial sections were stained with H&E (a) or analyzed by immunofluorescence for CD3, CXCR5, B220 (b); CD3, PNA, B220 (c); PCNA, PNA, B220 (d); CD21-CD35-FDCM1; CD11c, CXCL13 (f). All sections were counterstained with DAPI (blue). Yellow arrows point to CD3+ CXCR5+ T cells (a), PCNA+B220+ B cells (d) or CXCL13+CD11c+ cells (f). Original Magnification, 200X. One of two or more experiments shown.

Germinal center B cells (GC B cells) were identified as large, proliferating PCNA$^+$B220$^+$ blasts

2.5 DISCUSSION

Ninety percent of all *M. tuberculosis* infected individuals develop an immune response sufficient to control and contain the infection within pulmonary granulomas [229-230]. Containment is highly effective as most individuals go their lifetime without ever developing A-TB. There is a general consensus that the architecture of the granuloma contains Mtb-infected macrophages and multinucleated giant cells at the core with CD4$^+$ T cells, CD8$^+$ T cells, neutrophils, NK cells, and

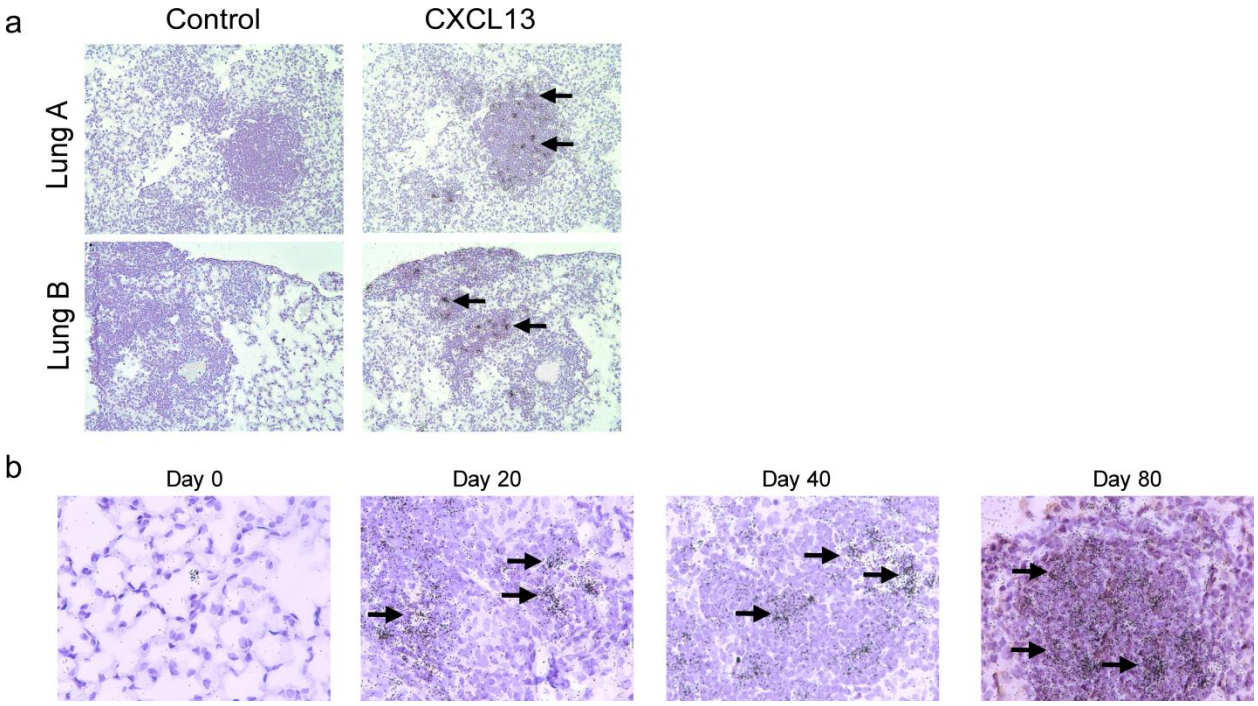

Figure 7: CXCL13 mRNA is localized in ectopic lymphoid follicles of Mtb-infected mice.

B6 mice were aerosol infected with ~100 cfu Mtb H37Rv and on day 50 post infection, FFPE serial sections were analyzed by ISH to determine localization of CXCL13 mRNA expression using a murine CXCL13 cRNA probe (a) during different points of infection (b). Black arrows point to localization of CXCL13 mRNA within granulomas. Original Magnification, 100X (a), and 600X (b). One of two or more experiments shown.

dendritic cells creating a perimeter around the infection [7, 229]. However, the functional and morphological characteristics that coordinate protective cross-talk in L-TB granulomas remain ill defined. Recently, areas of strong vascularization, B cell aggregation, and high proliferation markers were identified in patients with nonprogressive tuberculomas [223]. Furthermore, B cell aggregates containing $CD3^+$ T cells have been identified in humans, NHPs, and mice [11, 24, 78, 223]. Using immunofluorescence, we further characterized these distinct lymphoid aggregates as organized ectopic lymphoid organs containing FDC networks, proliferating GC B cells, $CXCR5^+$ T cells, and macrophages. Importantly, in NHPs that develop L-TB, we correlated the

organization of large organized ELOs containing $CXCR5^+$ T cells with immune control, while A-TB ELOs were associated with disorganized and smaller lymphoid aggregates. These findings establish a critical association of ectopic lymphoid structures in the protective immune response against Mtb.

Cxcl13 mRNA and protein were specifically expressed within ectopic lymphoid follicles and could not be detected in any other areas of the parenchyma or bronchovascular regions suggesting a critical role in Mtb induced ectopic lymphoid follicle formation. Expression of CXCL13 and CCL19/CCL21 is linked to ELO formation in other infectious disease such as *H. pylori* [204-207, 219] and influenza [124, 168], however, CXCL13 expression was pathological in *H. pylori* and was not required for ELO formation in influenza. CXCL13, and CCL19, but not CCL21 have been shown to be upregulated in the lungs of Mtb-infected mice [24]. Previous studies using *Cxcl13* deficient mice and *plt/plt* mice in Mtb infection have noted disruption of B cell aggregates and increased bacterial burden in the lung [24]. *Plt/plt* mice have a delayed accumulation of IFNγ producing T cells that is not observed in the absence of *Cxcl13* [24]. Decreased recruitment of IFNγ producing $CD4^+$ T cells in the lung was attributed to a decrease in DC migration to the draining lymph node (dLN) resulting in a delay of T cell priming and proliferation [24]. However, *ccr7* deficient mice were capable of ectopic proliferation of Ag85B-specific $CD4^+$ T cells in the lung and *plt/plt* mice still contained B cell follicles although smaller than wild type mice [24, 148]. These data suggest that CCL19/CCL21 are required for activated DC migration to the dLN, but decreased B cell follicle formation may be contributing to decreased lymphocyte accumulation rather than homeostatic chemokine expression. In contrast, *Cxcl13* deficient mice display complete disruption of B cell follicles within the lung and increased bacterial burden without defects in T cell priming [24]. Further, *Cxcl13* knockout mice contained

similar numbers of $CD4^+$ T cells to wild type mice in the lung suggesting the organization of immune cells in ectopic lymphoid follicles assists in macrophage activation and bacterial killing [24].

It has been previously noted that some granulomas are highly vascularized [223]. Vascularization is required for proper oxygen and nutrient supply to support cells and this is more often seen in the area occupied by ectopic lymphoid organs and in the periphery of the granuloma [223, 231-232]. Vascularized areas contained highly organized structures of macrophages and other antigen presenting cells surrounding by lymphocytes whereas active cavitary TB had disorganized lymphoid structures in these regions [223]. These observations suggest that the formation of ectopic lymphoid follicles in the vascularized region of the peripheral granuloma provides an ideal environment for cross-talk between the pathogen and host cellular immune response. The organization of these ELOs appear to be initiated by CXCL13 expression, but the cells and mechanism required for the protective properties of ectopic follicles requires further study.

2.6 ACKNOWLEDGEMENTS

The author would like to thank Javier Rangel-Moreno, PhD (University of Rochester, NY) for immunofluorescence staining and technical feedback and Beth A. Fallert-Junecko and Todd Reinhart, ScD (University of Pittsburgh, PA) for performing the CXCL13 in situ hybridization. Further, the author would like to thank Moises Selman, MD, Enrique Becerril-Villanueva, MD, Javier Baquera-Heredia, MD, and Lenin Pavon, MD for proving Mtb-infected human lung samples. Finally, we also thank Smriti Mehra and Deepak Kaushal, PhD for providing latent and

active NHP lung samples. This work was supported by Children's Hospital of Pittsburgh; NIH grants A1083541 and HL105427 to S.A. Khader, PhD; RR026006, AI091457, RR020159 and Tulane Primate Center base grant to D. Kaushal, PhD; HL69409 to T.D. Randall, PhD; and AI060422 to T.A. Reinhart, ScD; start-up funds from the Department of Medicine, University of Rochester, and AI91036 to J. Rangel-Moreno, PhD; and a Research Advisory Committee Grants from Children's Hospital of Pittsburgh of the UPMC Health System to S.R. Slight.

3.0 MECHANISMS UNDERLYING ECTOPIC LYMPHOID FOLLICLE FORMATION AND PROTECTION IN *M. TUBERCULOSIS* INFECTION

3.1 ABSTRACT

M. tuberculosis induced granulomas are central in providing conditions that promote immune cell interactions and bacterial containment. However, granulomas are present in both latent and active TB indicating structural and mechanistic immune differences must exist in granulomas that govern disease outcome. Recently, we have discovered that Mtb-infected lungs contain ectopic lymphoid follicles that correlate with protective immune control. To mechanistically address the cellular components necessary for protection and formation of ectopic lymphoid follicles, the TB mouse model was utilized. We discovered $CXCR5^+$ B cells and $CD4^+$ T cells, that produced Th1 proinflammatory cytokines, accumulated in the Mtb-infected lung. Further, mice deficient in *Cxcr5* were more susceptible to Mtb infection and do not form lymphoid follicles due to improper localization of $CD4^+$ T cells in the parenchyma, resulting in decreased macrophage activation. Defects in *Cxcr5* deficient mice could be rescued by the transfer of B6 $CD4^+$ T cells, but not *Cxcr5*-/- $CD4^+$ T cells. Finally, IL-6 and IL-21, cytokines important for T follicular helper cell CXCR5 expression, were required for optimal lymphoid follicle formation, but not for Mtb protective immunity. Our data demonstrate that $CD4^+CXCR5^+$ T cells play a

protective role in the immune response against TB and highlight their potential use for future TB vaccine design and therapy.

3.2 INTRODUCTION

Tuberculosis causes 2 million deaths a year despite the majority of infected individuals never developing symptoms [233]. The hallmark characterisitic of TB is the formation of the pulmonary granuloma, which requires coordination of multiple chemokines to recruit and organize immune cells [127]. Specific chemokine receptors have been implicated as important contributors to leukocyte accumulation, namely CXCR3 in the recruitment of T cells, CCR2 for macrophages and T cells, and CCR5 on myeloid cells (discussed in detail in Section 1.4). Further, the homeostatic chemokine CXCL13 is induced in the Mtb-infected lung and is critical for protective immunity [24]. CXCL13 is unique in that it is one of few chemokines that is non-redundant; there is only one receptor and one ligand. Its corresponding receptor, CXCR5, is expressed on Tfh cells and B cells and is responsible for the recruitment and organization of cells in the B cell follicle of SLOs [151, 153, 234].

Tfh cells are typically found within SLOs strategically positioned at the T-B cell border where they provide support for B cell expansion and differentiation by producing various cytokines, namely IL-21 [235-236]. High surface expression of ICOS and PD-1 on Tfh cells act as a co-stimulatory molecule inducing production of B helper cytokines and promoting long lived plasma cells, respectively [237-238]. Differentiation of Tfh cells is induced by IL-6 and IL-21 acting through STAT-3 to upregulate the transcription factor BCL-6 [239-243]. In addition, IL-12 produced

by human DCs was capable of driving differentiation of IL-21 producing Tfh cells suggesting Tfh cells may thrive in a Th1 environment [85, 244].

B cells also express CXCR5 for positioning within the follicles of SLOs and ELOs [151, 234]. The role of B cells (as described in section 1.2.4) is very much an enigma in TB. In the mouse model, Maglione et al. found low dose Mtb aerosol infection of B cell deficient mice had similar bacterial levels to wild type mice, but did not form follicles and had disrupted pulmonary architecture [77]. However, higher bacterial challenge resulted in exacerbated pathology with increased neutrophil infiltration and significantly higher bacterial burden in the lung [77]. In addition, Fcγ receptor IIB-/- mice have a decreased bacterial burden in the lung and enhanced Th1 cellular responses [245]. These data suggest that antibodies produced by B cells engage Fc receptors to modulate the Mtb immune response, in this case detrimentally [245]. The specific function and contribution of B cells continues to be investigated.

Recently, we have identified that ectopic lymphoid follicles containing $CXCR5^+$ cells are found within Mtb granulomas and formation correlates with protective immunity (as discussed in previous chapter). However, the mechanism of ELO formation and protective immunity against Mtb is uncertain. In this report, we show that CXCL13 recruits $CXCR5^+CD4^+$ T cells that are essential for ectopic lymphoid follicle formation within Mtb granulomas that mediate protective immunity. $CXCR5^+$ B cells are also found within the Mtb-infected lung, but these cells did not increase in frequency and B cell deficient mice were not more susceptible to Mtb challenge. Further, $CXCR5^+CD4^+$ T cells were found to produce the highest levels of Th1 proinflammatory cytokines and to localize near Mtb-infected macrophages driving activation and bacterial killing. Finally, the typical Tfh driving cytokines, IL-6 and IL-21, were required for optimal ectopic follicle formation, but not needed for protection. Our data prove that ectopic lymphoid follicle

formation in the granuloma is driven by CXCL13 and protective immunity is ascribed to Th1 cytokine producing $CXCR5^{+}CD4^{+}$ T cells.

3.3 MATERIALS AND METHODS

3.3.1 Mtb Infection in Mice

C57BL/6 (B6), *Il6*$^{-/-}$, *μMT*$^{-/-}$ (B cell deficient mice), *Cxcl13*$^{-/-}$ and *Cxcr5*$^{-/-}$ mice on the B6 background were purchased from The Jackson Laboratory, Bar Harbor, ME. *Il21*$^{-/-}$ mice were obtained from the Mutant Mouse Regional Resource Center (MMRC) and backcrossed to B6 mice for 10 generations. ESAT-6 (Early Secreted Antigenic Protein 6) αβ TCR transgenic (Tg) mice recognize IA^{b}/ESAT-6_{1-20} and were kindly provided by Dr. G. Winslow (Wadsworth Center, Albany, NY) and Dr. D. Woodland (Trudeau Institute, Saranac Lake, NY)[43]. The ESAT-6 TCR Tg mice were crossed and maintained on the *Rag1*$^{-/-}$ background. All mouse strains were bred and maintained at the Children's Hospital of Pittsburgh's animal facility. Experimental mice were age-and sex-matched and used between the ages of 6-8 wks in accordance with University of Pittsburgh International Animal Care and Use Committee guidelines. Mtb strain H37Rv was cultured in Proskauer Beck medium containing 0.05% Tween 80 to mid-log phase and frozen in 1 ml aliquots at -70^{o}C. Animals were aerosol infected with ~100 (low dose) or ~1000 (high dose) Colony Forming Units (CFU) of bacteria using a Glas-Col airborne infection system [227]. At given time points, organs were harvested, homogenized and serial dilutions of tissue homogenates plated on 7H11 plates and CFU determined. In some experiments, mice were subcutaneously vaccinated with ESAT6_{1-20} peptide (400 mg) emulsified with the adjuvant

containing MPL with TDM (Sigma-Aldrich) and DDA (ACROS organics) as described before [135]. On day 14 post vaccination, splenic $CD4^+$ T cells were sorted and cultured with irradiated APCs and Th polarizing conditions as described below. For generation of Th cell subsets, naïve ESAT-6 Tg $CD4^+$ T cells were cultured with BMDCs, $ESAT6_{1-20}$ peptide and cytokine cocktails. Tfh cells were cultured in Iscove's complete medium containing IL-21 (50ng/ml), anti-IL-4 (10μg/ml), anti-IFNγ (10μg/ml), and IL-2 (10U/ml); Th1 cells were cultured in complete DMEM containing IL-12 (10ng/ml), anti-IL-4 (10μg/ml) and IL-2 (10U/ml) [246]. Further, B6 mice were aerosol infected with ~100 cfu Mtb H37Rv and beginning at day 15 post infection, mice received 200 μg anti-CXCL13 antibody or isotype control antibody (R&D Biosystems) every other day until day 30 post infection on which organs were harvested.

3.3.2 Mtb Infection In NHPs

NHPs were infected as previously described in Section 2.3.2.

3.3.3 Lung and Spleen Single Cell Preparation

Lung tissue and the spleen were prepared as previously described [45]. Briefly, single cell suspensions were prepared from digested lung tissue or spleen by dispersing the tissue through a 70μm nylon tissue strainer (BD Falcon, Bedford, MA). The resultant suspension was treated with Gey's solution to remove residual red blood cells, washed twice, counted and used in assays described below.

3.3.4 Flow Cytometry

Single cell suspensions were stained with fluorochrome-labeled antibodies specific for CD3 (145-2C11), CD4 (RM4-5), CXCR5 (2G8), IFNγ (XMG1.2), TNFα (MP6-XT22), IL-21 (IL-21R-FC chimeric protein), IL-2 (JES6-5H4), Tbet (04-46) CD44 (IM7), Gr1 (RB6-8C5), CD11c (HL3), CD11b (M1/70), B220 (RA3-6B2), CD19 (ID3), Ly77 (GL7), CXCR3 (173), Bcl6 (7MG191E), ICOS (7E.17G9), PD-1(J43) and PNA (Sigma) or relevant isotype control antibodies. For intracellular analyses of cells, cells stimulated with phorbol myristate acetate (PMA-50ng/ml), ionomycin (750 ng/ml; Sigma Aldrich) or $ESAT6_{1-20}$ peptide (5 μg/ml) and Golgistop (BD Pharmingen), were surface stained, permeabilized with Cytofix-Cytoperm solution (BD Pharmingen) and stained for relevant cytokines. Cells were read using a Becton Dickinson FACS Aria flow cytometer using FACS Diva software. Cells were gated based on their forward by side scatter characteristics and the frequency of specific cell types was calculated using FlowJo (Tree Star Inc, CA). The mean fluorescent intensity was also calculated to determine expression levels of different molecules using FlowJo (Tree Star Inc, CA).

3.3.5 CXCL13 In Situ Hybridization

Performed as described in Section 2.3.5.

3.3.6 Morphometric Analysis and Immunofluorescence

Processing and staining was performed as mentioned in Section 2.3.4. Further, inducible NO Synthase (goat anti-mouse, M-19; Santa Cruz Biotechnology) and F4/80 (MCA497GA, Serotec)

were used. Primary Abs were detected with secondary Ab conjugated to Alexa fluor 568 for iNOS (Alexa fluor 568, donkey anti goat, Invitrogen).

3.3.7 Real-Time PCR

RNA was extracted as previously described [247]. RNA was treated with DNAse and reverse transcribed and cDNA was then amplified with FAM-labeled probe and PCR primers on the ABI Prism 7700 detection system. The log10 fold-induction of mRNA in experimental samples was calculated over signals derived from uninfected/control samples. The specific gene expression was calculated relative to GAPDH expression. The primer and probes sequences targeting genes encoding iNOS have been previously published [24].

3.3.8 Detection of IFN-γ-Producing Cells by ELISPOT Assay

ESAT-6_{1-20}-specific IFN-γ-producing IA^b-restricted T cells from infected lungs or spleen were enumerated using peptide-driven ELISpot as described [45]. Briefly, 96 well ELISpot plates were coated with monoclonal anti-mouse IFNγ blocked with media containing 10% FBS. Cells from lungs and spleen were seeded at an initial concentration of $5x10^5$ cells/well and subsequently diluted two fold. Irradiated B6 splenocytes were used as APCs at a concentration of $1x10^6$ cells/well in the presence of ESAT-6_{1-20} (10μg/ml) peptide and IL-2 (10U/ml). After 24 hrs, plates were washed and probed with biotinylated anti-mouse IFNγ. Spots were visualized and enumerated using a CTL-Immunospot S5 MicroAnalyzer. No spots were detected in cultures lacking antigen or when using cells from uninfected mice.

3.3.9 Protein Estimation by ELISA

Mouse Duoset ELISA antibody pairs from R&D Systems were used to detect IFNγ and IL-21 protein levels in the supernatant according to manufacturer's protocol. In some experiments protein levels were measured using a mouse Luminex assay (Linco/Millipore).

3.3.10 Adoptive Transfer of $CD4^+$ Cells

Naive $CD4^+$ T cells were isolated from single cell suspensions generated from lymph nodes and spleens of ESAT-6 TCR Tg mice, B6 and *Cxcr5*$^{-/-}$ mice using a positive $CD4^+$ T cell isolation kit (Miltenyi Biotech) as described [24]. For adoptive transfer into host mice, 2-5 x 10^6 naïve T cells were transferred intravenously, following which mice were rested for 24 hours and challenged with Mtb H37Rv by the aerosol route.

3.3.11 CXCL13 Chemotaxis Assay

B6 mice were aerosol infected with 100 cfu Mtb and sacrificed at day 50 post infection. Using a positive CD4+ T cell isolation kit (Miltenyi Biotech), CD4+ T cells were isolated and 1x10^5 cells were placed in 24 well transwell plate for chemotaxis assay to CXCL13 (500 ng/ml). CD4+ T cells were allowed to migrate for 90 minutes when they were stained with antibodies specific for CD4, ICOS, IFNγ, and BCL-6. Wells that did not contain CXCL13 were used as controls.

3.3.12 Statistics

Differences between the means of experimental groups were analyzed using the two tailed Student's t-test. Differences were considered significant when $p \leq 0.05$.

3.4 RESULTS

3.4.1 Activated $CD4^+CXCR5^+$ T cells accumulate in the lung during Mtb infection

Given that ectopic lymphoid structures associated with TB granulomas contained $CXCR5^+$ T cells, we next tested whether these cells were functionally important. The accumulation of activated, IFNγ-producing $CD4^+$ T cells normally occurs in the murine lung between days 15-21 following low dose Mtb infection [51, 80]. We found activated, $CD4^+$ $CXCR5^+$ T cells also accumulated in the lungs between days 15-21 (Figure 8a). Notably, a higher frequency and number of $CXCR5^+$ T cells was found in the activated $CD44^{hi}$ $CD4^+$ T cell subset when compared to unactivated naive $CD4^+$ $CD44^{lo}$ T cell subset (Figure 8b). In contrast, although a population of lung B cells also expressed CXCR5; this population did not increase in frequency following Mtb infection (Figure 8c). Furthermore, B cell deficient mice are not susceptible to low dose Mtb infection [76-77], suggesting that $CD4^+$ $CXCR5^+$ T cells, rather than $CXCR5^+$ B cells, play a dominant role in protective immunity in the low dose model of Mtb infection. In addition, lung activated $CD4^+$ $CXCR5^+$ T cells expressed significantly higher levels of Tfh-like cell markers, ICOS and PD1, when compared to activated $CD4^+$ $CXCR5^-$ T cells and unactivated naive $CD4^+$ T cells (Figure 8d).

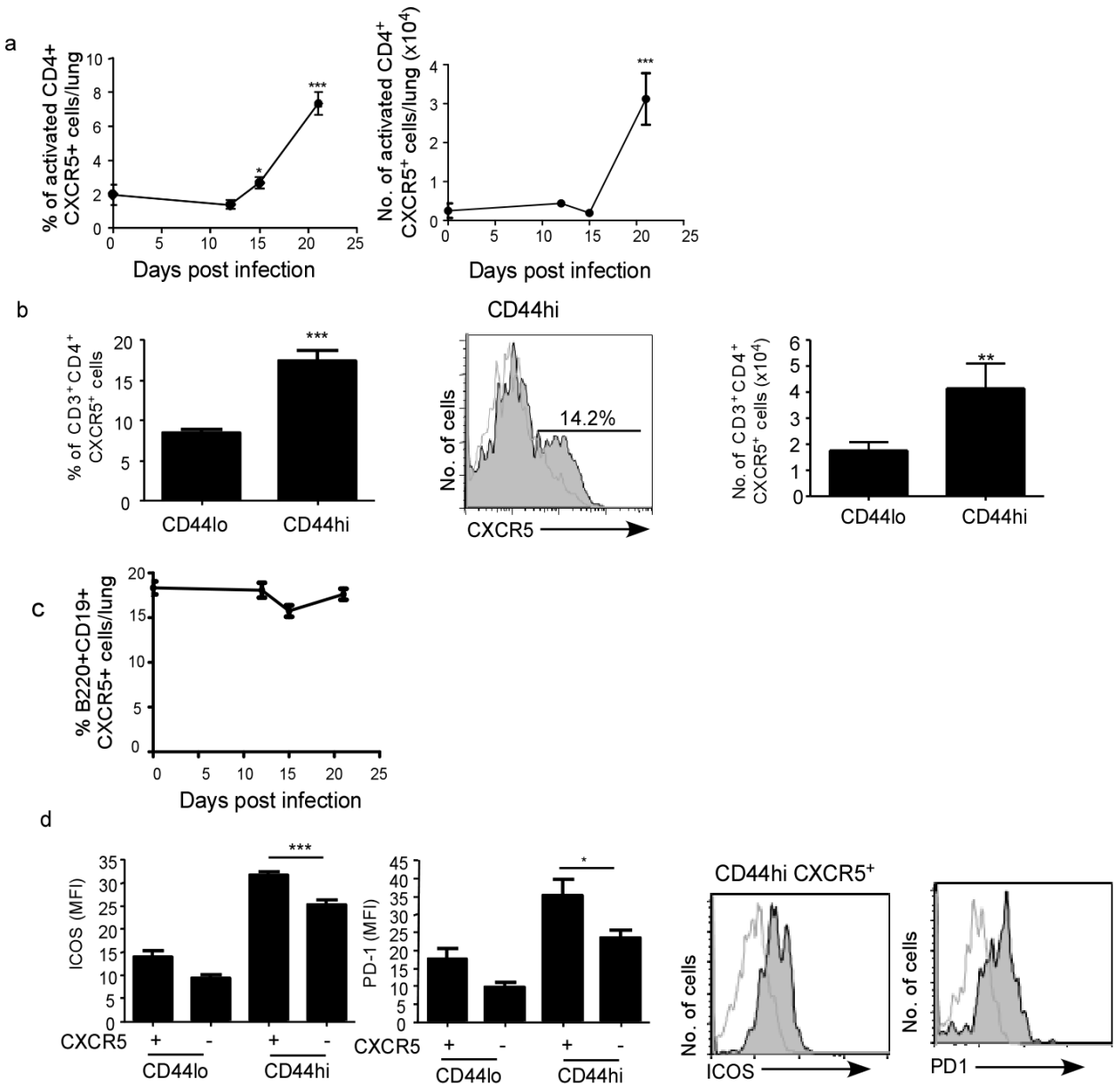

Figure 8: Activated CD4$^+$ CXCR5$^+$ T cells accumulate in the lung during Mtb infection and express both Tfh-like markers.

B6 mice were infected as in Figure 6. The frequency and number of activated CD4+ CXCR5+ T cells and B220+CD19+CXCR5+ B cells was determined by flow cytometry at different time points post infection (a,c). Frequency and number of activated (CD44hi) and unactivated (CD44lo) CD4+ CXCR5+ T cells were determined in Mtb-infected lungs on day 25 post infection by flow cytometry (b). A typical histogram showing CXCR5 specific staining (filled) within activated CD4+ T cells and relevant isotype control antibody (open) is shown (b). Expression of ICOS and PD-1 (d) on activated (CD44hi) and unactivated (CD44lo) CD4+ CXCR5+ and CD4+ CXCR5- T cells were calculated by determining the mean fluorescent intensity using flow cytometry. A typical histogram showing expression of PD1 and ICOS (filled) and relevant isotype control antibody (open) on activated CD4+ CXCR5+ cells is shown (d). The data points represent the mean (±SD) of values from 4-6 mice. (a-e). *p=0.05, ***p=0.0005. ns-not significant. One experiment representative of two.

3.4.2 Pulmonary $CD4^+CXCR5^+$ T cells produce proinflammatory cytokines

Importantly, we found that $ICOS^+$ $PD1^+$ $CD4^+$ T cell population was increased during infection (Figure 9a) and were enriched for expression of CXCR5 and CD44 (Figure 9b). As expected [248], activated $CD4^+$ $CXCR5^-$ T cells also expressed ICOS and PD-1, albeit at reduced levels (Figure 8d). Interestingly, activated $CD4^+$ $CXCR5^+$ T cells also expressed the highest levels of the proinflammatory cytokines IFNγ, TNFα and IL-2 (Figure 9c), individually, or in combination and cytokine-production by $CXCR5^+$ T cells was Mtb-specific (Figure 10a, b). However, only a small population of $CD4^+$ $CXCR5^+$ T cells produced IL-17 and IL-21 (Figure 10a). Despite increased expression of proinflammatory cytokine production in activated $CD4^+$ $CXCR5^+$ T cells, there were no differences in overall percentage (Figure 10a) or numbers of cytokine-producing cells between activated $CD4^+$ $CXCR5^+$ and $CD4^+$ $CXCR5^-$ T cells. In addition, $CD4^+$ $CXCR5^+$ population expressed higher levels of Bcl6, while expressing similar levels of Tbet as $CD4^+$ $CXCR5^-$ T cell populations (Figure 10c). These data together suggest that activated $CD4^+$ T cells express markers characteristic of Tfh-like cells such as ICOS, PD-1 and Bcl6, but also exhibit markers of Th1-like cells such as production of proinflammatory cytokines and expression of Tbet.

3.4.3 $CD4^+CXCR5^+$ T cells coexpress the chemokine receptor, CXCR3

We then determined if activated $CD4^+$ $CXCR5^+$ T cells expressed other chemokine receptors such as CXCR3, which are associated with Mtb-induced lung inflammatory T cell accumulation [136]. We detected expression of CXCR3 on a population of activated $CD4^+$ T cells (Figure 11a)

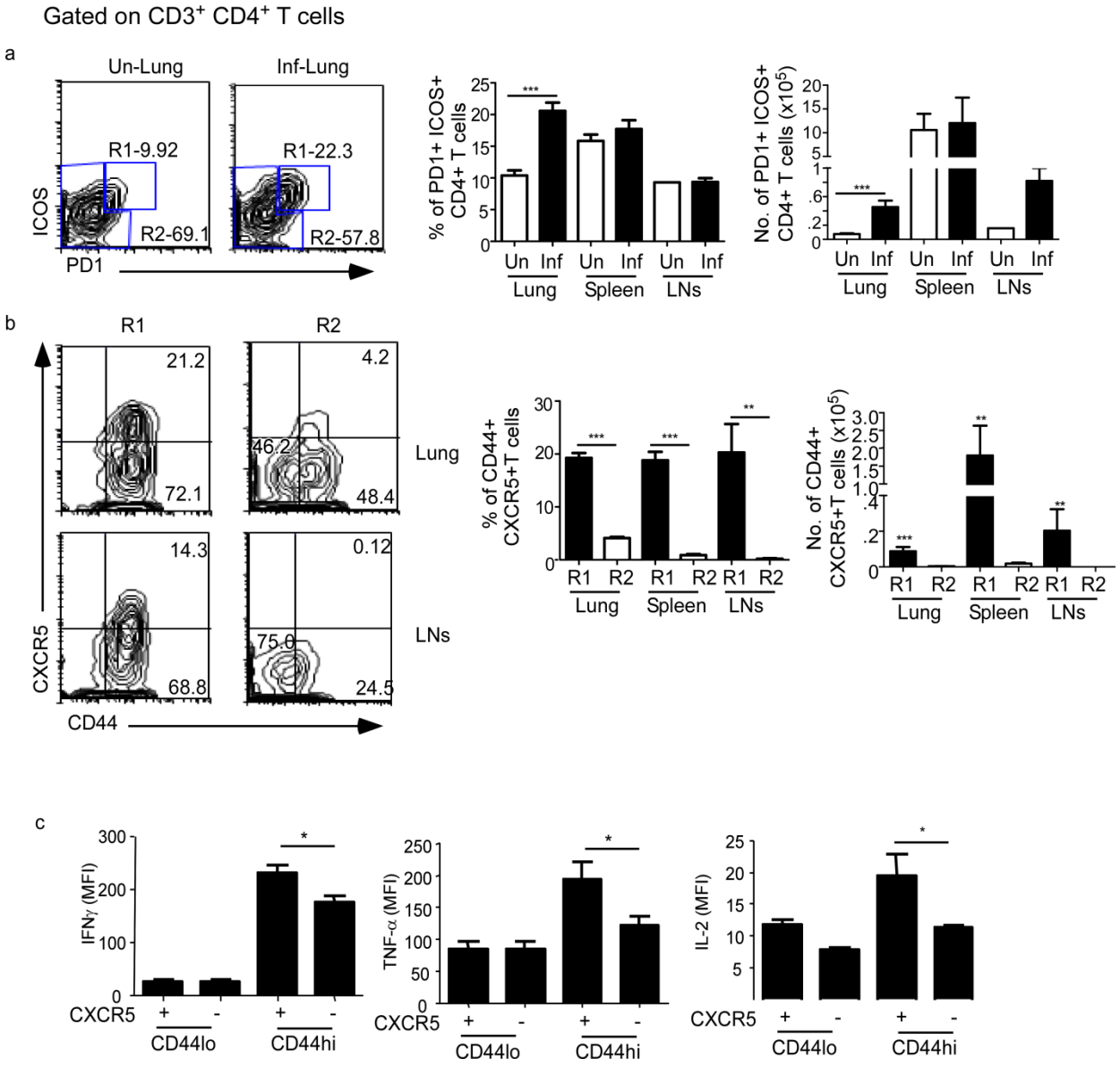

Figure 9: Pulmonary CD4$^+$ CXCR5$^+$ T cells produce proinflammatory cytokines.

On day 25 post infection, organs from uninfected (Un) and infected (Inf) B6 mice were assessed for the percentage or number of ICOS+ PD1+ within CD4+ T cells by flow cytometry (a). The expression of CD44 and CXCR5 and number of CD44+ CXCR5+ T cells within ICOS+PD1+ gate (R1) or ICOS-PD1- gate (R2) was calculated (b). Expression of IFNg, TNFa and IL-2 (c) on activated (CD44hi) and unactivated (CD44lo) CD4+ CXCR5+ and CD4+ CXCR5- T cells were calculated by determining the mean fluorescent intensity using flow cytometry. The data points represent the mean (±SD) of values from 4-6 mice. (A-D). **p=0.005, ***p=0.0005. One experiment representative of two.

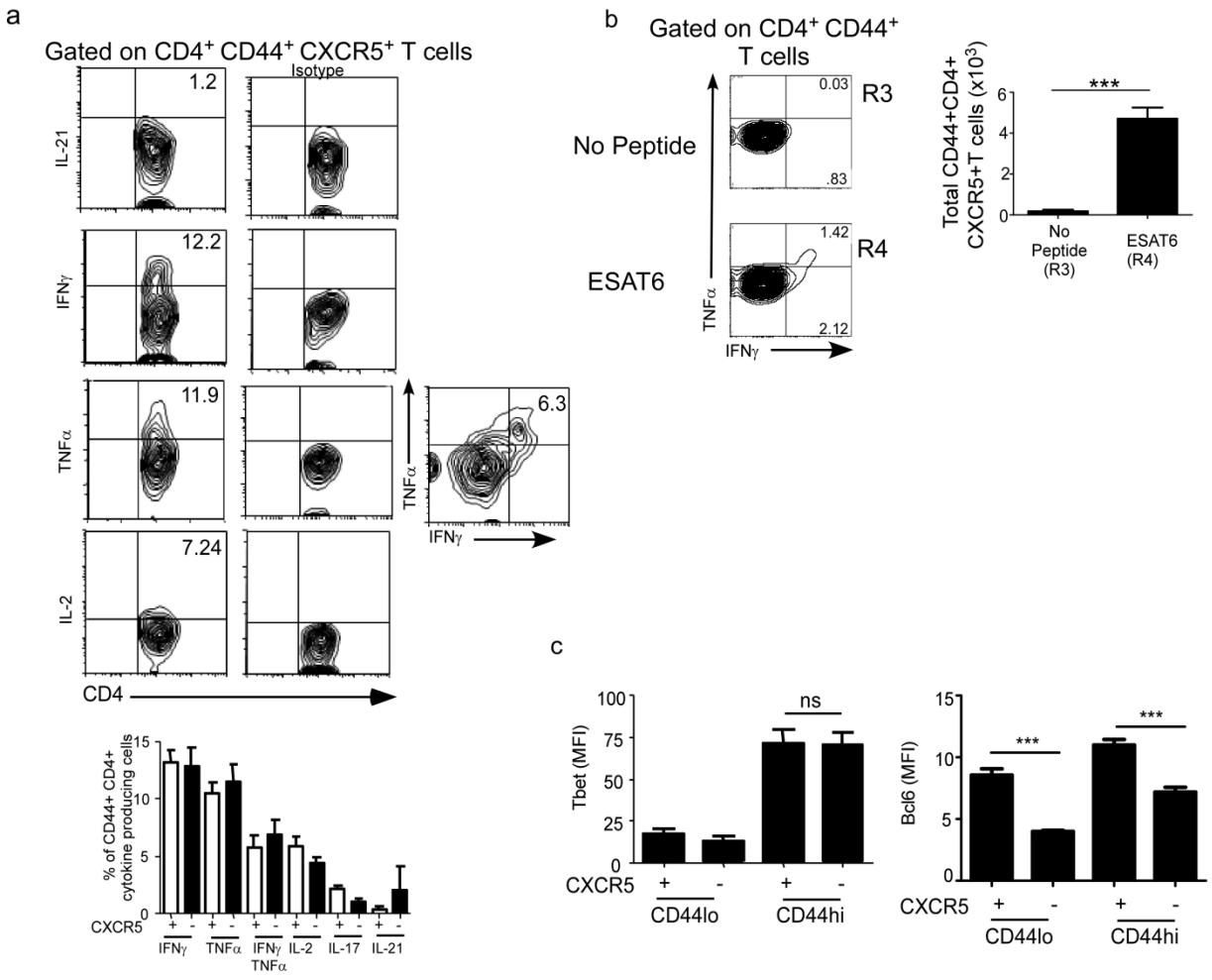

Figure 10: Pulmonary CD4$^+$ CXCR5$^+$ T cells produce proinflammatory cytokines.

On day 25 post infection, organs from uninfected (Un) and infected (Inf) B6 mice were assessed for the percentage of cytokine producing cells within CD44hi CXCR5+ and CD44hi CXCR5- was determined after stimulation with PMA/Ionomycin for 5 hours followed by intracellular staining and flow cytometry (a). A typical contour plot showing cytokine specific staining (left panel) within activated CD4+ CXCR5+ T cells and relevant isotype control antibody (right panel) shown. Cells from day 25 Mtb-infected lungs were stimulated with ESAT6 peptide and expression of CXCR5 was determined on CD44 hi IFNγ+TNFα+ cells (b). Expression of Tbet and Bcl6 (c) on activated (CD44hi) and unactivated (CD44lo) CD4+ CXCR5+ and CD4+ CXCR5- T cells were calculated by determining the mean fluorescent intensity using flow cytometry.The data points represent the mean (±SD) of values from 4-6 mice. (a-c). **p=0.005, ***p=0.0005. One experiment representative of two.

and found that a subset of $CXCR3^+$ $CD4^+$ T cells also co-expressed CXCR5 (Figure 11b). Surprisingly, we found that the $CD4^+$ $CXCR5^+$ T cell subset expressed the highest frequency and expression levels of IFNγ □(Figure 11c) and other proinflammatory cytokines, when compared to activated $CD4^+$ $CXCR3^+$ or $CD4^+$ $CXCR3^+$ $CXCR5^+$ T cell populations within Mtb-infected lungs (Figure 11c). Furthermore, in contrast to the localized expression of CXCL13 mRNA observed within lymphoid follicles (Figure 7 a, b), we found that mRNA for CXCL9, a CXCR3-ligand, was localized both within the inflammatory lesions as well as near blood vessels in the Mtb-infected murine lung (Figure 11d) and latently infected NHPs (Figure 11e). These data together suggest that Mtb-induced inflammatory chemokines such as CXCL9 are expressed near blood vessels and likely recruit activated $CD4^+$ T cells to the lung, but that CXCR5-CXCL13 interactions may be specifically required to localize potent cytokine-producing $CD4^+$ T cells within the lung parenchyma to organize lymphoid follicles and maximize mycobacterial control within granulomas.

3.4.4 CXCR5 expression is required for protective immunity against Mtb infection

To determine if there was a protective role for CXCR5 in immunity against TB, CXCR5-deficient (*Cxcr5*$^{-/-}$) mice were infected with Mtb and found to harbor higher lung bacterial burdens during early and chronic stages of infection, when compared to B6 mice (Figure 12a). In addition, CXCL13 neutralization also resulted in increased bacterial burden (Figure 12a) and

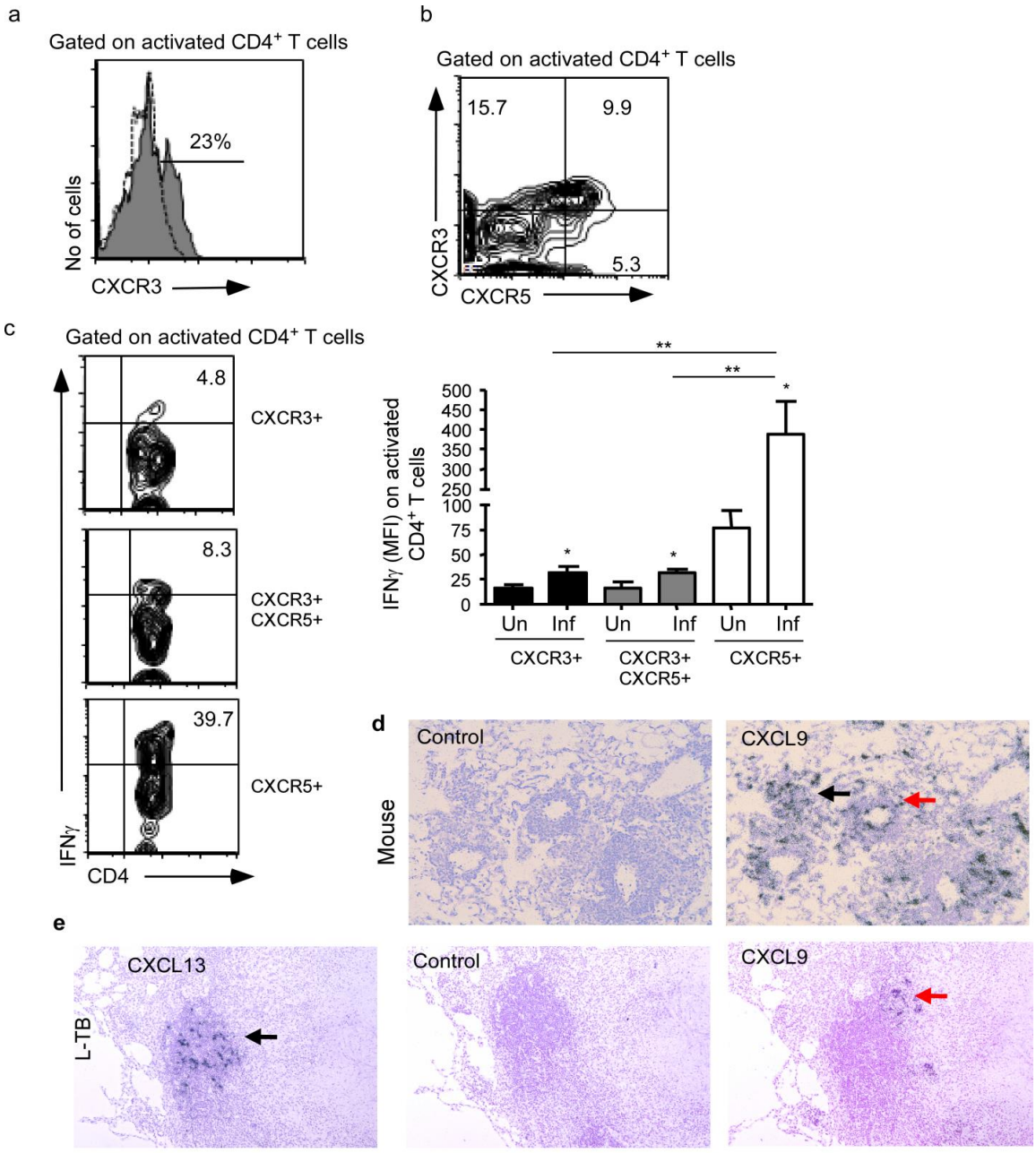

Figure 11: CD4$^+$ CXCR5$^+$ T cells also coexpress the chemokine receptor, CXCR3.

B6 mice were infected as in Figure 6 and lungs were harvested on day 25 post infection. The expression of CXCR3 (a), CXCR3 and CXCR5 (b) on activated CD4+ cells was determined by flow cytometry. A typical histogram with CXCR3 specific staining (filled) and relevant isotype control antibody within activated CD4+ T cells is shown (open) (a). A typical contour plot showing co-expression of CXCR3 and CXCR5 on activated CD4+ T cells is shown (b). The frequency and mean fluorescent intensity of IFNγ expression within activated CD4+ CXCR5+, CXCR5+CXCR3+ and CXCR3+ T cells was determined in cells stimulated with PMA/Ionomycin for 5 hours followed by intracellular staining and flow cytometry (c). The data points represent the mean (±SD) of values from 4-6 mice. (a-c). Lung FFPE serial sections were analyzed by ISH to determine localization of CXCL9 or CXCL13 mRNA expression in murine (d) or L-TB NHP (e). Black arrows point to mRNA localization within the lung parenchyma, while red arrows point to mRNA localization near blood vessels. *p=0.05, **p=0.005. Original magnification 100x. One experiment representative of two.

both *Cxcr5*$^{-/-}$ and *Cxcl13*$^{-/-}$ mice demonstrated decreased survival in response to high dose Mtb infection (Figure 12b). Using the low dose Mtb infection model, we found that the accumulation of total B cells (Figure 12c) was similar in B6 and *Cxcr5*$^{-/-}$ Mtb-infected lungs, while *Cxcr5*$^{-/-}$ Mtb-infected lungs showed impaired accumulation of lung GC B cells (Figure 12d). Furthermore, no differences in levels of ESAT-6-specific IgG1, IgG2a and IgG2b antibodies were found in B6 and *Cxcr5*$^{-/-}$ Mtb-infected mice. Therefore, we next assessed T cell responses, and found that despite lack of mediastinal lymph nodes and defective splenic architecture in *Cxcr5*$^{-/-}$ mice [249], comparable percentages of IFNγ–producing CD4^{+} cells (Figure 12 g, h) and number of Mtb-ESAT-6-specific, IFNγ-producing CD4^{+} cells (Figure 12e, f) were found in the lungs and spleen of *Cxcr5*$^{-/-}$ and B6 Mtb-infected mice. In addition, neither differences in frequency of total CD4^{+} T cells producing TNFα and IL-2, nor differences in expression levels of IFNγ, TNFα and IL-2 within CD4^{+} T cells were observed in B6 and *Cxcr5*$^{-/-}$ Mtb-infected lungs. The percentage of CD4^{+} T cells expressing Tfh-like cell markers ICOS and PD1 (Figure 13a), and the ability of activated ICOS^{+} PD1^{+} Th cells to produce IFNγ (Figure 13b), TNFα and IL-2 was also similar in B6 and *Cxcr5*$^{-/-}$ Mtb-infected lungs. To then address if *Cxcr5*$^{-/-}$ T cells had the potential to differentiate into cytokine-producing Th cell subsets, we immunized B6 and *Cxcr5*$^{-/-}$ mice with ESAT6 peptide in adjuvant and expanded splenic CD4^{+} T cells in vitro in the presence of Th1 or Tfh cell differentiation conditions. Similar to B6 CD4^{+} T cells, *Cxcr5*$^{-/-}$ CD4^{+} T cells produced IFNγ in response to Th1 polarizing conditions (Figure 13c) and produced IL-21 in response to Tfh cell differentiation conditions (Figure 13d). These data suggest that in the absence of CXCR5, B cells and cytokine producing antigen-specific T cells accumulate efficiently in the Mtb-infected lung.

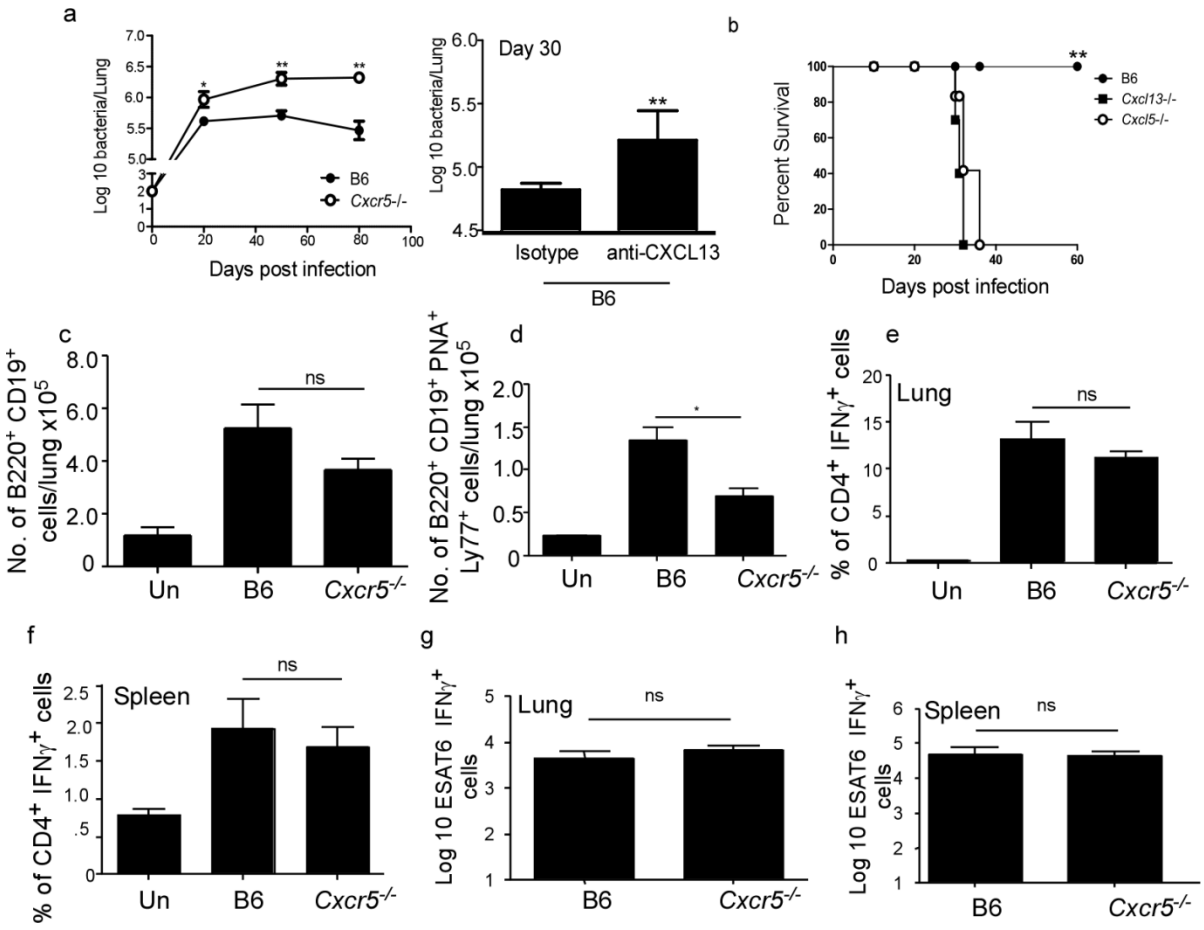

Figure 12: CXCR5 expression is required for protective immunity against Mtb infection.

B6 and Cxcr5-/- mice were infected or B6 Mtb-infected mice received CXCL13 neutralizing antibodies and lung bacterial burden determined (a). Survival of B6, *Cxcl13-/-* and *Cxcr5-/-* mice with high dose (1000 CFU) of aerosolized Mtb infection was determined (b). The number of total B cells (B220+ CD19+) (c) or GC B cells (B220+, CD19+, PNA+, and Ly77+) (d) was determined by flow cytometry in B6 and *Cxcr5-/-* Mtb-infected lungs on day 21 post infection. The total percentage of IFNγ producing CD4+ T cells in the lung (e) and spleen (f) were determined by intracellular staining and flow cytometry after stimulation with PMA/Ionomycin for 5 hours ex vivo. The number of ESAT-6 specific IFNγ-producing CD4+ T cells were determined in the lung (g) and spleen (h) by antigen-driven ELISpot assay. The data points represent the mean (±SD) of values from 4-6 mice. (a-h). *p=0.05, **=0.005, ***p=0.0005. One experiment representative of two.

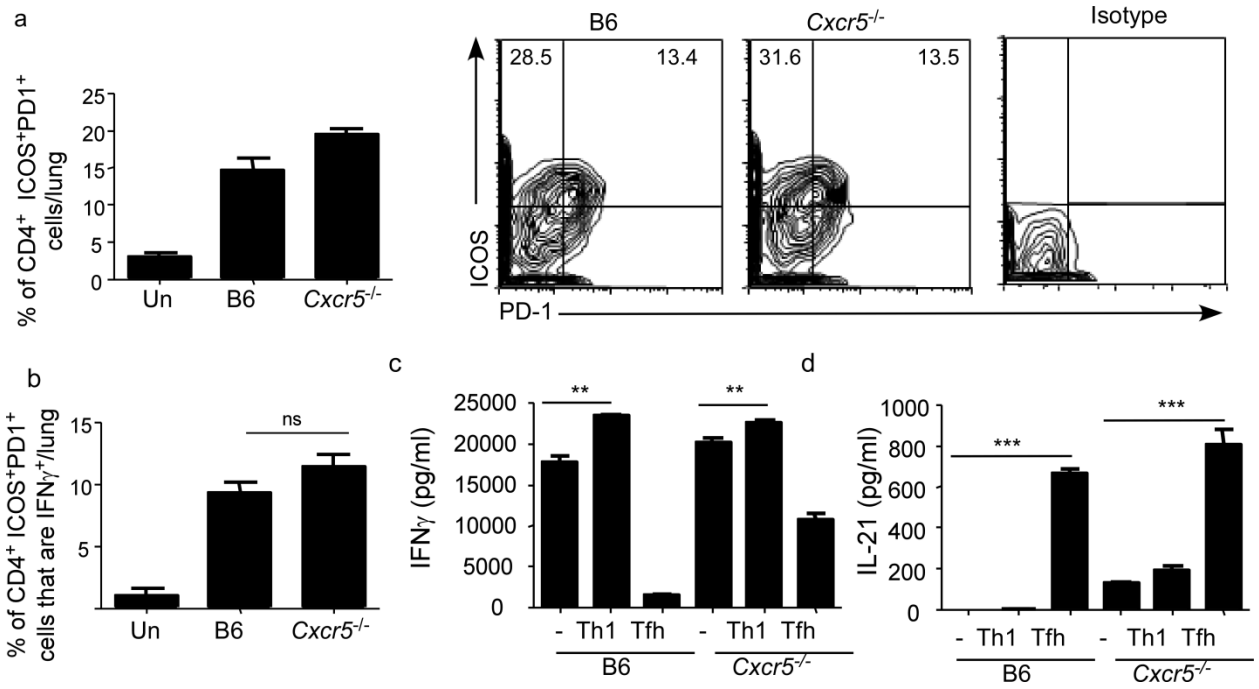

Figure 13: CXCR5 expression is not required for accumulation of cytokine-producing ICOS$^+$ PD1$^+$ T cells during Mtb infection.

B6 and *Cxcr5-/-* mice were infected as in Figure 3. The percentage of CD4+ T cells expressing ICOS and PD1 (a) and CD4+ ICOS+ PD1+ cells expressing IFNγ (b) was determined by intracellular staining with PMA/Ionomycin. B6 and *Cxcr5-/-* mice were subcutaneously vaccinated with $ESAT6_{1-20}$ peptide in adjuvant and on day 14 post vaccination, splenic CD4$^+$ T cells were cultured in vitro along with irradiated APCs and antigen under Th1 or Tfh cell differentiation conditions for 6 days as described in methods. At the end of the culture period, the CD4$^+$ T cells were re-stimulated with beads coated with anti-CD3/CD28 for 24 hours and culture supernatants assayed for IFNγ (c) or IL-21 (d) by ELISA. The data points represent the mean (±SD) of values from 4-6 mice (a-d). ns-not significant. One representative of two experiments is shown. *p=0.05. ns=not significant.

We therefore next addressed if the increased susceptibility in the *Cxcr5*$^{-/-}$ mice was due to defects in localization of T cells within lung inflammatory lesions. In support of a role for CXCR5 in correct T cell localization inside granulomas, CD3$^+$ T cells were dispersed throughout the organized lung granulomas in the B6 Mtb-infected mice (Figure 14a-upper panel). However, CD3$^+$ T cells were found as distinct perivascular cuffs in *Cxcr5*$^{-/-}$ Mtb-infected lungs and B6 mice that received CXCL13 neutralizing antibody (Figure 14b-lower panel, Figure 14c), resulting in disrupted granuloma formation (Figure 14a-lower panel) and defective lymphoid

structure generation (Figure 14d, e). These data together suggest that the increased susceptibility to Mtb infection seen in the *Cxcr5*$^{-/-}$ mice, is not due to impaired priming, generation or accumulation of cytokine-producing Tfh-like cells in the Mtb-infected lungs, but due to the inability of cytokine-producing CD4^{+} T cells to localize correctly within the Mtb-infected lung, and therefore unable to activate local macrophages to control Mtb.

3.4.5 B cell deficient mice localize T cells within the granuloma and control Mtb

We next addressed whether B cell lymphoid follicle formation within TB granulomas was a consequence of correct T cell localization and therefore a correlate of protection, but by itself not necessary for mediating the immune protection in Mtb-infected mice. We found that Mtb-infected B cell deficient mice (*μMT*$^{-/-}$) despite exhibiting disrupted granuloma formation and poorly formed lymphoid follicles in the lungs (Figure 15a-left panel), still controlled infection (Figure 15b) as previously described [76-77]. In addition, B cell deficient Mtb-infected mice generated and recruited similar numbers of ICOS^{+} PD1^{+} CXCR5^{+} T cells and accumulated similar numbers of antigen-specific IFNγ-producing cells to the lung (Figure 15c). Furthermore, immune control in B cell deficient mice coincided with well dispersed T cells localized in the inflammatory lesions in the lungs (Figure 15a-center panel) and resultant macrophage activation (Figure 15a-right panel, Figure 15d). These data together suggest that B cells are not required for bacterial control and T cell localization in the mouse. Further, that B cells are not required for macrophage activation, but that it is indeed T cell localization near Mtb-infected macrophages and the formation of ectopic follicles that is critical for host protective immunity.

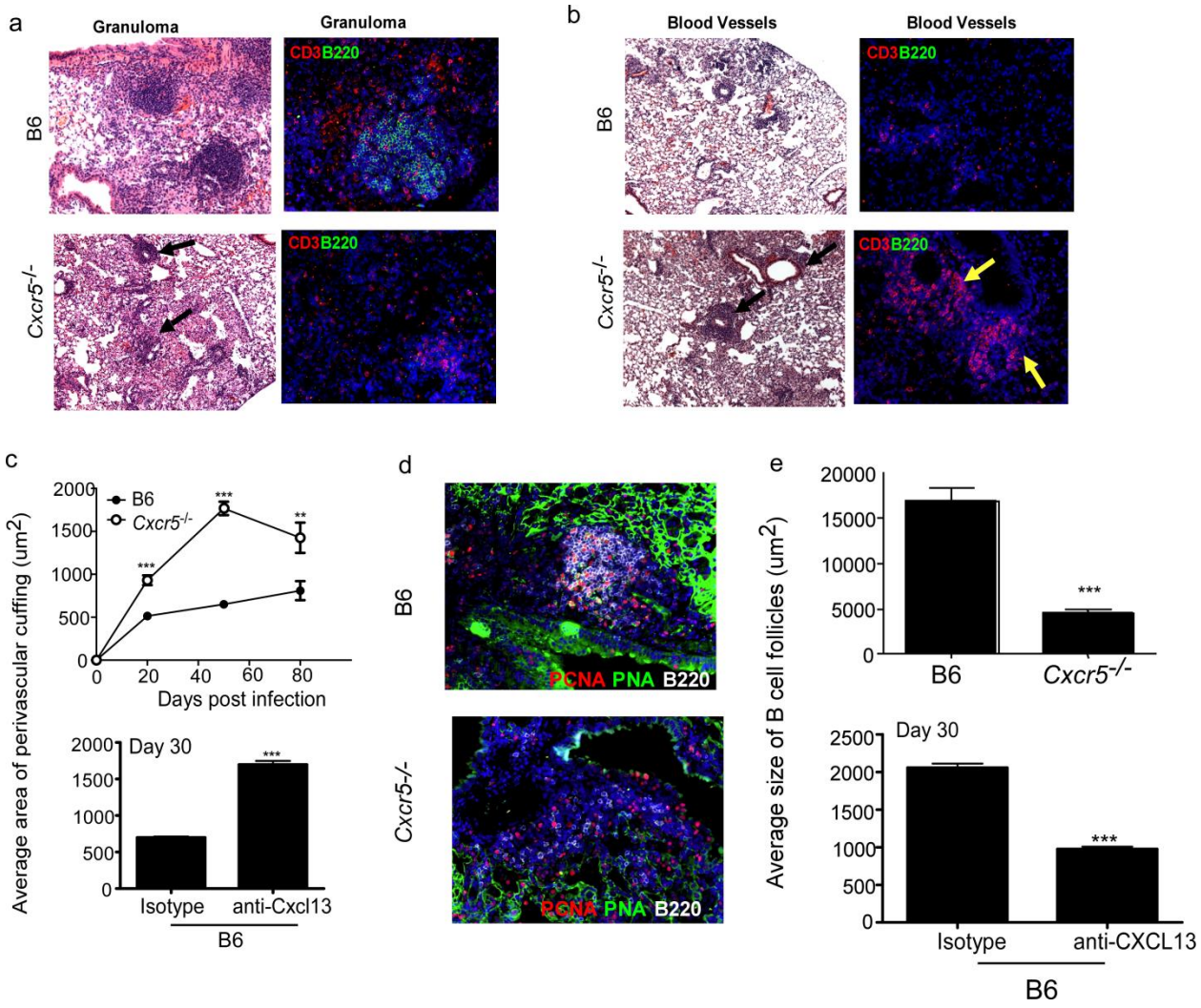

Figure 14: CXCR5 expression is required for ectopic lymphoid follicle formation during TB.

B6 and Cxcr5-/- mice were infected or B6 Mtb-infected mice received CXCL13 neutralizing antibodies. At day 50 post infection, FFPE lung sections were H&E stained or analyzed by immunofluorescence for CD3, B220 (a,b); Representative pictures of granulomas (a) and perivascular T cell cuffing (b) shown. Black and yellow arrows indicate T cell perivascular cuffing (b). Average area of perivascular cuffs was quantified using the the Zeiss Axioplan microscope (c). Error bars are not visible in day 30 B6 isotype group (c). B cell lymphoid follicles were detected with PCNA, PNA, and B220 at day 50 post infection (d). The average size of B cells follicles was quantified using the Zeiss Axioplan microscope (e). 100X magnification -H&E images; 200X magnification-fluorescent images. The data points represent the mean (±SD) of values from 4-6 mice (a-e). One representative of two experiments is shown. **p=0.005, ***p=0.0005. ns=not significant.

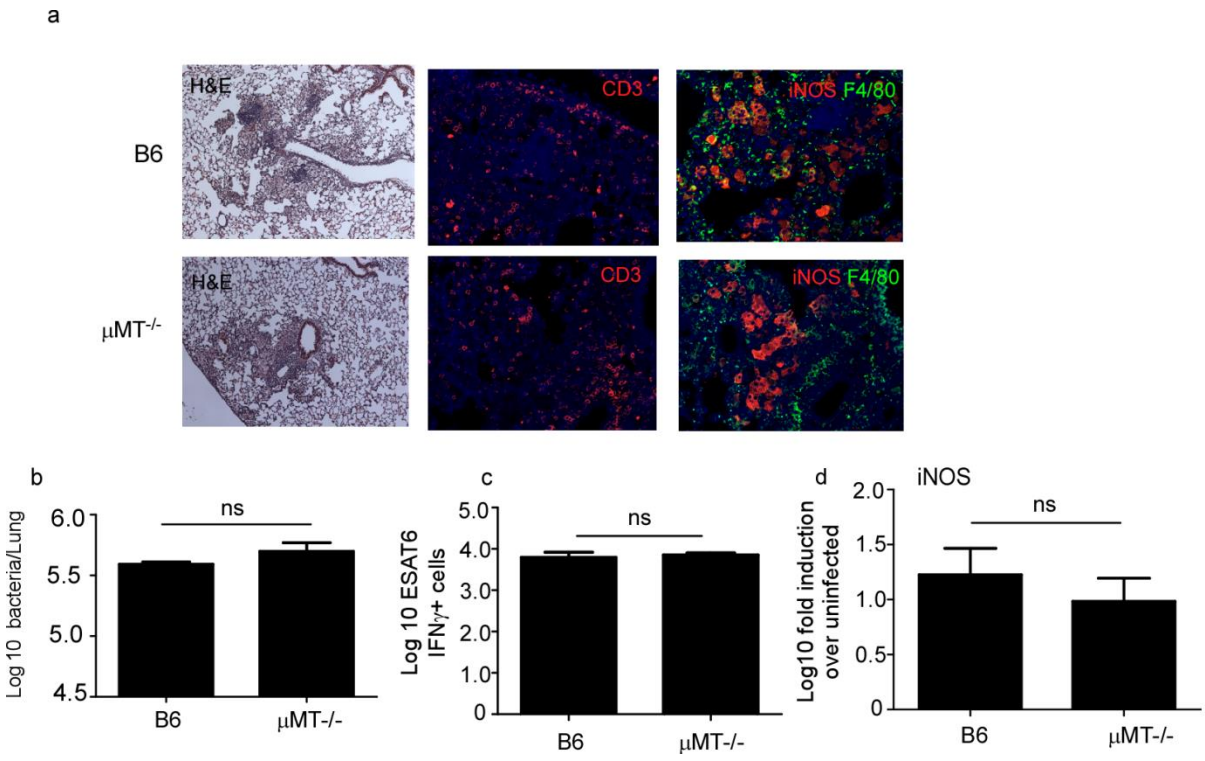

Figure 15: B cell deficient mice localize T cells within the granuloma and control Mtb.

B6 and μMT-/- mice were infected as described in Figure 6 and FFPE lung sections were stained with H&E or analyzed using antibodies specific for CD3 and iNOS, F4/80 (a); Representative pictures are shown. 50X magnification-H&E images, 200X magnification-fluorescent images. At day 50 post infection, bacterial burden was determined in the lung (b). The number of ESAT-6 specific IFNγ producing CD4+ T cells were determined in the lung by antigen driven ELISpot assay (c). Log10 fold induction of iNOS mRNA in B6 and μMT-/- Mtb-infected lungs relative to levels in uninfected lungs was determined by RT-PCR (d). The data points represent the mean (±SD) of values from 4-6 mice. (a-d). ns=not significant. One experiment representative of two.

3.4.6 $CD4^+$ T cells responsive to CXCL13 produce IFNγ and activate macrophages

In support of a role for CXCR5-CXCL13 in T cell localization within the lung for optimal macrophage activation, we found that $CD4^+$ T cells isolated from B6 Mtb-infected lungs migrated in response to CXCL13 in vitro, produced IFNγ and expressed Tfh-like cell markers, ICOS and Bcl6 (Figure 16a, b). Importantly, we found that despite similar numbers of lung macrophages and DCs in B6 and *Cxcr5*$^{-/-}$ Mtb-infected lungs (Figure 16c, d), *Cxcr5*$^{-/-}$ Mtb-

infected lungs had reduced induction of mRNA for the anti-mycobacterial molecule, iNOS (Figure 16e), and fewer iNOS^{+} macrophage-like cells were detected within the disorganized granulomas of *Cxcr5*$^{-/-}$ and *Cxcl13* deficient (*Cxcl13*$^{-/-}$) Mtb-infected lungs (Figure 16f). Furthermore, CD11c^{+} DCs and macrophages sorted from *Cxcr5*$^{-/-}$ and *Cxcl13*$^{-/-}$ Mtb-infected lungs, displayed lower iNOS mRNA expression, when compared to cells isolated from B6 Mtb-infected lungs (Figure 16g). These data together suggest that expression of CXCR5 is critical for strategic positioning of effector T cells within the lung for optimal macrophage activation, subsequent organization of lymphoid follicles and Mtb control.

3.4.7 Adoptive transfer of ESAT-6 Tg Th0 cells rescues Mtb-infected *Cxcr5*-/- mice

Our data suggests that localization of CD4^{+} CXCR5^{+} T cells within lymphoid structures is critical for generation of lymphoid structure formation, macrophage activation and mycobacterial immune control. Therefore, we determined if adoptive transfer of purified naïve ESAT-6-specific transgenic (Tg) T cells [43] capable of expressing CXCR5, into *Cxcr5*$^{-/-}$ mice would rescue T cell localization within the lung, macrophage activation and reverse susceptibility to TB. *Cxcr5*$^{-/-}$ mice that did not receive ESAT-6 Tg Th0 cells had higher bacterial burden (Figure 17a), contained numerous lymphocytic perivascular cuffs (Figure 17b), defective lymphoid follicle generation and reduced numbers of activated macrophages (Figure 17c-middle panel). In contrast, B6 Mtb-infected mice formed ectopic lymphoid structures characterized by lymphocytic infiltrates (Figure 17b, c), B cell follicles and granulomas with considerable numbers of iNOS-expressing macrophages (Figure 17c-upper panel). Importantly, adoptive transfer of ESAT-6 Tg Th0 cells into *Cxcr5*$^{-/-}$ mice decreased lung bacterial burden (Figure 17a),

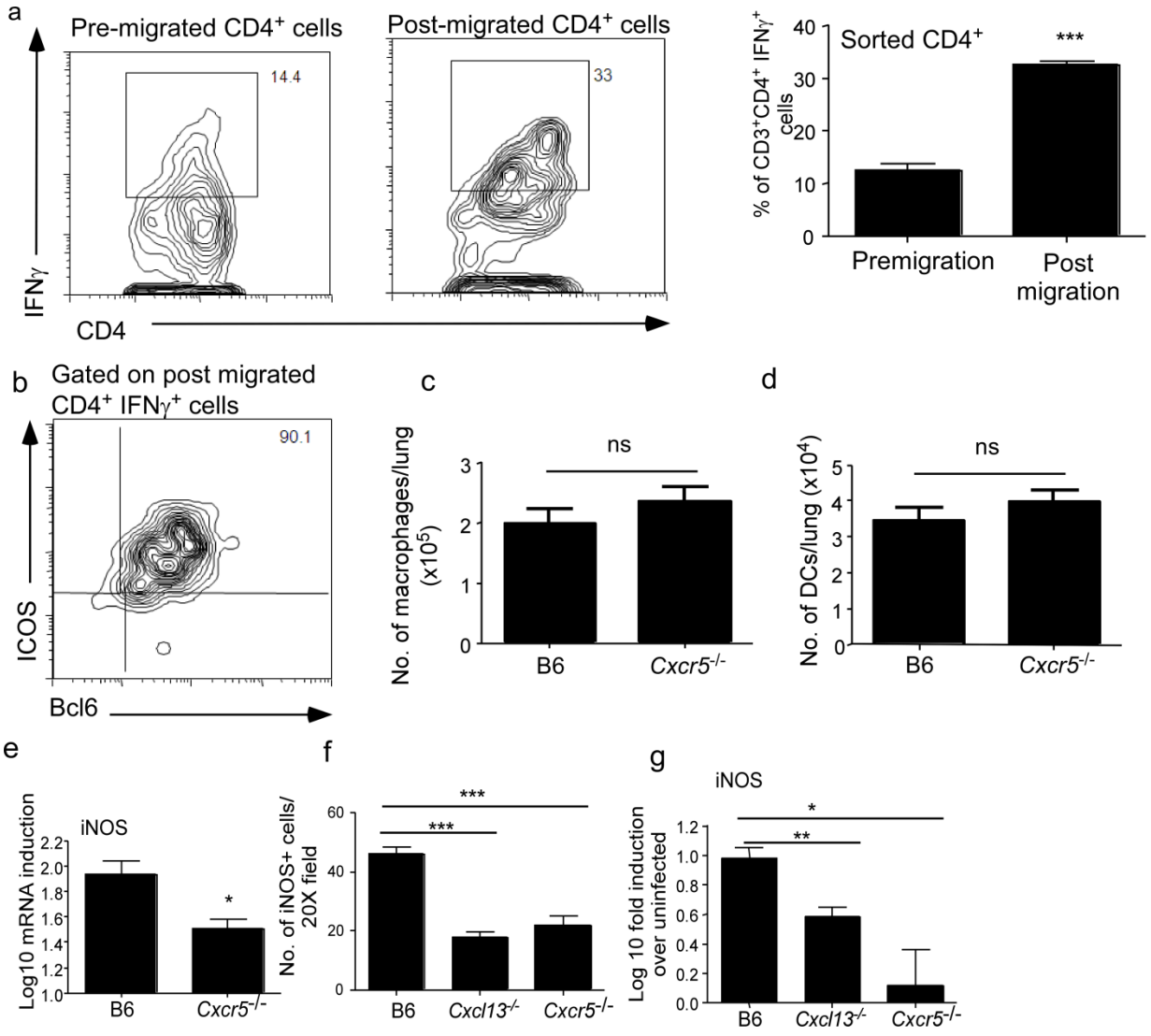

Figure 16: CD4$^+$ T cells responsive to CXCL13 produce IFNγ and are critical for macrophage activation.

CD4$^+$ T cells were sorted from day 21 Mtb-infected B6 lungs and assayed in vitro for chemotaxis migration assay towards CXCL13 (500 ng/ml). The ability of CD4$^+$ T cells to produce IFNγ pre- and post-migration was determined by intracellular staining and flow cytometry in PMA/Ionomycin stimulated cells (a). A representative contour plot showing surface expression of Bcl6 and ICOS on CD4+ T cells that was determined by flow cytometry (b). B6 and *Cxcr5-/-* mice were infected as mentioned in Figure 6. The number of lung macrophages (c) and dendritic cells (d) were determined by flow cytometry on day 21 post infection. Log10 fold induction of iNOS mRNA in B6 and *Cxcr5-/-* Mtb-infected lungs relative to levels in uninfected lungs was determined by RT-PCR on day 21 post infection (e). FFPE lung sections from day 21 Mtb-infected B6, *Cxcr5-/-* and *Cxcl13-/-* mice were analyzed by immunofluorescence for number of iNOS+ cells per granuloma (f). On day 21 post infection, lung CD11c+ cells were isolated from uninfected or Mtb-infected B6, *Cxcr5-/-* and *Cxcl13-/-* mice. iNOS mRNA expression in CD11c+ cells isolated from infected mice over levels detected in uninfected controls was determined by RT-PCR (g). The data points represent the mean (±SD) of values from 3-6 samples (a-g). *p=0.05, **p=0.005, p***=0.0005.

restored lung lymphocytic infiltrates, T cell localization, restored generation (Figure 17c) and organization of ectopic lymphoid follicles in *Cxcr5*$^{-/-}$ mice (Figure 17b, c), and activation of lung macrophages (Figure 17c-lower panel). Tracking of congenic, CD90.2^{+} ESAT-6 Tg cells in Mtb-infected congenic CD90.1^{+} mice, revealed that adoptively transferred naive Tg Th0 cells had underwent activation and acquired the expression of CXCR5, ICOS, PD-1 and the ability to produce proinflammatory cytokines (Figure 17d).

3.4.8 Adoptive Transfer of B6 but not *Cxcr5-/-* CD4^{+} T cells rescues Mtb-infected *Cxcr5-/-* mice

To definitely prove that CXCR5 expression on CD4+ T cells was responsible of for the rescue of *Cxcr5* deficient mice, *Cxcr5-/-* CD4^{+} T cells were utilized. We show that the increased bacterial burden (Figure 18a) and decreased lymphoid follicle organization (Figure 18b, c) and macrophage activation (Figure 18c, d) in Mtb-infected *Cxcr5*$^{-/-}$ mice could only be reversed by adoptive transfer of CD4^{+} T cells isolated from B6 mice, but not by transfer of CD4^{+} T cells isolated from *Cxcr5*$^{-/-}$ mice. These data together show that adoptive transfer of uncommitted Th0 cells, capable of acquiring expression of CXCR5, restored strategic T cell localization within the lung, formation of lymphoid structures and reversed susceptibility to TB.

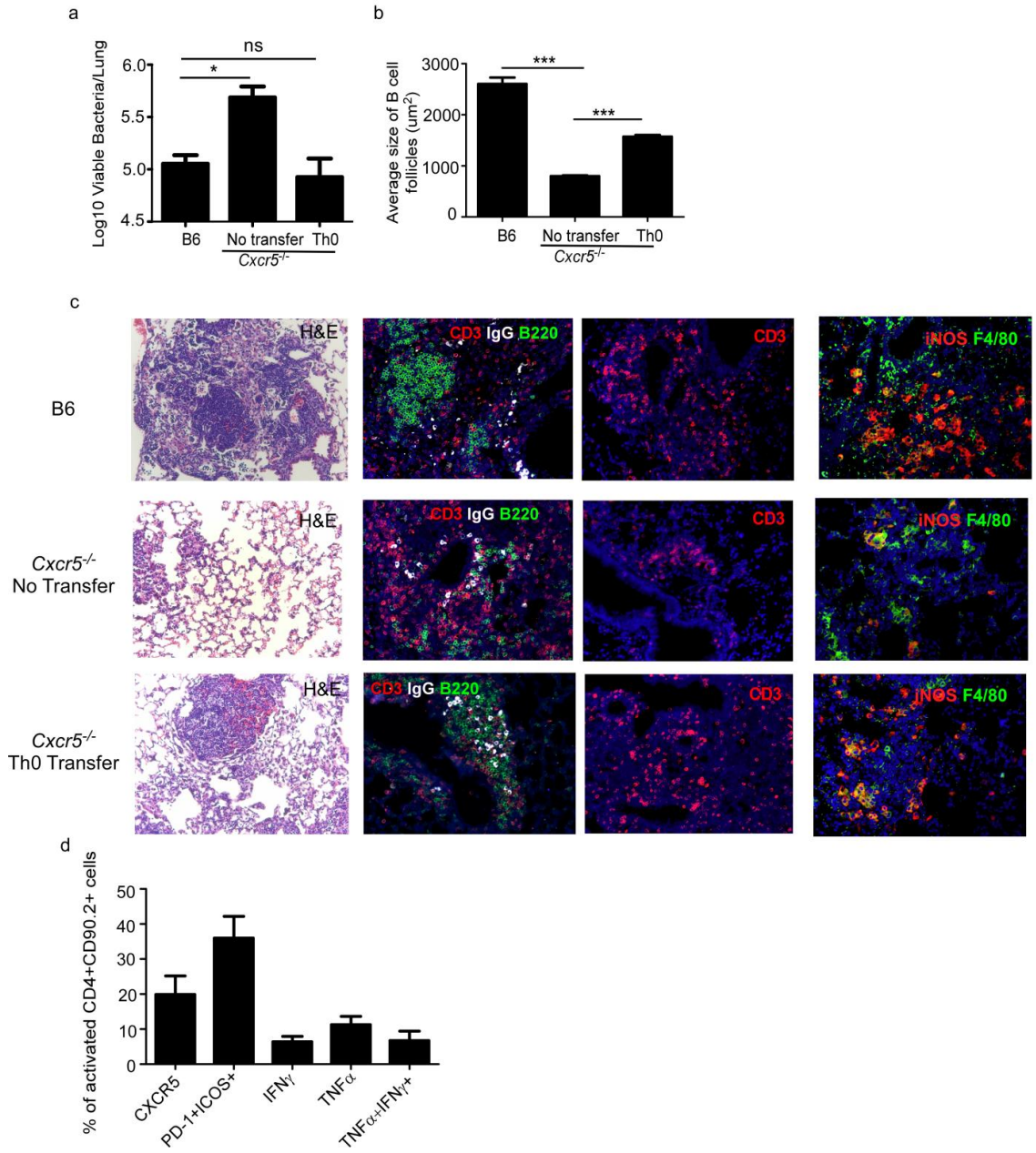

Figure 17: Adoptive transfer of ESAT-6 Tg Th0 cells rescues T cell localization and protection in *Cxcr5-/-* mice.

2-5x10^6 in vitro generated ESAT-6 Tg Th0 cells were adoptively transferred into *Cxcr5-/-* mice. 24 hours later, mice were infected as in Figure 6 and lung bacterial burden determined on day 50 (a). The average size of B cell lymphoid follicles was quantified in B6 and *Cxcr5-/-* Mtb-infected lungs on day 50 using the Zeiss Axioplan microscope (b). Pulmonary granuloma and B cell lymphoid follicle formation was assessed in FFPE lung sections that were stained with H&E; CD3, IgG, B220; CD3 alone; iNOS, F4/80 on day 50 (b,c). Original magnification for H&E sections, 50X; immunofluorescent sections, 200X. 2-5x10^6 ESAT-6 Tg $CD4^+$ Th0 cells were adoptively transferred into congenic CD90.1 B6 mice and infected as in Figure 6. The frequency of cells expressing different molecules was determined in PMA/Ionomycin stimulated CD90.2 Tg cells isolated from infected lungs on day 21 (d). The data points represent the mean (±SD) of values from 4-6 mice (a-d). *p=0.05, ***p=0.0005. ns-not significant.

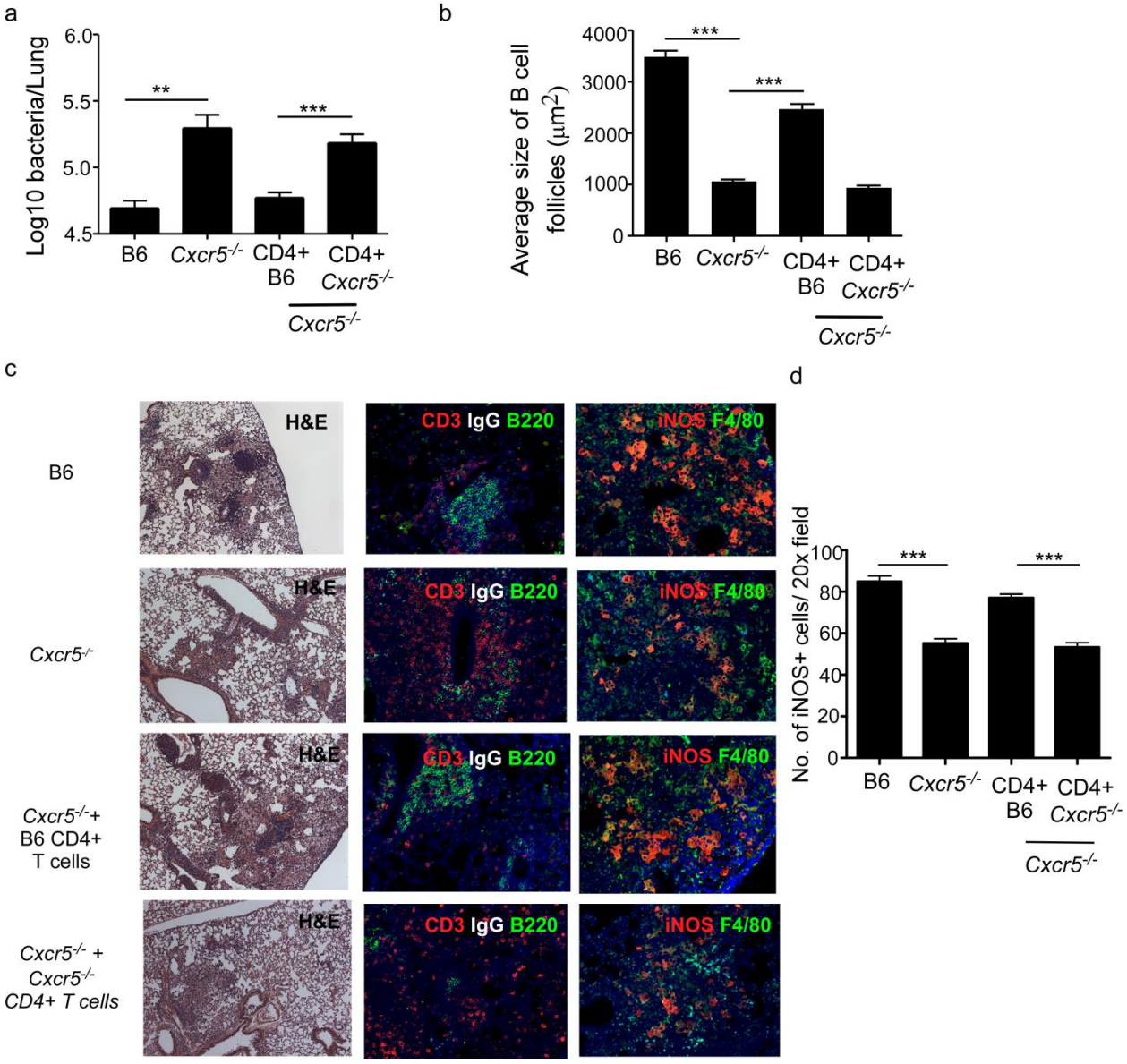

Figure 18: Adoptive transfer of B6, but not *Cxcr5*-/- CD4$^+$ T cells, rescues T cell localization and protection in *Cxcr5*-/- Mtb-infected mice.

2x10^6 CD4$^+$ B6 or *Cxcr5*-/- T cells were adoptively transferred into *Cxcr5*-/- mice. 24 hours later, mice were infected as in Figure 3 and lung bacterial burden determined on day 50 (a). The average size B cell lymphoid follicles was quantified in FFPE lung sections on day 50 using the Zeiss Axioplan microscope (b). Pulmonary granuloma and B cell lymphoid follicle formation was assessed in FFPE lung sections that were stained with H&E; CD3, IgG, B220; iNOS, F4/80 on day 50 (b,c). The number of iNOS$^+$ cells were quantitated using the Zeiss Axioplan Microscope (d). Original magnification for H&E sections, 50X; immunofluorescent sections, 200X. The data points represent the mean (+SD) of values from 4-6 mice (a-d). p**=0.005, ***=0.0005.

3.4.9 IL-6 and IL-21 are required for optimal B cell lymphoid follicle formation, but are not essential for Mtb control

IL-21 and IL-6 are required for polarization of Tfh cells [237, 241, 246]. Coincident with the early accumulation of $CD4^+$ $CXCR5^+$ Tfh-like cells in Mtb-infected lungs, IL-6, IL-21, ICOS and PD1 mRNA induction occurred in day 21-Mtb-infected lungs[80] (Table 4). Therefore, we tested whether absence of IL-6 and IL-21 impacts protective immunity to TB and found that B cell follicle formation was reduced, but not absent, in *Il21*$^{-/-}$ and *Il6*$^{-/-}$ Mtb-infected lungs (Figure 19 a,b,d,e) and did not impact lung bacterial control during Mtb infection (Figure 19 c, f) . These data suggest that although IL-6 and IL-21 are required for optimal generation of lymphoid structures, either IL-6 or IL-21 alone are sufficient for mediating protective immunity against TB.

Table 4: Genes induced during murine TB are associated with generation of Tfh-like cellular responses [80].

Fold induction of mRNA in Mtb-infected lungs over levels found in uninfected lungs shown. D-12, day 12 post infection; D-15, day 15 post infection; D-21, day 21 post infection. FC= fold change, q-val= q value.

			D-12		D-15		D-21	
EntrezID	Symbol	GeneName	FC	q-val	FC	q-val	FC	q-val
16193	IL6	Interleukin 6	-1.00	1.39	1.45	0.22	53.96	**0.0000**
60505	IL21	interleukin 21	1.00	1.09	-1.00	1.38	3.10	**0.0172**
54167	ICOS	inducible T-cell co-stimulator	-1.01	1.39	1.23	0.65	56.62	**0.0000**
58205	PDCD1LG2	programmed cell death 1 ligand 2	-1.02	1.34	1.01	1.36	15.14	**0.0001**
18566	PDCD1	programmed cell death 1	-1.01	1.37	-1.00	1.39	4.98	**0.0030**

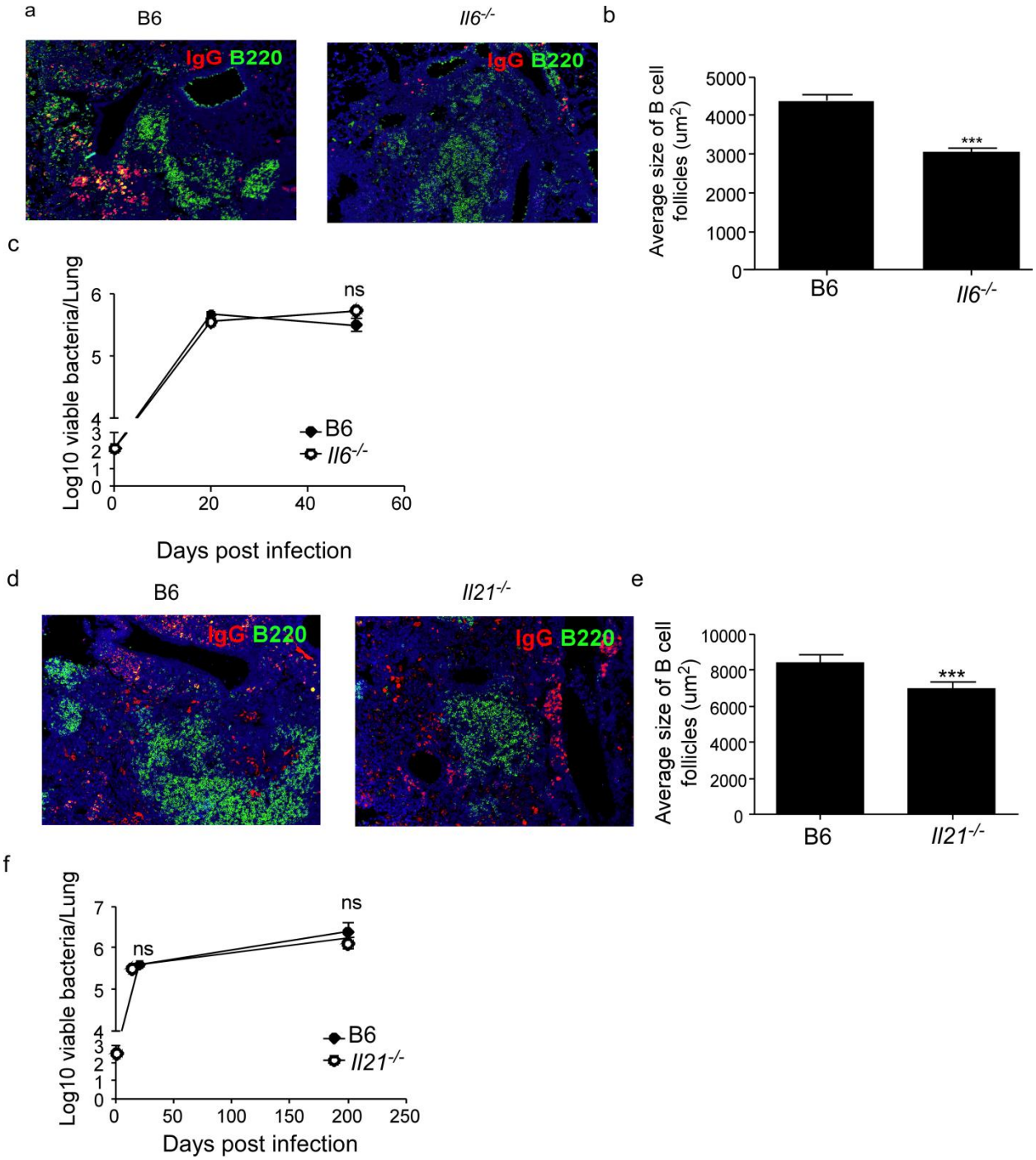

Figure 19: IL-6 and IL-21 are required for optimal B cell lymphoid follicle formation, but are not essential for Mtb control.

B6 and *Il6-/-* mice or B6 and *Il21-/-* mice were infected as in Figure 6. At day 50 post infection, FFPE lung sections were assessed for B cell lymphoid follicle organization by immunofluorescence, 200X magnification (a, d). The average size of B cell lymphoid follicles (b,e) and lung bacterial burden were determined at different time points post infection (c, d). The data points represent the mean (±SD) of values from 4-6 mice (a-f). ***p=0.0005. ns=not signigicant.

3.5 DISCUSSION

We have previously shown that ectopic lymphoid follicles in granulomas are associated with immune control (previous chapter), but the mechanism of formation and protective immunity in Mtb infection remain unknown. Using the mouse model of TB, we identified two CXCR5 expressing cell populations within the lung during Mtb infection, a $CD4^+$ T cell and $B220^+CD19^+$ B cell. We show that $CD4^+CXCR5^+$ T cells are the critical cellular component of ectopic lymphoid follicles that contribute to protective immunity against TB. $CD4^+CXCR5^+$ T cells expressed a Tfh-like cell phenotype, while concurrently also expressing Th1 cytokines and surface markers. Our data prove that potent activated Th1 cytokine producing $CXCR5^+$ Tfh-like cells localize to CXCL13 to position near Mtb-infected macrophages to activate and promote bacterial killing. Although, ectopic lymphoid follicle formation correlated with Mtb protective immunity, it was the recruitment of $CD4^+CXCR5^+$ T cells that specifically contributed to host defense against Mtb. Our results have far implications in the role of ectopic lymphoid follicles in infectious disease and autoimmunity. Further, these data has significant implications for future therapies and vaccine design against TB.

Using *Cxcr5* deficient mice, we found that expression of CXCR5 on T cells is not required for recruitment of T cells to the Mtb-infected lung, but is essential for T cell localization in the parenchyma near infected macrophages. Importantly, localized $CD4^+CXCR5^+$ T cells were required for macrophage activation and Mtb control in *Cxcr5* deficient mice. The *Cxcr5*-/- phenotype is unique in that these mice lack the majority of lymph nodes and have defective splenic architecture [249]. Despite the absence of lymph nodes, mice demonstrated no defects in T cell priming with similar numbers of Mtb-specific Th1 cytokine producing $CD4^+$ T cells in the lung, which is consistent with previous reports in other antigen models [250]. Further, similar

findings in SLO deficient B6 mice, which are still able to control Mtb, and *Ccr7-/-* mice show adaptive T cell responses that prime in the lung [148, 251]. *Cxcr5* deficient mice did not affect the number of $ICOS^{+}PD\text{-}1^{+}$ or $CXCR3^{+}CD4^{+}$ T helper cells arriving in the lung or the production of proinflammatory IFNγ and TNFα levels further substantiating that CXCR5 does not affect Tfh or Th1 effector expression. However, *Cxcr5*-/- mice did exhibit reduced activation determined by *iNOS* expression with similar numbers of myeloid cells in the lung suggesting T cell localization mediated by CXCR5 is necessary for myeloid cell activation and Mtb control. Importantly, mice that received Mtb-antigen specific $CD4^{+}$ T cells or wild type $CD4^{+}$ CXCR5 expressing T cells were able to rescue T cell localization, macrophage activation, ectopic lymphoid follicle formation, and bacterial control suggesting that it is indeed the CXCR5 expression on $CD4^{+}$ T cells that confers protective immunity in ectopic lymphoid follicles. This mechanism is likely conferred by localization of Th1 cytokine producing $CD4^{+}CXCR5^{+}$ T cells near Mtb-infected macrophages inducing activation and bacterial control. It is further possible that CXCR5 expressing T cells also regulate adhesion molecules and chemokine expression by other inflammatory cells inducing cellular organization, which should be further investigated.

It is becoming clear that some T helper cell phenotypes maintain a degree of plasticity [63, 252-253]. Although in vitro generated Tfh cells typically produce classic Tfh cytokines, namely IL-21, and lineage specific transcription factors (BCL-6), in vivo generated Tfh cells can co-express multiple transcription factors in addition to BCL-6 and produce IFNγ, IL-4, and IL-17a [237, 241, 246, 254-256]. Therefore, it appears Tfh cells are heterogeneous becoming either Th1/Th2/Th17 cells that are recruited to the B-T cell border for help and induction of class-switching in B cells or possibly being driven towards a lineage-specific phenotype in response to antigen stimulation. Tfh cells were driven towards a Th1 phenotype in response to immunization with a protein

antigen in adjuvant [257] and infection with *Leishmania major* [256] and *Toxoplasma gondii* [258] inducing class switching to IgG2a. In addition, in response to Th2 driving pathogens, *Schistosoma mansoni* [259] and *Heligmosomoides polygyrus* [255] drove generation of IL-4 producing Tfh cells. Recently, studies found that Tfh cells share a transition stage with Th1 cells through STAT4, which induced the expression of T-bet concomitantly with BCL-6 [258]. Cells were therefore capable of expressing dual lineage characteristics and functionalities. Our data support this model, as $CD4^+$ T cells generated during Mtb infection coexpressed both markers of Th1 and Tfh cells to become the highest producer of pro-inflammatory cytokines that were crucial for mediating protective immunity. Protective immunity produced by Th1 cytokine producing $CD4^+CXCR5^+$ T cells is consistent with studies showing that defense against Mtb is mediated by proinflammatory cytokines and $CD4^+$ T cells that can produce multiple Th1 cytokines [51, 106].

Expression of CXCR3 can also be found on a subset of $CD4^+CXCR5^+$ T cells. CXCR3 is a chemokine receptor normally associated with localization of Th1 cells and accordingly multiple CXCR3 ligands, CXCL9, CXCL10, and CXCL11 are induced in the Mtb-infected lung [35, 133, 260-262]. It is possible that $CD4^+CXCR5^+CXCR3^+$ T cells use CXCR3 and other chemokine receptors to get to the lung and use CXCR5 to position within the parenchyma near Mtb-infected macrophages for activation. Thus, it is tempting to speculate that CXCR3 may be down regulated upon arrival to the lung generating a $CXCR5^+CD4^+$ T cell population. Consistent with hypothesis, *Cxcr3-/-* are not more susceptible to Mtb infection, however, *Cxcr5*-/- and *Cxcl13*-/- have higher bacterial burdens and decreased macrophage activation with in the lung [24, 136]. Further, CCR2 [263], CCR5 [264], and CCR7 [148] deficient mice, chemokine receptors also expressed on T cells during Mtb infection, are also not more susceptible to low dose Mtb infection suggesting that redundancy in chemokine expression allow for $CD4^+$ T cells to arrive to the lung,

but only CXCR5 expression is indispensable for localization of $CD4^+$ T cells near infected macrophages.

The role of B cell effector functions and antibody responses in Mtb protective immunity is a ongoing area of study as some reports suggest B cells are not essential for protection, while others refute this claim. B cells are a principal component of the Mtb-infected lung with B cell aggregates observed in human TB granulomas [11, 79, 223], A-TB NHP granulomas [78], and Mtb-infected mouse granulomas [24, 147]. Recently, B cell deficient mice in a low dose aerosol model of Mtb infection controlled bacteria in the lung [77], which we also found in our low dose mouse model. Further, these mice had similar levels of macrophage activation compared to wild type mice. Importantly, although these mice did not form ectopic lymphoid follicles, they were still able to localize $CXCR5^+CD4^+$ T cells within the parenchyma. In addition, adoptive transfer of B6 T cells expressing CXCR5, but not *Cxcr5-/-* T cells were able to rescue ectopic lymphoid follicle formation, bacterial burden, and macrophage activation in *Cxcr5-/-* mice. These data suggest that despite both T cell and B cell populations expressing CXCR5, it is the $CXCR5^+CD4^+$ T cells population that is responsible for protective immunity. Ectopic lymphoid follicles appear to form in response to correct T cell localization within the lung and can be used as a correlate of protection, but the structure itself may not be necessary for Mtb control. Determining the direct role of $CXCR5^+CD4^+$ T cells and ectopic lymphoid follicles in Mtb-infected humans is a challenging task, but needs to be addressed to understand the potential use of these cells and markers in future treatment and prevention strategies.

3.6 ACKNOWLEDGEMENTS

The author would like to acknowledge Javier Rangel-Moreno, PhD for immunofluorescence staining and Alison Logar for technical assistance with flow cytometry. Further, the author would also like to thank you Radha Gopal, PhD for expertise in ELISpot assay and Yinyao Lin, PhD for assistance with animal infection and viable count. An additional thanks is offered to Nikhil Nuthalapati and Hillary Cleveland for assisting in mouse husbandry. Finally, we also thank Smriti Mehra and Deepak Kaushal, PhD for providing latent and active NHP lung samples and Beth A. Fallert-Junecko and Todd Reinhart, ScD (University of Pittsburgh, PA) for performing the CXCL13 in situ hybridization. This work was supported by Children's Hospital of Pittsburgh; NIH grants A1083541 and HL105427 to S.A. Khader, PhD; RR026006, AI091457, RR020159 and Tulane Primate Center base grant to D. Kaushal, PhD; HL69409 to T.D. Randall, PhD; and AI060422 to T.A. Reinhart, ScD; start-up funds from the Department of Medicine, University of Rochester, and AI91036 to J. Rangel-Moreno, PhD; T32 AI065380-08 grant to S.R. Slight; and a Research Advisory Committee Grants from Children's Hospital of Pittsburgh of the UPMC Health System to S.R. Slight and Y. Lin, PhD.

4.0 PULMONARY CXCL13 PRODUCTION DURING *M. TUBERCULOSIS* INFECTION

4.1 ABSTRACT

CXC chemokine ligand (CXCL)-13 is constitutively expressed in SLOs and is induced in the lung during *M. tuberculosis* infection. Localization of CXCL13 is confined within distinct ectopic lymphoid follicles near the granuloma. Although it is known that follicular dendritic cells and other stromal cells produce CXCL13 in the lymph node, the cellular source of CXCL13 in early and late TB infection remains to be defined. We found in Mtb-infected mice that stromal cells, FDCs, and DCs within the lung produced CXCL13. To determine whether hematopoietic or non-hematopoietic cells contributed more to immune protection and whether production was similar in both early (day 30) and late (day 50) infection, *Cxcl13* bone marrow chimeras were generated. Mice deficient in *Cxcl13* within non-hematopoietic cells were more susceptible early in infection, while both hematopoietic and non-hematopoietic cells producing CXCL13 were required for protective immunity in chronic Mtb infection. Further, non-hematopoietic *Cxcl13* deficient mice were unable to develop protective lymphoid follicles. Our data establish the importance of CXCL13 production in Mtb infection by both hematopoietic and non-hematopoietic cell subsets.

4.2 INTRODUCTION

CXCL13 is an 88 amino acid CXC-chemokine that was first discovered in 1998 and has sequence similarity to CXCL1, CXCL10, and CXCL12 although it performs a very different function [151, 234]. CXCL13 is a homeostatic chemokine that is normally expressed within SLOs and is important for B cell follicle formation and polarization of the germinal center light and dark zones [151, 234, 265]. Further, expression of CXCL13 is critical in ELO formation in certain autoimmune and infectious diseases indicating it is also an inducible chemokine (discussed in detail in Section 1.5). Initial production of CXCL13 in lymph node development is initiated by $CD4^+CD3^-$IL-7Rα^+ lymphoid tissue inducer (LTi) cells [266-267]. LTi cells express LT$\alpha\beta$ on their surface and engage the LTβR on mesenchymal cells to produce homeostatic chemokines, such as CXCL13 [267-268]. Mesenchymal cells differentiate into a variety of cells types including follicular dendritic cells, the main producer of CXCL13 in the SLO, and other stromal cells [172]. CXCL13 then recruits CXCR5 expressing cells, mature B cells and Tfh cells, within the lymph node [151, 153, 234]. B cells participate in CXCL13 production by upregulated LTα1β2 in response to the chemokine, which interacts with FDCs to further promote CXCL13 production [152]. In addition, Tfh cells also appear to play a role in the production of CXCL13 as genome wide approaches have suggested the *Cxcl13* gene is highly upregulated in this T cell lineage [269-270]. Thus multiple cell types are responsible for CXCL13 production in SLO formation and maintenance.

Other cell subsets have been implicated in the production of CXCL13 outside of SLOs, however, little is known regarding the production of CXCL13 in ELOs. In ectopic follicles of rheumatoid arthritis and ulcerative colitis patients, CXCL13 was produced by monocytes and macrophages, and FDCs [192]. Further, in human blood DCs exposed to influenza virus, CXCL13

protein could be detected in supernatants in just 8 hours [271]. In this study, we investigate the source of CXCL13 during Mtb infection in murine ectopic lymphoid follicles. We found that CXCL13 was produced by both hematopoietic and non-hematopoietic cells subsets, namely FDCs, non-FDC stromal cells, and DCs, but not lymphocytes. Further, we demonstrated that non-hematopoietic cell are critical for CXCL13 production early in Mtb infection while non-hematopoietic and hematopoietic subsets both contribute later during infection. These data suggest that multiple stromal and myeloid cell subsets are necessary for pulmonary CXCL13 induced ectopic lymphoid development in the Mtb-infected lung and that non-hematopoietic stromal cells are essential for early initiation.

4.3 MATERIAL AND METHODS

4.3.1 Mtb Infection in Mice

Mice were infected as previously described in Section 3.3.1.

4.3.2 Generation of Lung Cell Types

For generation of lung fibroblasts, lungs were perfused with 5 units/ml dispase followed by 1% low melting agarose in PBS, washed in PBS and incubated in dispase for 30 minutes at 37^{o}C. Single cell suspensions were then obtained from DNase/Collagenase treated lungs and fibroblasts generated by passaging 2-4 times. Lung alveolar macrophages were obtained by bronchoalveolar lavage as previously described [247]. Lung CD11c^{+} cells were sorted from single

cell lung suspensions using a magnetically labeled CD11c positive isolation kit (Miltenyi Biotech, CA). Mouse tracheal epithelial cells (MTECs) were generated using an air-liquid interface culture as previously described [272]. All the different cell types were stimulated with irradiated Mtb (100 μg/ml) for 24 hours and cells supernatants analyzed for CXCL13 protein.

4.3.3 Protein Estimation by ELISA

Mouse Duoset ELISA antibody pairs from R&D Systems were used to detect CXCL13 protein levels in the supernatant according to manufacturer's protocol. In some experiments protein levels were measured using a mouse Luminex assay (Linco/Millipore).

4.3.4 Generation of Bone Marrow Chimeric Mice

To generate chimeric mice, mice were given a medicated Sulfa-Trim diet containing 1.2% sulfamethoxazole and 0.2% trimethoprim (TestDiet) two weeks prior to irradiation. Mice were sub-lethally irradiated with 1000 rads in two doses (X-Rad 320). Mice were subsequently reconstituted with $10x10^6$ bone marrow cells from B6 or gene deficient mice via i.v. injection. Mice were allowed to reconstitute for 45 days while continuing to receive a Sulfa-Trim and acidified water diet following which they were used in experimental procedures.

4.3.5 Morphometric Analysis and Immunofluorescence

Immunofluorescence was performed as previously described in Section 2.3.4. In addition, DCs and stromal cells were stained with PE-hamster anti-mouse CD11c (HL3, BD Pharmingen) and

PE-mouse anti-mouse CD157 (BP3, BD Pharmingen). To amplify the signal, a rabbit, anti-PE antibody (Rockland Inc) was used, followed by its detection with Fab, donkey-anti rabbit-Cy3 (Jackson Immunoresearch Laboratories).

4.3.6 CXCL13 In Situ Hybridization

Performed as previously described in Section 2.3.5.

4.3.7 Statistics

Differences between the means of experimental groups were analyzed using the two tailed Student's t-test. Differences were considered significant when $p \leq 0.05$.

4.4 RESULTS

4.4.1 CXCL13 is produced by hematopoietic and non-hematopoietic cells during Mtb infection

Our data suggest that $CD4^+$ $CXCR5^+$ T cells producing proinflammatory cytokines that accumulate in the lung respond to a pulmonary CXCL13 gradient. Accordingly, CXCL13 is known to be produced by DCs [192, 273], FDCs [274-276] and stromal cells [277] in SLOs. Following Mtb infection, we detected increased expression of CXCL13 protein in lung homogenates (uninfected: 42+/- 10.03 pg/ml, Mtb-infected: 452.96 +/- 82.3, p=0.001) and CXCL13 protein was found to co-localize with lung $BP3^+$ stromal cells, CD21-$CD35^+$ FDCs and $CD11c^+$ DCs in

ELOs (Figure 20a). Furthermore, when lung alveolar macrophages, $CD11c^+$ cells, mouse tracheal epithelial cells and fibroblasts were exposed to Mtb in vitro, CXCL13 protein was detected in supernatants from myeloid cells and fibroblasts, but not epithelial cell supernatants, suggesting that both hematopoietic and non-hematopoietic cells produce CXCL13 during Mtb infection (Figure 20b). Also, both $CD11c^+$ and $CD11c^-$ cells isolated from Mtb-infected B6 lungs expressed CXCL13 mRNA (Figure 20c).

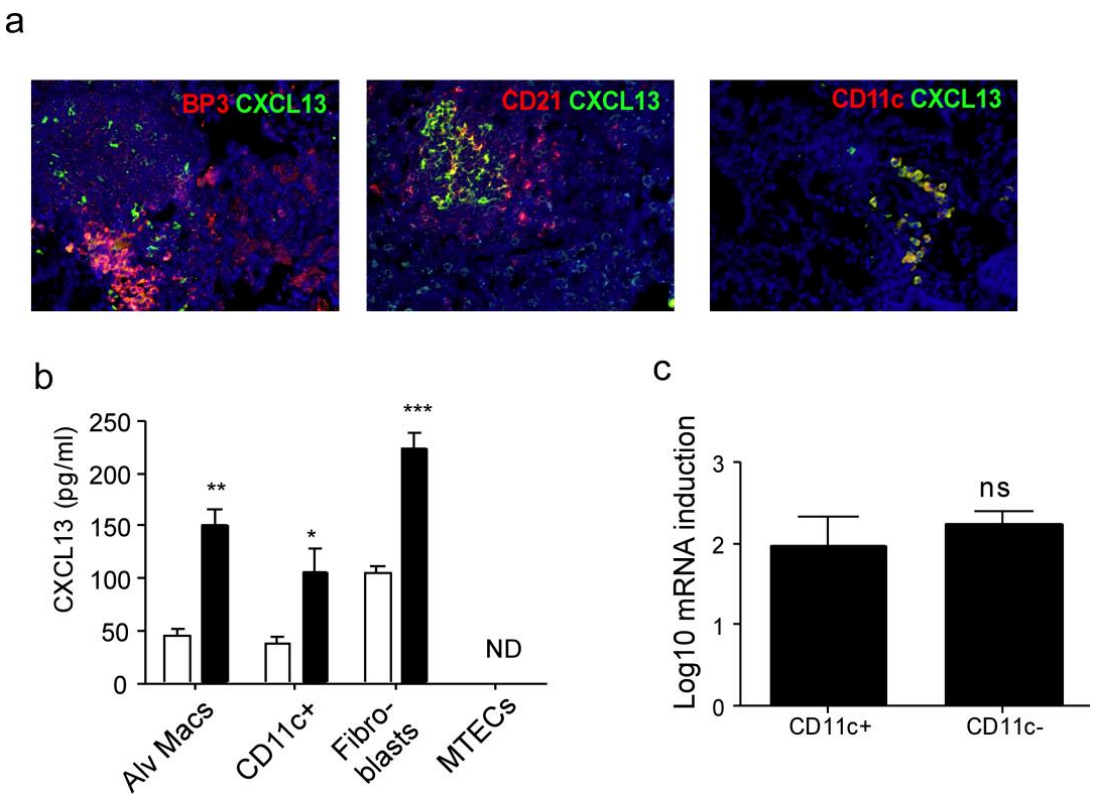

Figure 20: CXCL13 is produced by stromal and myeloid cells in Mtb infection.

FFPE lung sections from B6 Mtb-infected mice were assessed for CXCL13-producing populations by immunofluorescence (a). Alveolar macrophages, lung CD11c+ cells, lung fibroblasts, and mouse tracheal epithelial cells (MTECs) were left untreated or treated with irradiated Mtb (100 mg/ml) for 24 hours and supernatants assayed for CXCL13 protein (b). ND-not detectable. CD11c+ and CD11c- cells were sorted from B6 Mtb-infected lungs (day 50 post infection) and log10 fold induction of CXCL13 mRNA relative to GAPDH was determined by RT-PCR (c). Immunofluorescence original magnification 200X. The data points represent the mean (±SD) of values from 3-4 samples (a-b) or from 4-6 mice (c). *p=0.05, **=0.005, ***p=0.0005. ns= not significant. One experiment representative of two is shown.

4.4.2 CXCL13 by different cell populations is critical in early and late Mtb infection

To delineate the protective contributions of CXCL13 production by hematopoietic and non-hematopoietic cells, we infected hematopoietic *Cxcl13*$^{-/-}$ bone marrow chimeric (BMC) mice (B6 host/-/- BM) or non-hematopoietic *Cxcl13*$^{-/-}$ BMC mice (-/- host/B6 BM) with Mtb. As expected [24], complete *Cxcl13*$^{-/-}$ BMC mice (-/-host/-/- BM) were more susceptible to Mtb infection than complete B6 BMC mice (B6 host/B6 BM) (Figure 21a). Interestingly, non-hematopoietic, but not hematopoietic *Cxcl13*$^{-/-}$ BMC mice had increased lung bacterial burden at early time points (Figure 21a), while at later time points, both hematopoietic and non-hematopoietic *Cxcl13*$^{-/-}$ BMC mice had increased lung bacterial burden (Figure 21b), decreased T cell localization within the lung and reduced lymphoid structure formation when compared to B6 Mtb-infected lungs (Figure 21c, d). Furthermore, hematopoietic *Cxcl13*$^{-/-}$ BMC mice which were protected during early infection, had more distinct T cell localization within the lung, highly organized B cell lymphoid follicle structures (Figure 21 c, d) and increased CXCL13 mRNA expression within lymphoid structures (Figure 21e). These data show that both hematopoietic and non-hematopoietic sources of CXCL13 are required for lymphoid structure formation and protective immunity against Mtb infection, but that non-hematopoietic sources of CXCL13 are required for early protective immunity during TB.

4.5 DISCUSSION

Using the Mtb mouse model, we demonstrated that FDCs, non-FDC stromal cells, and DCs, all produce CXCL13 within pulmonary ectopic lymphoid follicles. However, we did not

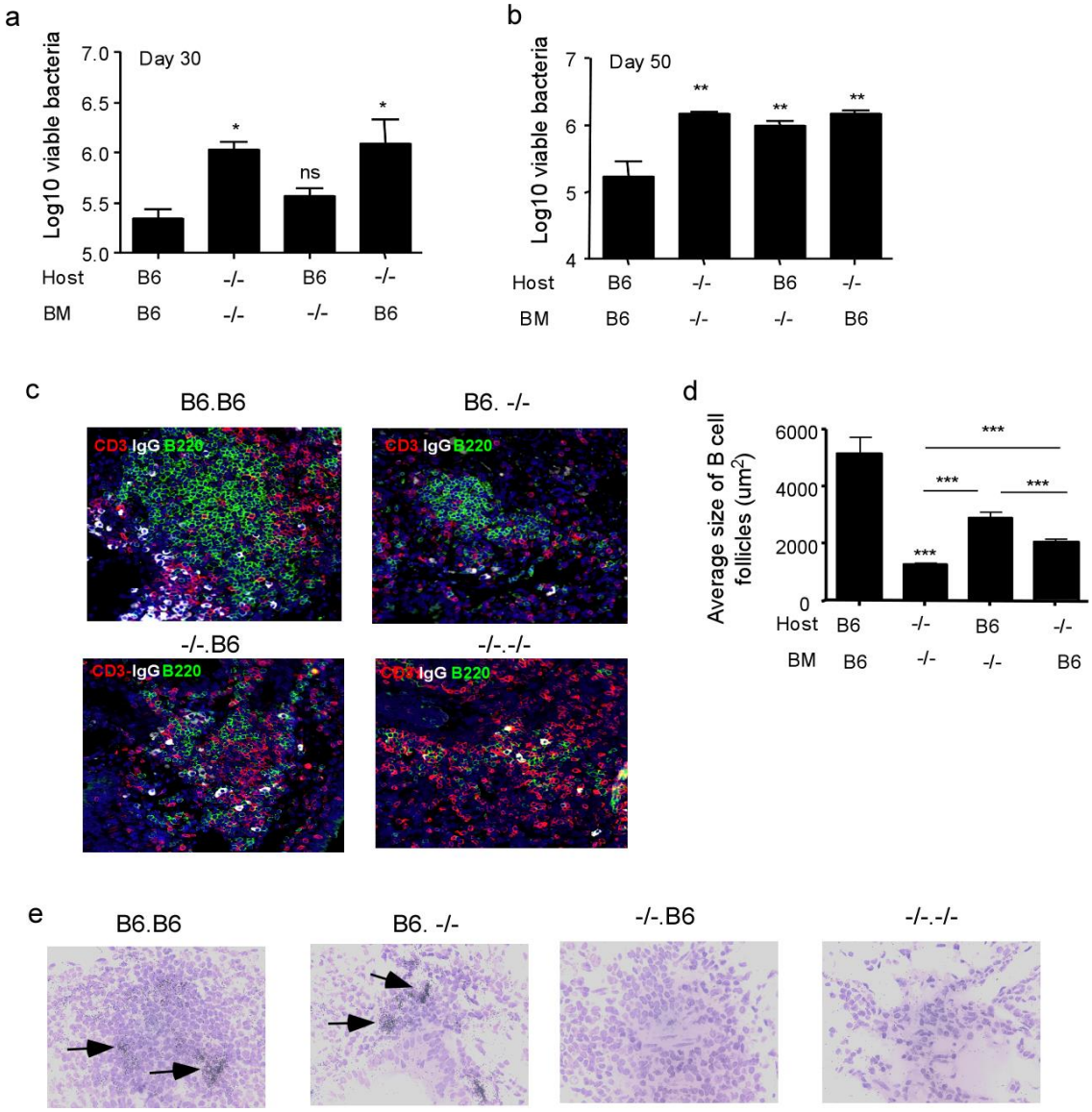

Figure 21: CXCL13 is produced by hematopoietic and non-hematopoietic cells and required for Mtb control.

Hematopoietic Cxcl13-/- BMC mice (B6 host/-/- BM), non-hematopoietic Cxcl13-/- BMC mice (-/- host/B6 BM), complete Cxcl13-/- BMC mice (-/- host/-/-BM) and complete B6 BMC mice (B6 host/B6 BM) were infected with Mtb and lung bacterial burden determined on day 30 (a) and day 50 (b). Pulmonary B cell lymphoid follicles were detected in FFPE lung sections (day 50) by immunofluorescent staining for CD3, IgG, and B220; DAPI (blue) was used to detect nuclei (c). Average size of the B cell lymphoid follicles was quantified using the Zeiss Axioplan microscope (day 50) (d). Day 30 FFPE lung sections were assayed for CXCL13 mRNA localization by ISH (e). Black arrows indicate CXCL13 localization within granulomas (e). ISH original magnification 600X. Immunofluorescence original magnification 200X. The data points represent the mean (±SD) from 4-6 mice (a-e). *p=0.05, **=0.005, ***p=0.0005. ns= not significant. One experiment representative of two is shown.

observe CXCL13 localization with any lymphocytic subset as implied by previous genome array studies [269-270]. Further, in vitro data verified the capability of both stromal and myeloid cells to produce CXCL13 in response to Mtb. In addition, we characterized the importance of different cell subsets in the initiation of ectopic lymphoid follicle formation and we found that non-hematopoietic subsets are essential for the earliest production of CXCL13 in the Mtb-infected lung as *Cxcl13-/-* non-hematopoietic bone marrow chimeric mice were unable to control infection and to form ectopic lymphoid follicles. However, later during infection (day 50), when inflammatory immune cells have infiltrated the lung, both non-hematopoietic and hematopoietic cell subsets contributed to ectopic lymphoid follicle formation and protective immunity against Mtb. Our data prove that different cellular sources of CXCL13 in ectopic lymphoid tissues can impact progression of disease and protective outcomes in chronic infections. Further, varying sources of CXCL13 ensure that $CXCR5^+$ cells respond and migrate to the lung to elicit the highest protective immune response against Mtb.

With our data and previous studies [170, 184, 191, 194], a likely mechanism of ectopic lymphoid follicle development unfolds. It is probable that either LTi cells or TNFα and LT-α induced by Mtb initiate production of CXCL13 in stromal cells. As infection progresses, FDCs and reticular networks develop further contributing to CXCL13 production. Further, inflammatory myeloid cells are recruited in large numbers to the lung, which also have the potential to produce CXCL13 later in infection. Upon formation of ectopic lymphoid follicles, B cells likely establish a positive feedback loop with FDCs promoting the maintenance of CXCL13 [152], however, this help is dispensable in Mtb infection. Induction of CXCL13 further recruits a Tfh-like Th1 proinflammatory producing $CD4^+CXCR5^+$ T cells that localizes near Mtb-infected macrophages promoting activation and bacterial killing and thus immune control in the lung. Additional

studies are required to understand the earliest mechanisms of CXCL13 production in FDCs, stromal cells, and DCs, but these studies are clear in the importance of CXCL13 for immune control of Mtb and protective ectopic lymphoid follicle formation in the lung. These studies have contributed greatly to the understanding of Mtb immune responses and the formation of ectopic lymphoid organs during infection.

4.6 ACKNOWLEDGEMENTS

The author would like to acknowledge Javier Rangel-Moreno, PhD for immunofluorescence staining and Beth A. Fallert-Junecko and Todd Reinhart, ScD (University of Pittsburgh, PA) for performing the CXCL13 in situ hybridization. Further, the author would like to also thank John Alcorn, PhD for assistance in isolation of alveolar macrophages and David Askew for mouse tracheal epithelial cell isolation and maintenance. This work was supported by Children's Hospital of Pittsburgh; NIH grants A1083541 and HL105427 to S.A. Khader, PhD; HL69409 to T.D. Randall, PhD; and AI060422 to T.A. Reinhart, ScD; start-up funds from the Department of Medicine, University of Rochester, and AI91036 to J. Rangel-Moreno, PhD; T32 AI065380-08 institutional training grant (PART) to S.R. Slight; and a Research Advisory Committee Grants from Children's Hospital of Pittsburgh of the UPMC Health System to S.R. Slight.

5.0 CONCLUSIONS, SIGNIFICANCE AND FUTURE DIRECTIONS

M. tuberculosis is the causative agent of the disease that causes tuberculosis, which has multiple outcomes including active, latent and reactivated disease [229, 278]. Latent TB patients are asymptomatic and 90% can live a lifetime harboring the bacteria without ever developing reactivated infection and complications [278]. Further, these patients are at little risk to other individuals as bacteria is only transmitted during active infection [278]. Thus, the immune components required for maintaining latent infection are important in understanding protective immunity and immune control. It was previously understood that $CD4^+$ Th1 cells are necessary to activate macrophages through IFNγ and TNFα production, which stimulates macrophages to upregulate iNOS and contribute to bacterial killing [51]. Further, the granuloma, the hallmark of Mtb infection, is thought to facilitate cross-talk and provide a physical barrier for the prevention of bacterial spread and to limit pathology. However, the granuloma forms in both active and latent disease indicating immune differences exist in generating a functional and protective granuloma. The lack of latent Mtb infection models limits the work in this area. However, using a combination of human, NHP, which develop latent disease, and the Mtb mouse model, which is invaluable for mechanistic studies, evidence has emerged on granuloma formation in latent, active, and chronic disease.

Previous work has established the presence of B cell lymphoid aggregates within the granuloma of humans [11], NHPs [78], and mice [24, 77]. Development of lymphoid follicles was

associated with development of L-TB in some humans [223]. Our data proves that these lymphoid follicles are ectopic lymphoid organs that indeed correlate with immune control as 100% of L-TB NHPs formed ectopic follicles while only 33% of samples from NHPs with A-TB contained proliferating GC B cells, FDCs, and $CXCR5^+$ T cells. Importantly, we mechanistically addressed the formation of ectopic lymphoid follicles and the cells required for protective immunity. We found that expression of CXCL13 by stromal cells, FDCs, and DCs were critical for ectopic lymphoid follicle formation and recruitment of $CXCR5^+$ T cells within the lung. CXCL13 was not required for $CXCR5^+$ T cells to migrate to the lung, but was required for specific localization within the lung parenchyma. $CXCR5^+$ T cells, which express dual characteristics of Tfh and Th1 cells, are essential for controlling Mtb infection in mice by their production of Th1 proinflammatory cytokines that promote macrophage activation and further contribute to ectopic lymphoid follicle development. This protective model is summarized in Figure 25.

Our study highlights the importance of CXCL13 induction, $CXCR5^+$ T cell recruitment and formation of ectopic lymphoid follicles in the generation of a protective Mtb immune response. Further, these data support the hypothesis that T helper cells exhibit degrees of plasticity and can express multiple lineage characteristics. In addition, they support the idea that effective granuloma formation does contribute to protective immunity and that significant differences exist in both morphological and physiological parameters indicating future diagnostic tools may easily be able to differentiate between active and latent TB disease.

Although it is difficult to mechanistically determine the role of the CXCL13/CXCR5 axis in human TB, much work can be performed to validate this hypothesis. Our data translated into humans could have extensive implications in diagnostics of L-TB and A-TB and can

potentially indicate those individuals reverting to active disease. CXCL13 levels or CXCR5 expression in the serum or BAL could differentiate those with L-TB, A-TB, or those at risk for reactivation. In humans, individuals with specific genetic mutations are predisposed to increased mycobacterial infections such as those in the IFNγ locus (discussed in section 1.3.2). It is possible that specific populations with single-nucleotide polymorphisms in the *Cxcr5* or *Cxcl13*

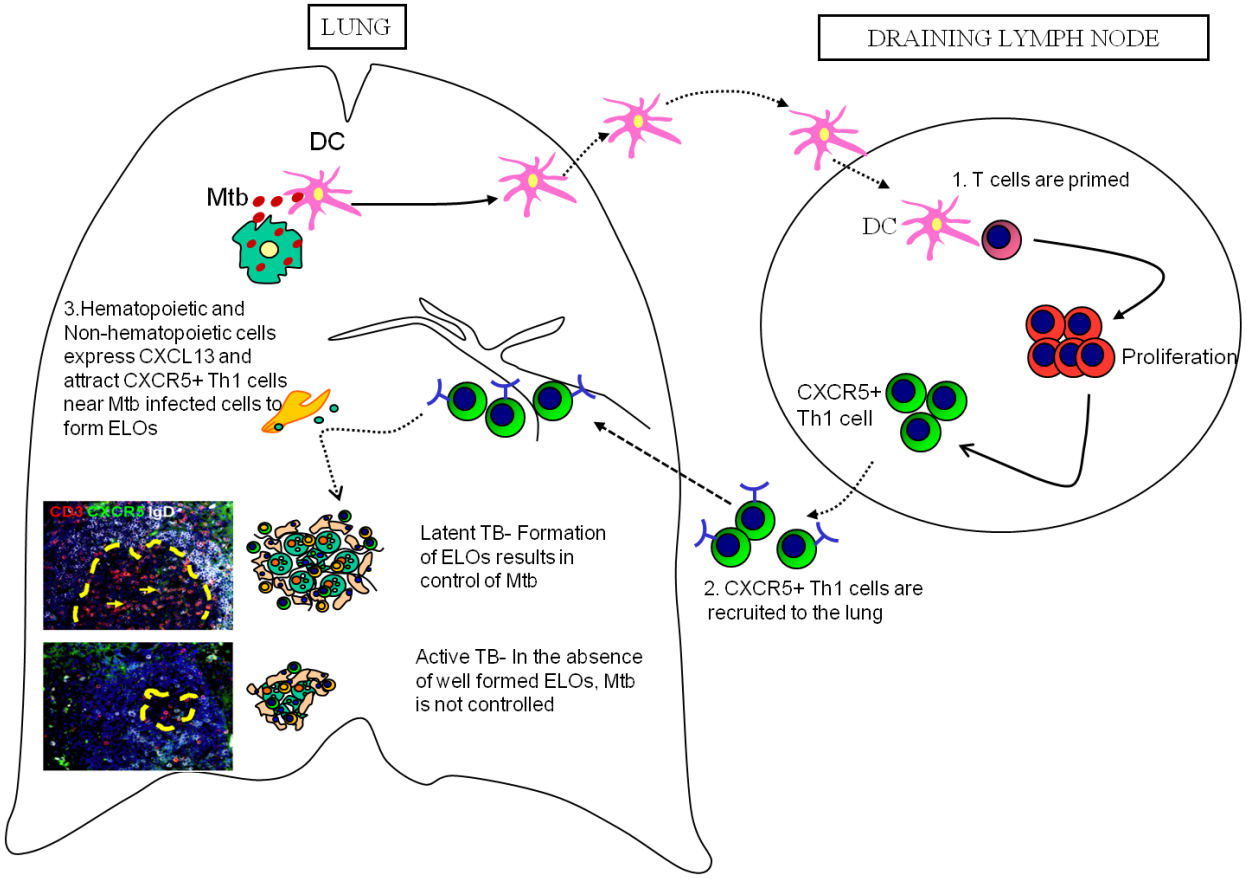

Figure 22: CXCR5 expressing T cells mediate protective immunity against tuberculosis.

Dendritic cells become activated following uptake and processing of Mtb antigen in the lung. Following activation, DCs upregulate CCR7 and migrate to the draining lymph node in response to CCL19/CCL21 chemokines. DCs present antigen to naïve T helper cells, which differentiate into Tfh-like Th1 cells, which express CXCR5. CXCR5+ Th1 cells migrate to the lung in response to inflammatory chemokines. Upon arrival to the lung, CXCR5+ Th1 cells use CXCL13 to specifically localize to Mtb-infected phagocytes within the parenchyma. Localization of CXCR5+ T cells typically results in the formation of ectopic lymphoid follicles containing CXCR5+ T cells, GC B cells, FDCs, and other myeloid cells, which are strongly associated with latent TB. Localized CXCR5+ Th1 cells produce IFNγ and TNFα, which act to activate macrophages and kill Mtb thereby assisting in the host protective immune response.

locus may have a higher incidence rate of Mtb infections and have a higher risk for reactivation. Further, our study also provides the rationale for targeting CXCR5 expression on memory T cells in vaccine immunity. Accordingly, studies have reported that the use of IL-6 as a vaccine adjuvant drives CXCR5 expression on T cells suggesting this is a distinct possibility [279]. Therefore our mechanistic studies using the mouse model of Mtb may have a broader relevance in human TB disease. Our findings may also have direct implications in other diseases both autoimmune and infectious. These results with other studies implicate ectopic lymphoid follicles as both mediators of protection and autoimmune pathology suggesting location and circumstances determine the role of this structure.

The future directions of this investigation will involve study of the mechanisms driving induction of CXCL13 and ectopic lymphoid follicle formation. Previous studies [35] have found pulmonary expression of TNF-α and LT-α in Mtb-infected mice, both known to induce CXCL13 expression, but it is not known if one, both, or neither of these cytokines is responsible. Further, it is also possible that Mtb may directly induce CXCL13 expression through TLR stimulation [280]. IL-17, which is implicated in the formation of ELOs in influenza [176], is also induced during Mtb infection [80]. Further, *Il-23-/-* mice lacked organized ELOs later in infection suggesting IL-17 may play a role in maintenance of ELO formation during chronic TB [281]. Moreover, the impact of *Cxcl13* and *Cxcr5* deficiency, on vascular adhesion molecule expression, chemokine production, and chemokine receptor expression should be investigated as these may also contribute to correct localization of T cells within the granuloma. To gain further insight, it would also be beneficial to take advantage of gene expression microarrays to define specific activation profiles of $CXCR5^+$ and CXCR5- $CD4^+$ T cells.

Additional studies investigated the protective role of CXCR5/CXCL13 and ELO formation in vaccine induced immunity is essential. Indeed, further work done in our lab indicates ELOs are induced in mice mucosally vaccinated with $ESAT6_{1-20}$ peptide and formation is dependent upon CXCL13 expression [282]. Further, *Cxcl13-/-* mice were unable to generate a protective vaccine induced immune response following challenge with Mtb [282]. Induction of CXCL13 was dependent upon IL-17, but not IFNγ production suggesting IL-17 is also involved in protective vaccine induced ELO formation [282]. It is clear that expression of CXCL13 is essential in the Mtb mouse model for protective vaccine induced immunity.

Our data further support the idea that T helper cells are plastic, capable of expressing dual characteristics of both Tfh and Th1 lineage cells. Tfh cells appear to be the most dynamic subset as in vitro Tfh cells can become Th1, Th2, and Th17 cells [283]. Further, Th1 cells pass through a Tfh-like transition before they become fully committed Th1 cells [258]. It is possible that this Tfh-like Th1 transition state is critical in Mtb immunity. $CXCR5^{+}CD4^{+}$ T cells in Mtb infection could utilize CXCR5 expression to migrate into the parenchyma and position in the granuloma, but then down regulate CXCR5 and become fully committed Th1 cells. The exact benefit of T cell plasticity in Mtb infection and the cytokines that drive this transition require further study.

In summary, our data describe a novel and previously undescribed role for $CD4^{+}CXCR5^{+}$ Th cells in Mtb protective immunity through localized proinflammatory cytokine production and macrophage activation. As we further elucidate the immune mechanisms required for protective immunity against TB, targeted efforts can be made to improve vaccine strategies, diagnostics, and treatment against this pulmonary pathogen.

6.0 RELEVANT PUBLICATIONS

1. **Slight SR,** Rangel-Moreno J, Gopal R, Lin Y, Fallert Junecko BA, Mehra S, Selman M, Becerril-Villanueva E, Baquera-Heredia J, Pavon L, Kaushal D, Reinhart TA, Randall TD, and Khader SA. (2013). $CXCR5^{+}$ T helper cells mediate protective immunity against tuberculosis. *J Clin Invest*. 123 (2): 712-726.

2. **Slight SR** and Khader SA. (2012). Chemokines shape the immune response to tuberculosis. *Cytokine Crowth Factor Rev.* 24 (2): 105-113.

BIBLIOGRAPHY

1. Andersen P. Vaccine strategies against latent tuberculosis infection. Trends Microbiol 2007;15:7-13.
2. Kumar S, Vaidyanathan B, Gayathri S, Rajam L. Systemic onset juvenile idiopathic arthritis with macrophage activation syndrome misdiagnosed as Kawasaki disease: case report and literature review. Rheumatology international 2010.
3. Lange C, Mori T. Advances in the diagnosis of tuberculosis. Respirology 2010;15:220-40.
4. Zumla A, Raviglione M, Hafner R, von Reyn CF. Tuberculosis. The New England journal of medicine 2013;368:745-55.
5. Druszczynska M, Kowalewicz-Kulbat M, Fol M, Wlodarczyk M, Rudnicka W. Latent M. tuberculosis infection--pathogenesis, diagnosis, treatment and prevention strategies. Polish journal of microbiology / Polskie Towarzystwo Mikrobiologow = The Polish Society of Microbiologists 2012;61:3-10.
6. Ramakrishnan L. Revisiting the role of the granuloma in tuberculosis. Nature reviews Immunology 2012;12:352-66.
7. Ulrichs T, Kaufmann SH. New insights into the function of granulomas in human tuberculosis. The Journal of pathology 2006;208:261-9.
8. Flynn JL, Chan J, Lin PL. Macrophages and control of granulomatous inflammation in tuberculosis. Mucosal immunology 2011;4:271-8.
9. Davis JM, Ramakrishnan L. The role of the granuloma in expansion and dissemination of early tuberculous infection. Cell 2009;136:37-49.
10. Helming L, Gordon S. The molecular basis of macrophage fusion. Immunobiology 2007;212:785-93.
11. Ulrichs T, Kosmiadi GA, Trusov V, et al. Human tuberculous granulomas induce peripheral lymphoid follicle-like structures to orchestrate local host defence in the lung. The Journal of pathology 2004;204:217-28.
12. Fenhalls G, Wong A, Bezuidenhout J, van Helden P, Bardin P, Lukey PT. In situ production of gamma interferon, interleukin-4, and tumor necrosis factor alpha mRNA in human lung tuberculous granulomas. Infection and immunity 2000;68:2827-36.
13. Koch R. Classics in infectious diseases. The etiology of tuberculosis: Robert Koch. Berlin, Germany 1882. Reviews of infectious diseases 1982;4:1270-4.
14. Padilla-Carlin DJ, McMurray DN, Hickey AJ. The guinea pig as a model of infectious diseases. Comparative medicine 2008;58:324-40.
15. Lurie MB. The Correlation between the Histological Changes and the Fate of Living Tubercle Bacilli in the Organs of Tuberculous Rabbits. The Journal of experimental medicine 1932;55:31-54.

16. Nedeltchev GG, Raghunand TR, Jassal MS, Lun S, Cheng QJ, Bishai WR. Extrapulmonary dissemination of Mycobacterium bovis but not Mycobacterium tuberculosis in a bronchoscopic rabbit model of cavitary tuberculosis. Infection and immunity 2009;77:598-603.
17. Davis JM, Clay H, Lewis JL, Ghori N, Herbomel P, Ramakrishnan L. Real-time visualization of mycobacterium-macrophage interactions leading to initiation of granuloma formation in zebrafish embryos. Immunity 2002;17:693-702.
18. Swaim LE, Connolly LE, Volkman HE, Humbert O, Born DE, Ramakrishnan L. Mycobacterium marinum infection of adult zebrafish causes caseating granulomatous tuberculosis and is moderated by adaptive immunity. Infection and immunity 2006;74:6108-17.
19. Beamer GL, Turner J. Murine models of susceptibility to tuberculosis. Archivum immunologiae et therapiae experimentalis 2005;53:469-83.
20. Orme IM. The kinetics of emergence and loss of mediator T lymphocytes acquired in response to infection with Mycobacterium tuberculosis. Journal of immunology 1987;138:293-8.
21. Middlebrook G. An apparatus for airborne infection of mice. Proceedings of the Society for Experimental Biology and Medicine Society for Experimental Biology and Medicine 1952;80:105-10.
22. Ratcliffe HL, Palladino VS. Tuberculosis induced by droplet nuclei infection; initial homogeneous response of small mammals (rats, mice, guinea pigs, and hamsters) to human and to bovine bacilli, and the rate and pattern of tubercle development. The Journal of experimental medicine 1953;97:61-8.
23. Rhoades ER, Frank AA, Orme IM. Progression of chronic pulmonary tuberculosis in mice aerogenically infected with virulent Mycobacterium tuberculosis. Tubercle and lung disease : the official journal of the International Union against Tuberculosis and Lung Disease 1997;78:57-66.
24. Khader SA, Rangel-Moreno J, Fountain JJ, et al. In a murine tuberculosis model, the absence of homeostatic chemokines delays granuloma formation and protective immunity. J Immunol 2009;183:8004-14.
25. Driver ER, Ryan GJ, Hoff DR, et al. Evaluation of a mouse model of necrotic granuloma formation using C3HeB/FeJ mice for testing of drugs against Mycobacterium tuberculosis. Antimicrob Agents Chemother 2012;56:3181-95.
26. Kaushal D, Mehra S, Didier PJ, Lackner AA. The non-human primate model of tuberculosis. Journal of medical primatology 2012;41:191-201.
27. Schlesinger LS, Bellinger-Kawahara CG, Payne NR, Horwitz MA. Phagocytosis of Mycobacterium tuberculosis is mediated by human monocyte complement receptors and complement component C3. Journal of immunology 1990;144:2771-80.
28. Ernst JD. Macrophage receptors for Mycobacterium tuberculosis. Infection and immunity 1998;66:1277-81.
29. Beharka AA, Gaynor CD, Kang BK, Voelker DR, McCormack FX, Schlesinger LS. Pulmonary surfactant protein A up-regulates activity of the mannose receptor, a pattern recognition receptor expressed on human macrophages. Journal of immunology 2002;169:3565-73.

30. Gaynor CD, McCormack FX, Voelker DR, McGowan SE, Schlesinger LS. Pulmonary surfactant protein A mediates enhanced phagocytosis of Mycobacterium tuberculosis by a direct interaction with human macrophages. Journal of immunology 1995;155:5343-51.
31. Bhatt K, Salgame P. Host innate immune response to Mycobacterium tuberculosis. Journal of clinical immunology 2007;27:347-62.
32. Aderem A, Underhill DM. Mechanisms of phagocytosis in macrophages. Annual review of immunology 1999;17:593-623.
33. Fratti RA, Chua J, Vergne I, Deretic V. Mycobacterium tuberculosis glycosylated phosphatidylinositol causes phagosome maturation arrest. Proceedings of the National Academy of Sciences of the United States of America 2003;100:5437-42.
34. Chua J, Vergne I, Master S, Deretic V. A tale of two lipids: Mycobacterium tuberculosis phagosome maturation arrest. Current opinion in microbiology 2004;7:71-7.
35. Kang PB, Azad AK, Torrelles JB, et al. The human macrophage mannose receptor directs Mycobacterium tuberculosis lipoarabinomannan-mediated phagosome biogenesis. The Journal of experimental medicine 2005;202:987-99.
36. Vergne I, Fratti RA, Hill PJ, Chua J, Belisle J, Deretic V. Mycobacterium tuberculosis phagosome maturation arrest: mycobacterial phosphatidylinositol analog phosphatidylinositol mannoside stimulates early endosomal fusion. Molecular biology of the cell 2004;15:751-60.
37. van Kooyk Y, Engering A, Lekkerkerker AN, Ludwig IS, Geijtenbeek TB. Pathogens use carbohydrates to escape immunity induced by dendritic cells. Current opinion in immunology 2004;16:488-93.
38. van Kooyk Y, Geijtenbeek TB. DC-SIGN: escape mechanism for pathogens. Nature reviews Immunology 2003;3:697-709.
39. Tailleux L, Neyrolles O, Honore-Bouakline S, et al. Constrained intracellular survival of Mycobacterium tuberculosis in human dendritic cells. Journal of immunology 2003;170:1939-48.
40. Krutzik SR, Modlin RL. The role of Toll-like receptors in combating mycobacteria. Seminars in immunology 2004;16:35-41.
41. Quesniaux V, Fremond C, Jacobs M, et al. Toll-like receptor pathways in the immune responses to mycobacteria. Microbes and infection / Institut Pasteur 2004;6:946-59.
42. Wolf AJ, Desvignes L, Linas B, et al. Initiation of the adaptive immune response to Mycobacterium tuberculosis depends on antigen production in the local lymph node, not the lungs. The Journal of experimental medicine 2008;205:105-15.
43. Reiley WW, Calayag MD, Wittmer ST, et al. ESAT-6-specific CD4 T cell responses to aerosol Mycobacterium tuberculosis infection are initiated in the mediastinal lymph nodes. Proceedings of the National Academy of Sciences of the United States of America 2008;105:10961-6.
44. Gallegos AM, Pamer EG, Glickman MS. Delayed protection by ESAT-6-specific effector CD4+ T cells after airborne M. tuberculosis infection. The Journal of experimental medicine 2008;205:2359-68.
45. Khader SA, Partida-Sanchez S, Bell G, et al. Interleukin 12p40 is required for dendritic cell migration and T cell priming after Mycobacterium tuberculosis infection. The Journal of experimental medicine 2006;203:1805-15.

46. Robinson RT, Khader SA, Martino CA, et al. Mycobacterium tuberculosis infection induces il12rb1 splicing to generate a novel IL-12Rbeta1 isoform that enhances DC migration. The Journal of experimental medicine 2010;207:591-605.
47. Winslow GM, Cooper A, Reiley W, Chatterjee M, Woodland DL. Early T-cell responses in tuberculosis immunity. Immunological reviews 2008;225:284-99.
48. Saunders BM, Frank AA, Orme IM, Cooper AM. CD4 is required for the development of a protective granulomatous response to pulmonary tuberculosis. Cellular immunology 2002;216:65-72.
49. Wolf AJ, Linas B, Trevejo-Nunez GJ, et al. Mycobacterium tuberculosis infects dendritic cells with high frequency and impairs their function in vivo. Journal of immunology 2007;179:2509-19.
50. Cooper AM, Kipnis A, Turner J, Magram J, Ferrante J, Orme IM. Mice lacking bioactive IL-12 can generate protective, antigen-specific cellular responses to mycobacterial infection only if the IL-12 p40 subunit is present. Journal of immunology 2002;168:1322-7.
51. Cooper AM, Khader SA. The role of cytokines in the initiation, expansion, and control of cellular immunity to tuberculosis. Immunological reviews 2008;226:191-204.
52. Kaufmann SH. Protection against tuberculosis: cytokines, T cells, and macrophages. Annals of the rheumatic diseases 2002;61 Suppl 2:ii54-8.
53. Korn T, Bettelli E, Gao W, et al. IL-21 initiates an alternative pathway to induce proinflammatory T(H)17 cells. Nature 2007;448:484-7.
54. Veldhoen M, Hocking RJ, Atkins CJ, Locksley RM, Stockinger B. TGFbeta in the context of an inflammatory cytokine milieu supports de novo differentiation of IL-17-producing T cells. Immunity 2006;24:179-89.
55. Zhou L, Ivanov, II, Spolski R, et al. IL-6 programs T(H)-17 cell differentiation by promoting sequential engagement of the IL-21 and IL-23 pathways. Nature immunology 2007;8:967-74.
56. Zhu J, Yamane H, Paul WE. Differentiation of effector CD4 T cell populations (*). Annual review of immunology 2010;28:445-89.
57. Khader SA, Pearl JE, Sakamoto K, et al. IL-23 compensates for the absence of IL-12p70 and is essential for the IL-17 response during tuberculosis but is dispensable for protection and antigen-specific IFN-gamma responses if IL-12p70 is available. Journal of immunology 2005;175:788-95.
58. Aujla SJ, Chan YR, Zheng M, et al. IL-22 mediates mucosal host defense against Gram-negative bacterial pneumonia. Nature medicine 2008;14:275-81.
59. Gopal R, Lin Y, Obermajer N, et al. IL-23-dependent IL-17 drives Th1-cell responses following Mycobacterium bovis BCG vaccination. European journal of immunology 2012;42:364-73.
60. Ottenhoff TH. New pathways of protective and pathological host defense to mycobacteria. Trends in microbiology 2012;20:419-28.
61. Scott-Browne JP, Shafiani S, Tucker-Heard G, et al. Expansion and function of Foxp3-expressing T regulatory cells during tuberculosis. The Journal of experimental medicine 2007;204:2159-69.
62. Shafiani S, Tucker-Heard G, Kariyone A, Takatsu K, Urdahl KB. Pathogen-specific regulatory T cells delay the arrival of effector T cells in the lung during early tuberculosis. The Journal of experimental medicine 2010;207:1409-20.

63. Nakayamada S, Takahashi H, Kanno Y, O'Shea JJ. Helper T cell diversity and plasticity. Curr Opin Immunol 2012;24:297-302.
64. Caccamo N, Guggino G, Joosten SA, et al. Multifunctional CD4(+) T cells correlate with active Mycobacterium tuberculosis infection. European journal of immunology 2010;40:2211-20.
65. Turner J, D'Souza CD, Pearl JE, et al. CD8- and CD95/95L-dependent mechanisms of resistance in mice with chronic pulmonary tuberculosis. American journal of respiratory cell and molecular biology 2001;24:203-9.
66. Mogues T, Goodrich ME, Ryan L, LaCourse R, North RJ. The relative importance of T cell subsets in immunity and immunopathology of airborne Mycobacterium tuberculosis infection in mice. The Journal of experimental medicine 2001;193:271-80.
67. Muller I, Cobbold SP, Waldmann H, Kaufmann SH. Impaired resistance to Mycobacterium tuberculosis infection after selective in vivo depletion of L3T4+ and Lyt-2+ T cells. Infection and immunity 1987;55:2037-41.
68. Orme IM, Collins FM. Adoptive protection of the Mycobacterium tuberculosis-infected lung. Dissociation between cells that passively transfer protective immunity and those that transfer delayed-type hypersensitivity to tuberculin. Cellular immunology 1984;84:113-20.
69. Stenger S, Mazzaccaro RJ, Uyemura K, et al. Differential effects of cytolytic T cell subsets on intracellular infection. Science 1997;276:1684-7.
70. Stenger S, Hanson DA, Teitelbaum R, et al. An antimicrobial activity of cytolytic T cells mediated by granulysin. Science 1998;282:121-5.
71. Woodworth JS, Behar SM. Mycobacterium tuberculosis-specific CD8+ T cells and their role in immunity. Critical reviews in immunology 2006;26:317-52.
72. Bold TD, Ernst JD. CD4+ T cell-dependent IFN-gamma production by CD8+ effector T cells in Mycobacterium tuberculosis infection. Journal of immunology 2012;189:2530-6.
73. Kumararatne DS. Tuberculosis and immunodeficiency--of mice and men. Clinical and experimental immunology 1997;107:11-4.
74. Glatman-Freedman A, Casadevall A. Serum therapy for tuberculosis revisited: reappraisal of the role of antibody-mediated immunity against Mycobacterium tuberculosis. Clinical microbiology reviews 1998;11:514-32.
75. Doffinger R, Patel S, Kumararatne DS. Human immunodeficiencies that predispose to intracellular bacterial infections. Current opinion in rheumatology 2005;17:440-6.
76. Turner J, Frank AA, Brooks JV, Gonzalez-Juarrero M, Orme IM. The progression of chronic tuberculosis in the mouse does not require the participation of B lymphocytes or interleukin-4. Exp Gerontol 2001;36:537-45.
77. Maglione PJ, Xu J, Chan J. B cells moderate inflammatory progression and enhance bacterial containment upon pulmonary challenge with Mycobacterium tuberculosis. J Immunol 2007;178:7222-34.
78. Phuah JY, Mattila JT, Lin PL, Flynn JL. Activated B cells in the granulomas of nonhuman primates infected with Mycobacterium tuberculosis. The American journal of pathology 2012;181:508-14.
79. Tsai MC, Chakravarty S, Zhu G, et al. Characterization of the tuberculous granuloma in murine and human lungs: cellular composition and relative tissue oxygen tension. Cellular microbiology 2006;8:218-32.

80. Kang DD, Lin Y, Moreno JR, Randall TD, Khader SA. Profiling early lung immune responses in the mouse model of tuberculosis. PloS one 2011;6:e16161.
81. Gately MK, Renzetti LM, Magram J, et al. The interleukin-12/interleukin-12-receptor system: role in normal and pathologic immune responses. Annual review of immunology 1998;16:495-521.
82. Holscher C, Atkinson RA, Arendse B, et al. A protective and agonistic function of IL-12p40 in mycobacterial infection. Journal of immunology 2001;167:6957-66.
83. Feng CG, Jankovic D, Kullberg M, et al. Maintenance of pulmonary Th1 effector function in chronic tuberculosis requires persistent IL-12 production. Journal of immunology 2005;174:4185-92.
84. Filipe-Santos O, Bustamante J, Chapgier A, et al. Inborn errors of IL-12/23- and IFN-gamma-mediated immunity: molecular, cellular, and clinical features. Seminars in immunology 2006;18:347-61.
85. Ma CS, Suryani S, Avery DT, et al. Early commitment of naive human CD4(+) T cells to the T follicular helper (T(FH)) cell lineage is induced by IL-12. Immunology and cell biology 2009;87:590-600.
86. Dorman SE, Picard C, Lammas D, et al. Clinical features of dominant and recessive interferon gamma receptor 1 deficiencies. Lancet 2004;364:2113-21.
87. MacMicking JD, Nathan C, Hom G, et al. Altered responses to bacterial infection and endotoxic shock in mice lacking inducible nitric oxide synthase. Cell 1995;81:641-50.
88. MacMicking JD, Taylor GA, McKinney JD. Immune control of tuberculosis by IFN-gamma-inducible LRG-47. Science 2003;302:654-9.
89. Gutierrez MG, Master SS, Singh SB, Taylor GA, Colombo MI, Deretic V. Autophagy is a defense mechanism inhibiting BCG and Mycobacterium tuberculosis survival in infected macrophages. Cell 2004;119:753-66.
90. Desvignes L, Ernst JD. Interferon-gamma-responsive nonhematopoietic cells regulate the immune response to Mycobacterium tuberculosis. Immunity 2009;31:974-85.
91. Shams H, Wizel B, Weis SE, Samten B, Barnes PF. Contribution of CD8(+) T cells to gamma interferon production in human tuberculosis. Infection and immunity 2001;69:3497-501.
92. Cooper AM, Dalton DK, Stewart TA, Griffin JP, Russell DG, Orme IM. Disseminated tuberculosis in interferon gamma gene-disrupted mice. The Journal of experimental medicine 1993;178:2243-7.
93. Flynn JL, Chan J, Triebold KJ, Dalton DK, Stewart TA, Bloom BR. An essential role for interferon gamma in resistance to Mycobacterium tuberculosis infection. The Journal of experimental medicine 1993;178:2249-54.
94. Nandi B, Behar SM. Regulation of neutrophils by interferon-gamma limits lung inflammation during tuberculosis infection. J Exp Med 2011;208:2251-62.
95. Mootoo A, Stylianou E, Arias MA, Reljic R. TNF-alpha in tuberculosis: a cytokine with a split personality. Inflammation & allergy drug targets 2009;8:53-62.
96. Keane J, Gershon S, Wise RP, et al. Tuberculosis associated with infliximab, a tumor necrosis factor alpha-neutralizing agent. The New England journal of medicine 2001;345:1098-104.
97. Wallis RS, Broder M, Wong J, Beenhouwer D. Granulomatous infections due to tumor necrosis factor blockade: correction. Clinical infectious diseases : an official publication of the Infectious Diseases Society of America 2004;39:1254-5.

98. Flynn JL, Goldstein MM, Chan J, et al. Tumor necrosis factor-alpha is required in the protective immune response against Mycobacterium tuberculosis in mice. Immunity 1995;2:561-72.
99. Lin PL, Myers A, Smith L, et al. Tumor necrosis factor neutralization results in disseminated disease in acute and latent Mycobacterium tuberculosis infection with normal granuloma structure in a cynomolgus macaque model. Arthritis and rheumatism 2010;62:340-50.
100. Chakravarty SD, Zhu G, Tsai MC, et al. Tumor necrosis factor blockade in chronic murine tuberculosis enhances granulomatous inflammation and disorganizes granulomas in the lungs. Infection and immunity 2008;76:916-26.
101. Bean AG, Roach DR, Briscoe H, et al. Structural deficiencies in granuloma formation in TNF gene-targeted mice underlie the heightened susceptibility to aerosol Mycobacterium tuberculosis infection, which is not compensated for by lymphotoxin. Journal of immunology 1999;162:3504-11.
102. Garcia I, Miyazaki Y, Marchal G, Lesslauer W, Vassalli P. High sensitivity of transgenic mice expressing soluble TNFR1 fusion protein to mycobacterial infections: synergistic action of TNF and IFN-gamma in the differentiation of protective granulomas. European journal of immunology 1997;27:3182-90.
103. Algood HM, Lin PL, Yankura D, Jones A, Chan J, Flynn JL. TNF influences chemokine expression of macrophages in vitro and that of CD11b+ cells in vivo during Mycobacterium tuberculosis infection. Journal of immunology 2004;172:6846-57.
104. Barry SM, Lipman MC, Bannister B, Johnson MA, Janossy G. Purified protein derivative-activated type 1 cytokine-producing CD4+ T lymphocytes in the lung: a characteristic feature of active pulmonary and nonpulmonary tuberculosis. The Journal of infectious diseases 2003;187:243-50.
105. Keane J, Shurtleff B, Kornfeld H. TNF-dependent BALB/c murine macrophage apoptosis following Mycobacterium tuberculosis infection inhibits bacillary growth in an IFN-gamma independent manner. Tuberculosis 2002;82:55-61.
106. Gallegos AM, van Heijst JW, Samstein M, Su X, Pamer EG, Glickman MS. A gamma interferon independent mechanism of CD4 T cell mediated control of M. tuberculosis infection in vivo. PLoS pathogens 2011;7:e1002052.
107. Yang CS, Yuk JM, Jo EK. The role of nitric oxide in mycobacterial infections. Immune network 2009;9:46-52.
108. Chan J, Xing Y, Magliozzo RS, Bloom BR. Killing of virulent Mycobacterium tuberculosis by reactive nitrogen intermediates produced by activated murine macrophages. The Journal of experimental medicine 1992;175:1111-22.
109. Chan J, Tanaka K, Carroll D, Flynn J, Bloom BR. Effects of nitric oxide synthase inhibitors on murine infection with Mycobacterium tuberculosis. Infection and immunity 1995;63:736-40.
110. Beisiegel M, Kursar M, Koch M, et al. Combination of host susceptibility and virulence of Mycobacterium tuberculosis determines dual role of nitric oxide in the protection and control of inflammation. The Journal of infectious diseases 2009;199:1222-32.
111. Flynn JL, Scanga CA, Tanaka KE, Chan J. Effects of aminoguanidine on latent murine tuberculosis. Journal of immunology 1998;160:1796-803.

112. Nicholson S, Bonecini-Almeida Mda G, Lapa e Silva JR, et al. Inducible nitric oxide synthase in pulmonary alveolar macrophages from patients with tuberculosis. The Journal of experimental medicine 1996;183:2293-302.
113. Aston C, Rom WN, Talbot AT, Reibman J. Early inhibition of mycobacterial growth by human alveolar macrophages is not due to nitric oxide. Am J Respir Crit Care Med 1998;157:1943-50.
114. Jagannath C, Actor JK, Hunter RL, Jr. Induction of nitric oxide in human monocytes and monocyte cell lines by Mycobacterium tuberculosis. Nitric oxide : biology and chemistry / official journal of the Nitric Oxide Society 1998;2:174-86.
115. Kwon OJ. The role of nitric oxide in the immune response of tuberculosis. Journal of Korean medical science 1997;12:481-7.
116. Rich EA, Torres M, Sada E, Finegan CK, Hamilton BD, Toossi Z. Mycobacterium tuberculosis (MTB)-stimulated production of nitric oxide by human alveolar macrophages and relationship of nitric oxide production to growth inhibition of MTB. Tubercle and lung disease : the official journal of the International Union against Tuberculosis and Lung Disease 1997;78:247-55.
117. Azad AK, Sadee W, Schlesinger LS. Innate immune gene polymorphisms in tuberculosis. Infection and immunity 2012;80:3343-59.
118. Mehrad B, Keane MP, Strieter RM. Chemokines as mediators of angiogenesis. Thromb Haemost 2007;97:755-62.
119. Rollins BJ. Chemokines. Blood 1997;90:909-28.
120. Zlotnik A, Yoshie O. Chemokines: a new classification system and their role in immunity. Immunity 2000;12:121-7.
121. Zlotnik A, Yoshie O, Nomiyama H. The chemokine and chemokine receptor superfamilies and their molecular evolution. Genome Biol 2006;7:243.
122. Moser B, Loetscher P. Lymphocyte traffic control by chemokines. Nat Immunol 2001;2:123-8.
123. Rangel-Moreno J, Hartson L, Navarro C, Gaxiola M, Selman M, Randall TD. Inducible bronchus-associated lymphoid tissue (iBALT) in patients with pulmonary complications of rheumatoid arthritis. The Journal of clinical investigation 2006;116:3183-94.
124. Rangel-Moreno J, Moyron-Quiroz JE, Hartson L, Kusser K, Randall TD. Pulmonary expression of CXC chemokine ligand 13, CC chemokine ligand 19, and CC chemokine ligand 21 is essential for local immunity to influenza. Proc Natl Acad Sci U S A 2007;104:10577-82.
125. Schmidt C, Plate A, Angele B, et al. A prospective study on the role of CXCL13 in Lyme neuroborreliosis. Neurology 2011;76:1051-8.
126. Winter S, Loddenkemper C, Aebischer A, et al. The chemokine receptor CXCR5 is pivotal for ectopic mucosa-associated lymphoid tissue neogenesis in chronic Helicobacter pylori-induced inflammation. J Mol Med (Berl) 2010;88:1169-80.
127. Slight SR, Khader SA. Chemokines shape the immune responses to tuberculosis. Cytokine Growth Factor Rev 2012.
128. Rhoades ER, Cooper AM, Orme IM. Chemokine response in mice infected with Mycobacterium tuberculosis. Infect Immun 1995;63:3871-7.
129. Sadek MI, Sada E, Toossi Z, Schwander SK, Rich EA. Chemokines induced by infection of mononuclear phagocytes with mycobacteria and present in lung alveoli during active pulmonary tuberculosis. Am J Respir Cell Mol Biol 1998;19:513-21.

130. Saukkonen JJ, Bazydlo B, Thomas M, Strieter RM, Keane J, Kornfeld H. Beta-chemokines are induced by Mycobacterium tuberculosis and inhibit its growth. Infect Immun 2002;70:1684-93.
131. Loetscher M, Loetscher P, Brass N, Meese E, Moser B. Lymphocyte-specific chemokine receptor CXCR3: regulation, chemokine binding and gene localization. Eur J Immunol 1998;28:3696-705.
132. Groom JR, Luster AD. CXCR3 ligands: redundant, collaborative and antagonistic functions. Immunol Cell Biol 2011;89:207-15.
133. Fuller CL, Flynn JL, Reinhart TA. In situ study of abundant expression of proinflammatory chemokines and cytokines in pulmonary granulomas that develop in cynomolgus macaques experimentally infected with Mycobacterium tuberculosis. Infection and immunity 2003;71:7023-34.
134. Lin PL, Pawar S, Myers A, et al. Early events in Mycobacterium tuberculosis infection in cynomolgus macaques. Infect Immun 2006;74:3790-803.
135. Khader SA, Bell GK, Pearl JE, et al. IL-23 and IL-17 in the establishment of protective pulmonary CD4+ T cell responses after vaccination and during Mycobacterium tuberculosis challenge. Nat Immunol 2007;8:369-77.
136. Seiler P, Aichele P, Bandermann S, et al. Early granuloma formation after aerosol Mycobacterium tuberculosis infection is regulated by neutrophils via CXCR3-signaling chemokines. European journal of immunology 2003;33:2676-86.
137. Hasan Z, Jamil B, Khan J, et al. Relationship between circulating levels of IFN-gamma, IL-10, CXCL9 and CCL2 in pulmonary and extrapulmonary tuberculosis is dependent on disease severity. Scand J Immunol 2009;69:259-67.
138. Hasan Z, Jamil B, Ashraf M, et al. ESAT6-induced IFNgamma and CXCL9 can differentiate severity of tuberculosis. PLoS One 2009;4:e5158.
139. Tang NL, Fan HP, Chang KC, et al. Genetic association between a chemokine gene CXCL-10 (IP-10, interferon gamma inducible protein 10) and susceptibility to tuberculosis. Clin Chim Acta 2009;406:98-102.
140. Cyster JG. Chemokines and cell migration in secondary lymphoid organs. Science 1999;286:2098-102.
141. Cyster JG. Chemokines and the homing of dendritic cells to the T cell areas of lymphoid organs. J Exp Med 1999;189:447-50.
142. Gunn MD, Kyuwa S, Tam C, et al. Mice lacking expression of secondary lymphoid organ chemokine have defects in lymphocyte homing and dendritic cell localization. J Exp Med 1999;189:451-60.
143. Gunn MD, Tangemann K, Tam C, Cyster JG, Rosen SD, Williams LT. A chemokine expressed in lymphoid high endothelial venules promotes the adhesion and chemotaxis of naive T lymphocytes. Proc Natl Acad Sci U S A 1998;95:258-63.
144. Saeki H, Moore AM, Brown MJ, Hwang ST. Cutting edge: secondary lymphoid-tissue chemokine (SLC) and CC chemokine receptor 7 (CCR7) participate in the emigration pathway of mature dendritic cells from the skin to regional lymph nodes. J Immunol 1999;162:2472-5.
145. Bhatt K, Hickman SP, Salgame P. Cutting edge: a new approach to modeling early lung immunity in murine tuberculosis. J Immunol 2004;172:2748-51.

146. Arias MA, Pantoja AE, Jaramillo G, et al. Chemokine receptor expression and modulation by Mycobacterium tuberculosis antigens on mononuclear cells from human lymphoid tissues. Immunology 2006;118:171-84.
147. Kahnert A, Hopken UE, Stein M, Bandermann S, Lipp M, Kaufmann SH. Mycobacterium tuberculosis triggers formation of lymphoid structure in murine lungs. The Journal of infectious diseases 2007;195:46-54.
148. Olmos S, Stukes S, Ernst JD. Ectopic activation of Mycobacterium tuberculosis-specific CD4+ T cells in lungs of CCR7-/- mice. J Immunol 2010;184:895-901.
149. Cyster JG, Ngo VN, Ekland EH, Gunn MD, Sedgwick JD, Ansel KM. Chemokines and B-cell homing to follicles. Curr Top Microbiol Immunol 1999;246:87-92; discussion 3.
150. Wang X, Cho B, Suzuki K, et al. Follicular dendritic cells help establish follicle identity and promote B cell retention in germinal centers. J Exp Med 2011;208:2497-510.
151. Legler DF, Loetscher M, Roos RS, Clark-Lewis I, Baggiolini M, Moser B. B cell-attracting chemokine 1, a human CXC chemokine expressed in lymphoid tissues, selectively attracts B lymphocytes via BLR1/CXCR5. The Journal of experimental medicine 1998;187:655-60.
152. Ansel KM, Ngo VN, Hyman PL, et al. A chemokine-driven positive feedback loop organizes lymphoid follicles. Nature 2000;406:309-14.
153. Schaerli P, Willimann K, Lang AB, Lipp M, Loetscher P, Moser B. CXC chemokine receptor 5 expression defines follicular homing T cells with B cell helper function. The Journal of experimental medicine 2000;192:1553-62.
154. Suto H, Katakai T, Sugai M, Kinashi T, Shimizu A. CXCL13 production by an established lymph node stromal cell line via lymphotoxin-beta receptor engagement involves the cooperation of multiple signaling pathways. Int Immunol 2009;21:467-76.
155. Rangel-Moreno J, Hartson L, Navarro C, Gaxiola M, Selman M, Randall T. Inducible bronchus-associated lymphoid tissue (iBALT) in patients with pulmonary complications of rheumatoid arthritis. Journal of Clinical Investigations 2006;116:3183-94.
156. Hogg JC, Chu F, Utokaparch S, et al. The nature of small-airway obstruction in chronic obstructive pulmonary disease. N Engl J Med 2004;350:2645-53.
157. Schreiber T, Ehlers S, Aly S, et al. Selectin ligand-independent priming and maintenance of T cell immunity during airborne tuberculosis. J Immunol 2006;176:1131-40.
158. Pabst R, Gehrke I. Is the bronchus-associated lymphoid tissue (BALT) an integral structure of the lung in normal mammals, including humans? American journal of respiratory cell and molecular biology 1990;3:131-5.
159. Foo SY, Phipps S. Regulation of inducible BALT formation and contribution to immunity and pathology. Mucosal immunology 2010;3:537-44.
160. Bienenstock J, Johnston N, Perey DY. Bronchial lymphoid tissue. I. Morphologic characteristics. Laboratory investigation; a journal of technical methods and pathology 1973;28:686-92.
161. Sminia T, van der Brugge-Gamelkoorn GJ, Jeurissen SH. Structure and function of bronchus-associated lymphoid tissue (BALT). Critical reviews in immunology 1989;9:119-50.
162. Suzuki K, Grigorova I, Phan TG, Kelly LM, Cyster JG. Visualizing B cell capture of cognate antigen from follicular dendritic cells. The Journal of experimental medicine 2009;206:1485-93.

163. van der Brugge-Gamelkoorn GJ, van de Ende MB, Sminia T. Non-lymphoid cells of bronchus-associated lymphoid tissue of the rat in situ and in suspension. With special reference to interdigitating and follicular dendritic cells. Cell and tissue research 1985;239:177-82.
164. Kosco-Vilbois MH, Gray D, Scheidegger D, Julius M. Follicular dendritic cells help resting B cells to become effective antigen-presenting cells: induction of B7/BB1 and upregulation of major histocompatibility complex class II molecules. The Journal of experimental medicine 1993;178:2055-66.
165. Milne RW, Bienenstodk J, Perey DY. The influence of antigenic stimulation on the ontegeny of lymphoid aggregates and immunoglobulin-containing cells in mouse bronchial and intestinal mucosa. Journal of the Reticuloendothelial Society 1975;17:361-9.
166. GeurtsvanKessel CH, Willart MA, Bergen IM, et al. Dendritic cells are crucial for maintenance of tertiary lymphoid structures in the lung of influenza virus-infected mice. The Journal of experimental medicine 2009;206:2339-49.
167. Halle S, Dujardin HC, Bakocevic N, et al. Induced bronchus-associated lymphoid tissue serves as a general priming site for T cells and is maintained by dendritic cells. The Journal of experimental medicine 2009;206:2593-601.
168. Moyron-Quiroz JE, Rangel-Moreno J, Kusser K, et al. Role of inducible bronchus associated lymphoid tissue (iBALT) in respiratory immunity. Nature medicine 2004;10:927-34.
169. Xu B, Wagner N, Pham LN, et al. Lymphocyte homing to bronchus-associated lymphoid tissue (BALT) is mediated by L-selectin/PNAd, alpha4beta1 integrin/VCAM-1, and LFA-1 adhesion pathways. The Journal of experimental medicine 2003;197:1255-67.
170. Carragher DM, Rangel-Moreno J, Randall TD. Ectopic lymphoid tissues and local immunity. Semin Immunol 2008;20:26-42.
171. Luther SA, Lopez T, Bai W, Hanahan D, Cyster JG. BLC expression in pancreatic islets causes B cell recruitment and lymphotoxin-dependent lymphoid neogenesis. Immunity 2000;12:471-81.
172. Randall TD, Carragher DM, Rangel-Moreno J. Development of secondary lymphoid organs. Annual review of immunology 2008;26:627-50.
173. Goodnow CC. Chance encounters and organized rendezvous. Immunological reviews 1997;156:5-10.
174. Ansel KM, McHeyzer-Williams LJ, Ngo VN, McHeyzer-Williams MG, Cyster JG. In vivo-activated CD4 T cells upregulate CXC chemokine receptor 5 and reprogram their response to lymphoid chemokines. The Journal of experimental medicine 1999;190:1123-34.
175. Rangel-Moreno J, Carragher D, Randall TD. Role of lymphotoxin and homeostatic chemokines in the development and function of local lymphoid tissues in the respiratory tract. Inmunologia 2007;26:13-28.
176. Rangel-Moreno J, Carragher DM, de la Luz Garcia-Hernandez M, et al. The development of inducible bronchus-associated lymphoid tissue depends on IL-17. Nature immunology 2011;12:639-46.
177. Cupedo T, Kraal G, Mebius RE. The role of CD45+CD4+CD3- cells in lymphoid organ development. Immunological reviews 2002;189:41-50.

178. Shilling RA, Williams JW, Perera J, et al. Autoreactive T and B cells Induce Development of BALT-like Tissue in the Lung. American journal of respiratory cell and molecular biology 2013.
179. Ingegnoli F, Sciascera A, Galbiati V, Corbelli V, D'Ingianna E, Fantini F. Bronchus-associated lymphoid tissue lymphoma in a patient with primary Sjogren's syndrome. Rheumatology international 2008;29:207-9.
180. Salomonsson S, Jonsson MV, Skarstein K, et al. Cellular basis of ectopic germinal center formation and autoantibody production in the target organ of patients with Sjogren's syndrome. Arthritis and rheumatism 2003;48:3187-201.
181. Sato A, Hayakawa H, Uchiyama H, Chida K. Cellular distribution of bronchus-associated lymphoid tissue in rheumatoid arthritis. American journal of respiratory and critical care medicine 1996;154:1903-7.
182. Magliozzi R, Howell O, Vora A, et al. Meningeal B-cell follicles in secondary progressive multiple sclerosis associate with early onset of disease and severe cortical pathology. Brain : a journal of neurology 2007;130:1089-104.
183. Serafini B, Rosicarelli B, Magliozzi R, Stigliano E, Aloisi F. Detection of ectopic B-cell follicles with germinal centers in the meninges of patients with secondary progressive multiple sclerosis. Brain pathology 2004;14:164-74.
184. Lee Y, Chin RK, Christiansen P, et al. Recruitment and activation of naive T cells in the islets by lymphotoxin beta receptor-dependent tertiary lymphoid structure. Immunity 2006;25:499-509.
185. Kendall PL, Yu G, Woodward EJ, Thomas JW. Tertiary lymphoid structures in the pancreas promote selection of B lymphocytes in autoimmune diabetes. Journal of immunology 2007;178:5643-51.
186. Weyand CM, Goronzy JJ. Ectopic germinal center formation in rheumatoid synovitis. Annals of the New York Academy of Sciences 2003;987:140-9.
187. Jonsson MV, Skarstein K. Follicular dendritic cells confirm lymphoid organization in the minor salivary glands of primary Sjogren's syndrome. Journal of oral pathology & medicine : official publication of the International Association of Oral Pathologists and the American Academy of Oral Pathology 2008;37:515-21.
188. Jonsson MV, Szodoray P, Jellestad S, Jonsson R, Skarstein K. Association between circulating levels of the novel TNF family members APRIL and BAFF and lymphoid organization in primary Sjogren's syndrome. Journal of clinical immunology 2005;25:189-201.
189. Manzo A, Bombardieri M, Humby F, Pitzalis C. Secondary and ectopic lymphoid tissue responses in rheumatoid arthritis: from inflammation to autoimmunity and tissue damage/remodeling. Immunol Rev 2010;233:267-85.
190. Corsiero E, Bombardieri M, Manzo A, Bugatti S, Uguccioni M, Pitzalis C. Role of lymphoid chemokines in the development of functional ectopic lymphoid structures in rheumatic autoimmune diseases. Immunology letters 2012;145:62-7.
191. Astorri E, Bombardieri M, Gabba S, Peakman M, Pozzilli P, Pitzalis C. Evolution of ectopic lymphoid neogenesis and in situ autoantibody production in autoimmune nonobese diabetic mice: cellular and molecular characterization of tertiary lymphoid structures in pancreatic islets. J Immunol 2010;185:3359-68.

192. Carlsen HS, Baekkevold ES, Morton HC, Haraldsen G, Brandtzaeg P. Monocyte-like and mature macrophages produce CXCL13 (B cell-attracting chemokine 1) in inflammatory lesions with lymphoid neogenesis. Blood 2004;104:3021-7.
193. Columba-Cabezas S, Griguoli M, Rosicarelli B, et al. Suppression of established experimental autoimmune encephalomyelitis and formation of meningeal lymphoid follicles by lymphotoxin beta receptor-Ig fusion protein. J Neuroimmunol 2006;179:76-86.
194. Szekanecz Z, Vegvari A, Szabo Z, Koch AE. Chemokines and chemokine receptors in arthritis. Front Biosci (Schol Ed) 2010;2:153-67.
195. Reksten TR, Jonsson MV, Szyszko EA, Brun JG, Jonsson R, Brokstad KA. Cytokine and autoantibody profiling related to histopathological features in primary Sjogren's syndrome. Rheumatology 2009;48:1102-6.
196. Gatumu MK, Jonsson MV, Oijordsbakken G, Skarstein K. Nuclear BCL10 in primary Sjogren's syndrome. Journal of oral pathology & medicine : official publication of the International Association of Oral Pathologists and the American Academy of Oral Pathology 2009;38:501-7.
197. Kim HJ, Krenn V, Steinhauser G, Berek C. Plasma cell development in synovial germinal centers in patients with rheumatoid and reactive arthritis. Journal of immunology 1999;162:3053-62.
198. Aloisi F, Columba-Cabezas S, Franciotta D, et al. Lymphoid chemokines in chronic neuroinflammation. J Neuroimmunol 2008;198:106-12.
199. Barone F, Bombardieri M, Manzo A, et al. Association of CXCL13 and CCL21 expression with the progressive organization of lymphoid-like structures in Sjogren's syndrome. Arthritis Rheum 2005;52:1773-84.
200. Henry RA, Kendall PL. CXCL13 blockade disrupts B lymphocyte organization in tertiary lymphoid structures without altering B cell receptor bias or preventing diabetes in nonobese diabetic mice. Journal of immunology 2010;185:1460-5.
201. Chen SC, Vassileva G, Kinsley D, et al. Ectopic expression of the murine chemokines CCL21a and CCL21b induces the formation of lymph node-like structures in pancreas, but not skin, of transgenic mice. Journal of immunology 2002;168:1001-8.
202. Martin AP, Coronel EC, Sano G, et al. A novel model for lymphocytic infiltration of the thyroid gland generated by transgenic expression of the CC chemokine CCL21. Journal of immunology 2004;173:4791-8.
203. Fan L, Reilly CR, Luo Y, Dorf ME, Lo D. Cutting edge: ectopic expression of the chemokine TCA4/SLC is sufficient to trigger lymphoid neogenesis. Journal of immunology 2000;164:3955-9.
204. Shomer NH, Fox JG, Juedes AE, Ruddle NH. Helicobacter-induced chronic active lymphoid aggregates have characteristics of tertiary lymphoid tissue. Infection and immunity 2003;71:3572-7.
205. Watanabe T, Suda T, Hirono H, et al. Successful treatment of mucosa-associated lymphoid tissue lymphoma in a patient with gastric and rectal lesions with metachronous and ectopic development. Rare tumors 2011;3:e24.
206. Park JH, Seok SH, Cho SA, et al. The high prevalence of Helicobacter sp. in porcine pyloric mucosa and its histopathological and molecular characteristics. Veterinary microbiology 2004;104:219-25.

207. Zaitoun AM. The prevalence of lymphoid follicles in Helicobacter pylori associated gastritis in patients with ulcers and non-ulcer dyspepsia. Journal of clinical pathology 1995;48:325-9.
208. Leinweber B, Colli C, Chott A, Kerl H, Cerroni L. Differential diagnosis of cutaneous infiltrates of B lymphocytes with follicular growth pattern. The American Journal of dermatopathology 2004;26:4-13.
209. Kerl H, Fink-Puches R, Cerroni L. Diagnostic criteria of primary cutaneous B-cell lymphomas and pseudolymphomas. The Keio journal of medicine 2001;50:269-73.
210. Colli C, Leinweber B, Mullegger R, Chott A, Kerl H, Cerroni L. Borrelia burgdorferi-associated lymphocytoma cutis: clinicopathologic, immunophenotypic, and molecular study of 106 cases. Journal of cutaneous pathology 2004;31:232-40.
211. Suda T, Chida K, Hayakawa H, et al. Development of bronchus-associated lymphoid tissue in chronic hypersensitivity pneumonitis. Chest 1999;115:357-63.
212. Brodie SJ, de la Rosa C, Howe JG, Crouch J, Travis WD, Diem K. Pediatric AIDS-associated lymphocytic interstitial pneumonia and pulmonary arterio-occlusive disease: role of VCAM-1/VLA-4 adhesion pathway and human herpesviruses. The American journal of pathology 1999;154:1453-64.
213. Marolda J, Pace B, Bonforte RJ, Kotin NM, Rabinowitz J, Kattan M. Pulmonary manifestations of HIV infection in children. Pediatric pulmonology 1991;10:231-5.
214. Baskerville A, Ramsay AD, Addis BJ, et al. Interstitial pneumonia in simian immunodeficiency virus infection. The Journal of pathology 1992;167:241-7.
215. Gould SJ, Isaacson PG. Bronchus-associated lymphoid tissue (BALT) in human fetal and infant lung. The Journal of pathology 1993;169:229-34.
216. Vernooy JH, Dentener MA, van Suylen RJ, Buurman WA, Wouters EF. Long-term intratracheal lipopolysaccharide exposure in mice results in chronic lung inflammation and persistent pathology. American journal of respiratory cell and molecular biology 2002;26:152-9.
217. Phillips RJ, Burdick MD, Hong K, et al. Circulating fibrocytes traffic to the lungs in response to CXCL12 and mediate fibrosis. The Journal of clinical investigation 2004;114:438-46.
218. Delventhal S, Hensel A, Petzoldt K, Pabst R. Effects of microbial stimulation on the number, size and activity of bronchus-associated lymphoid tissue (BALT) structures in the pig. International journal of experimental pathology 1992;73:351-7.
219. Allen LA. The role of the neutrophil and phagocytosis in infection caused by Helicobacter pylori. Current opinion in infectious diseases 2001;14:273-7.
220. Dogan A, Du M, Koulis A, Briskin MJ, Isaacson PG. Expression of lymphocyte homing receptors and vascular addressins in low-grade gastric B-cell lymphomas of mucosa-associated lymphoid tissue. The American journal of pathology 1997;151:1361-9.
221. Nakashima Y, Isomoto H, Matsushima K, et al. Enhanced expression of CXCL13 in human Helicobacter pylori-associated gastritis. Digestive diseases and sciences 2011;56:2887-94.
222. Wiley JA, Richert LE, Swain SD, et al. Inducible bronchus-associated lymphoid tissue elicited by a protein cage nanoparticle enhances protection in mice against diverse respiratory viruses. PLoS One 2009;4:e7142.

223. Ulrichs T, Kosmiadi GA, Jorg S, et al. Differential organization of the local immune response in patients with active cavitary tuberculosis or with nonprogressive tuberculoma. The Journal of infectious diseases 2005;192:89-97.
224. Saunders BM, Britton WJ. Life and death in the granuloma: immunopathology of tuberculosis. Immunology and cell biology 2007;85:103-11.
225. Mehra S, Golden NM, Dutta NK, et al. Reactivation of latent tuberculosis in rhesus macaques by co-infection with Simian
Immunodeficiency Virus. J Med Primatol 2011;40:485-94.
226. Mehra S, Golden NA, Stuckey K, et al. The Mycobacterium tuberculosis Stress Response Factor SigH Is Required for Bacterial Burden as Well as Immunopathology in Primate Lungs. J Infect Dis 2012;205:1203-13.
227. Roberts A, Cooper A, Belisle J, Turner J, Gonzalez-Juarerro M, Orme I. Murine Models of Tuberculosis. In: Kaufmann S, Kabelitz D, eds. Methods in Microbiology. Second ed. London: Academic Press; 2002:433-62.
228. Fallert BA, Reinhart TA. Improved detection of simian immunodeficiency virus RNA by in situ hybridization in fixed tissue sections: combined effects of temperatures for tissue fixation and probe hybridization. J Virol Methods 2002;99:23-32.
229. Flynn JL, Chan J. Immunology of tuberculosis. Annual review of immunology 2001;19:93-129.
230. Kaufmann SH. How can immunology contribute to the control of tuberculosis? Nature reviews Immunology 2001;1:20-30.
231. Alatas F, Alatas O, Metintas M, Ozarslan A, Erginel S, Yildirim H. Vascular endothelial growth factor levels in active pulmonary tuberculosis. Chest 2004;125:2156-9.
232. Aly S, Laskay T, Mages J, Malzan A, Lang R, Ehlers S. Interferon-gamma-dependent mechanisms of mycobacteria-induced pulmonary immunopathology: the role of angiostasis and CXCR3-targeted chemokines for granuloma necrosis. J Pathol 2007;212:295-305.
233. Watts G. WHO annual report finds world at a crossroad on tuberculosis. BMJ 2012;345:e7051.
234. Gunn MD, Ngo VN, Ansel KM, Ekland EH, Cyster JG, Williams LT. A B-cell-homing chemokine made in lymphoid follicles activates Burkitt's lymphoma receptor-1. Nature 1998;391:799-803.
235. Bryant VL, Ma CS, Avery DT, et al. Cytokine-mediated regulation of human B cell differentiation into Ig-secreting cells: predominant role of IL-21 produced by CXCR5+ T follicular helper cells. Journal of immunology 2007;179:8180-90.
236. Crotty S. Follicular helper CD4 T cells (TFH). Annual review of immunology 2011;29:621-63.
237. Bauquet AT, Jin H, Paterson AM, et al. The costimulatory molecule ICOS regulates the expression of c-Maf and IL-21 in the development of follicular T helper cells and TH-17 cells. Nature immunology 2009;10:167-75.
238. Good-Jacobson KL, Szumilas CG, Chen L, Sharpe AH, Tomayko MM, Shlomchik MJ. PD-1 regulates germinal center B cell survival and the formation and affinity of long-lived plasma cells. Nature immunology 2010;11:535-42.
239. Nurieva RI, Chung Y, Martinez GJ, et al. Bcl6 mediates the development of T follicular helper cells. Science 2009;325:1001-5.

240. Yu D, Rao S, Tsai LM, et al. The transcriptional repressor Bcl-6 directs T follicular helper cell lineage commitment. Immunity 2009;31:457-68.
241. Vogelzang A, McGuire HM, Yu D, Sprent J, Mackay CR, King C. A fundamental role for interleukin-21 in the generation of T follicular helper cells. Immunity 2008;29:127-37.
242. Eto D, Lao C, DiToro D, et al. IL-21 and IL-6 are critical for different aspects of B cell immunity and redundantly induce optimal follicular helper CD4 T cell (Tfh) differentiation. PloS one 2011;6:e17739.
243. Ma CS, Avery DT, Chan A, et al. Functional STAT3 deficiency compromises the generation of human T follicular helper cells. Blood 2012;119:3997-4008.
244. Schmitt N, Morita R, Bourdery L, et al. Human dendritic cells induce the differentiation of interleukin-21-producing T follicular helper-like cells through interleukin-12. Immunity 2009;31:158-69.
245. Maglione PJ, Xu J, Casadevall A, Chan J. Fc gamma receptors regulate immune activation and susceptibility during Mycobacterium tuberculosis infection. Journal of immunology 2008;180:3329-38.
246. Nurieva RI, Chung Y, Hwang D, et al. Generation of T follicular helper cells is mediated by interleukin-21 but independent of T helper 1, 2, or 17 cell lineages. Immunity 2008;29:138-49.
247. Lin Y, Ritchea S, Logar A, et al. Interleukin-17 Is Required for T Helper 1 Cell Immunity and Host Resistance to the Intracellular Pathogen Francisella tularensis. Immunity 2009;31:799-810.
248. Francisco LM, Sage PT, Sharpe AH. The PD-1 pathway in tolerance and autoimmunity. Immunol Rev 2010;236:219-42.
249. Forster R, Mattis AE, Kremmer E, Wolf E, Brem G, Lipp M. A putative chemokine receptor, BLR1, directs B cell migration to defined lymphoid organs and specific anatomic compartments of the spleen. Cell 1996;87:1037-47.
250. Haynes NM, Allen CD, Lesley R, Ansel KM, Killeen N, Cyster JG. Role of CXCR5 and CCR7 in follicular Th cell positioning and appearance of a programmed cell death gene-1high germinal center-associated subpopulation. Journal of immunology 2007;179:5099-108.
251. Day TA, Koch M, Nouailles G, et al. Secondary lymphoid organs are dispensable for the development of T-cell-mediated immunity during tuberculosis. European journal of immunology 2010;40:1663-73.
252. Zhu J, Paul WE. Heterogeneity and plasticity of T helper cells. Cell research 2010;20:4-12.
253. Zhou L, Chong MM, Littman DR. Plasticity of CD4+ T cell lineage differentiation. Immunity 2009;30:646-55.
254. King C, Tangye SG, Mackay CR. T follicular helper (TFH) cells in normal and dysregulated immune responses. Annual review of immunology 2008;26:741-66.
255. King IL, Mohrs M. IL-4-producing CD4+ T cells in reactive lymph nodes during helminth infection are T follicular helper cells. The Journal of experimental medicine 2009;206:1001-7.
256. Reinhardt RL, Liang HE, Locksley RM. Cytokine-secreting follicular T cells shape the antibody repertoire. Nature immunology 2009;10:385-93.

257. Fazilleau N, McHeyzer-Williams LJ, Rosen H, McHeyzer-Williams MG. The function of follicular helper T cells is regulated by the strength of T cell antigen receptor binding. Nature immunology 2009;10:375-84.
258. Nakayamada S, Kanno Y, Takahashi H, et al. Early Th1 cell differentiation is marked by a Tfh cell-like transition. Immunity 2011;35:919-31.
259. Glatman Zaretsky A, Taylor JJ, King IL, Marshall FA, Mohrs M, Pearce EJ. T follicular helper cells differentiate from Th2 cells in response to helminth antigens. The Journal of experimental medicine 2009;206:991-9.
260. Annunziato F, Galli G, Cosmi L, et al. Molecules associated with human Th1 or Th2 cells. European cytokine network 1998;9:12-6.
261. Sauty A, Dziejman M, Taha RA, et al. The T cell-specific CXC chemokines IP-10, Mig, and I-TAC are expressed by activated human bronchial epithelial cells. Journal of immunology 1999;162:3549-58.
262. Xie JH, Nomura N, Lu M, et al. Antibody-mediated blockade of the CXCR3 chemokine receptor results in diminished recruitment of T helper 1 cells into sites of inflammation. Journal of leukocyte biology 2003;73:771-80.
263. Scott HM, Flynn JL. Mycobacterium tuberculosis in chemokine receptor 2-deficient mice: influence of dose on disease progression. Infection and immunity 2002;70:5946-54.
264. Algood HM, Flynn JL. CCR5-deficient mice control Mycobacterium tuberculosis infection despite increased pulmonary lymphocytic infiltration. Journal of immunology 2004;173:3287-96.
265. Allen CD, Ansel KM, Low C, et al. Germinal center dark and light zone organization is mediated by CXCR4 and CXCR5. Nature immunology 2004;5:943-52.
266. Ngo VN, Korner H, Gunn MD, et al. Lymphotoxin alpha/beta and tumor necrosis factor are required for stromal cell expression of homing chemokines in B and T cell areas of the spleen. The Journal of experimental medicine 1999;189:403-12.
267. Taylor RT, Patel SR, Lin E, et al. Lymphotoxin-independent expression of TNF-related activation-induced cytokine by stromal cells in cryptopatches, isolated lymphoid follicles, and Peyer's patches. Journal of immunology 2007;178:5659-67.
268. Drayton DL, Ying X, Lee J, Lesslauer W, Ruddle NH. Ectopic LT alpha beta directs lymphoid organ neogenesis with concomitant expression of peripheral node addressin and a HEV-restricted sulfotransferase. The Journal of experimental medicine 2003;197:1153-63.
269. Kim CH, Lim HW, Kim JR, Rott L, Hillsamer P, Butcher EC. Unique gene expression program of human germinal center T helper cells. Blood 2004;104:1952-60.
270. Vermi W, Lonardi S, Bosisio D, et al. Identification of CXCL13 as a new marker for follicular dendritic cell sarcoma. The Journal of pathology 2008;216:356-64.
271. Piqueras B, Connolly J, Freitas H, Palucka AK, Banchereau J. Upon viral exposure, myeloid and plasmacytoid dendritic cells produce 3 waves of distinct chemokines to recruit immune effectors. Blood 2006;107:2613-8.
272. You Y, Richer EJ, Huang T, Brody SL. Growth and differentiation of mouse tracheal epithelial cells: selection of a proliferative population. Am J Physiol Lung Cell Mol Physiol 2002;283:L1315-21.
273. Vermi W, Facchetti F, Riboldi E, et al. Role of dendritic cell-derived CXCL13 in the pathogenesis of Bartonella henselae B-rich granuloma. Blood 2006;107:454-62.

274. Takemura S, Braun A, Crowson C, et al. Lymphoid neogenesis in rheumatoid synovitis. J Immunol 2001;167:1072-80.
275. Mazzucchelli L, Blaser A, Kappeler A, et al. BCA-1 is highly expressed in Helicobacter pylori-induced mucosa-associated lymphoid tissue and gastric lymphoma. J Clin Invest 1999;104:R49-54.
276. Shi K, Hayashida K, Kaneko M, et al. Lymphoid chemokine B cell-attracting chemokine-1 (CXCL13) is expressed in germinal center of ectopic lymphoid follicles within the synovium of chronic arthritis patients. J Immunol 2001;166:650-5.
277. Lisignoli G, Toneguzzi S, Piacentini A, et al. Human osteoblasts express functional CXC chemokine receptors 3 and 5: activation by their ligands, CXCL10 and CXCL13, significantly induces alkaline phosphatase and beta-N-acetylhexosaminidase release. J Cell Physiol 2003;194:71-9.
278. Connell DW, Berry M, Cooke G, Kon OM. Update on tuberculosis: TB in the early 21st century. European respiratory review : an official journal of the European Respiratory Society 2011;20:71-84.
279. Dienz O, Eaton SM, Bond JP, et al. The induction of antibody production by IL-6 is indirectly mediated by IL-21 produced by CD4+ T cells. The Journal of experimental medicine 2009;206:69-78.
280. Perrier P, Martinez FO, Locati M, et al. Distinct transcriptional programs activated by interleukin-10 with or without lipopolysaccharide in dendritic cells: induction of the B cell-activating chemokine, CXC chemokine ligand 13. Journal of immunology 2004;172:7031-42.
281. Khader SA, Guglani L, Rangel-Moreno J, et al. IL-23 is required for long-term control of Mycobacterium tuberculosis and B cell follicle formation in the infected lung. J Immunol 2011;187:5402-7.
282. Gopal R, Rangel-Moreno J, Slight S, et al. Interleukin-17-dependent CXCL13 mediates mucosal vaccine-induced immunity against tuberculosis. Mucosal Immunol 2013.
283. Lu KT, Kanno Y, Cannons JL, et al. Functional and epigenetic studies reveal multistep differentiation and plasticity of in vitro-generated and in vivo-derived follicular T helper cells. Immunity 2011;35:622-32.